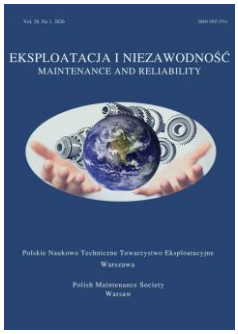

Eksploatacja i Niezawodnosc – Maintenance and Reliability
Volume 28 (2026), Issue 1
journal homepage: http://www.ein.org.pl

Article citation info:
Peng C, Li J, Ren L, Li D, Chen J, Remaining useful life prediction of binary stochastic degradation equipment based on mixed Copula functions, Eksploatacja i Niezawodnosc – Maintenance and Reliability 2026: 28(1) http://doi.org/10.17531/ein/209903

Remaining useful life prediction of binary stochastic degradation equipment based on mixed Copula functions

Indexed by:
Web of Science Group

Caihua Peng[a], Jianhua Li[a,*], Lina Ren[a], Dachao Li[a], Jintao Chen[a]

[a] School of Mechanical and Electrical Engineering, Lanzhou University of Technology, Lanzhou 730050, China

Highlights

- A remaining useful life prediction method based on mixed Copula functions is proposed.
- A stochastic degradation model considering multiple degradation modes is established.
- Comparative analysis shows that the proposed method results in smaller prediction errors.

Abstract

To address the issue of distorted correlation characterization in existing multivariate correlation-based remaining useful life (RUL) prediction methods for degrading equipment—caused by relying solely on a single Copula function to model interdependencies among multiple degradation features—this paper proposes an RUL prediction method based on mixed Copula functions. First, a stochastic degradation model incorporating multiple degradation modes is established based on the Wiener process. Second, a mixed Copula function composed of linear combinations of Gumbel, Clayton, and Frank Copulas is constructed to capture the complex correlations among degradation features, and a stepwise maximum likelihood method is employed to estimate the model parameters. Finally, validation through simulated degradation datasets, LED lighting system degradation data, and metal crack propagation data demonstrates that the proposed method achieves smaller prediction errors and higher accuracy compared to existing single Copula-based methods, confirming its superiority.

Keywords
degradation modeling, Wiener process, Mixed Copula functions, remaining useful life prediction

1. Introduction

With the continuous development of high-tech, modern industrial equipment is evolving towards high automation and integration. Due to the comprehensive effects of factors such as vibration impacts, operating condition transitions, mechanical wear, chemical erosion, load variations, and energy consumption throughout their lifecycles, these types of equipment inevitably experience degradation in performance and health status, eventually leading to equipment failure and even causing irreparable loss of life and property. If the RUL of equipment can be predicted before failure, and appropriate maintenance strategies can be adopted accordingly, catastrophic accidents can be effectively avoided, thereby achieving the goals of cost reduction and property protection [1-3]. As a core technology of prognostics and health management, RUL prediction is the prerequisite and foundation for making scientifically informed maintenance decisions for equipment. Therefore, accurately predicting the RUL of equipment to reduce the risk of sudden failures holds significant theoretical significance and engineering practical value [4,5].

Existing literature categorizes methods for predicting

(*) Corresponding author.
E-mail addresses: C. Peng (ORCID: 0000-0002-9026-969X) pch5616854@163.com, J. Li (ORCID: 0000-0001-7777-8580) li_jh@vip.sina.com, L. Ren (ORCID: 0000-0003-1350-1819) sunnyren331@sina.com, D. Li (ORCID: 0009-0006-2260-5272) dachaoli@lut.edu.cn, J. Chen (ORCID: 0000-0003-2299-8820) jtao_chen@163.com

equipment lifetime into two main groups: physics-based methods and data-driven methods [6-8]. Physics-based methods utilize the knowledge of equipment's mechanical dynamics combined with monitoring data to predict lifetime, primarily relying on specific physical models of the equipment. However, due to unclear failure mechanisms and diverse failure modes of most equipment, it is challenging to establish accurate physical models, thereby limiting the applicability of physics-based methods in lifetime prediction [9-10]. Data-driven lifetime prediction methods do not require knowledge of the equipment's physical model, they directly utilize monitoring data or historical degradation data of similar equipment to estimate lifetime, thus attracting significant attention from scholars both domestically and internationally [11-13].

Due to the high randomness of the degradation failure process of the equipment, most existing studies adopt stochastic processes to describe the performance degradation process, believing that stochastic processes can more accurately depict the trajectory of equipment performance degradation. Among these, modeling methods based on Wiener processes have been used widely in degradation modeling and lifetime prediction due to their favorable mathematical properties [14-27]. The Wiener process is a stochastic process extensively used for features with increasing or decreasing non-monotonic characteristics. In practical applications, the non-monotonic characteristics of degradation data arise from differences in equipment loads and variations in internal and external environments, making Wiener processes suitable for degradation modeling and lifetime prediction of equipment.

In response to the characteristic of equipment degradation trajectories exhibiting linear degradation, Kahle et al. [14] proposed a simple linear Wiener process degradation model, providing parameter estimation methods and definitions for equipment lifetime. Wang et al. [15] introduced a RUL prediction method for metallized film capacitors based on the linear Wiener process. Li et al. [16] addressed variations in performance among different units in the same batch of equipment due to factors such as processing techniques, design errors, and functional differences. They proposed a linear Wiener process that considers the randomness of drift parameters for predicting the lifetime of momentum wheels. Si et al. [17] considering measurement errors as a source of uncertainty, derived the PDF for RUL using Bayesian inference and the EM algorithm. Peng et al. [18] proposed a linear Wiener degradation model with a drift factor following a skew-normal distribution for predicting the RUL of equipment. In cases where the degradation trajectory of equipment displays linear segments, Zhang et al. [19] proposed a two-stage linear Wiener process, successfully applied to predicting the RUL of batteries. Guan et al. [20] introduced a two-stage linear Wiener process that accounts for measurement errors, aimed at predicting the RUL of bearings.

The linear Wiener degradation model is only applicable to situations where the degradation trajectory has a linear trend, whereas the degradation trajectories of most equipment are characterized by nonlinearity. In order to improve the generality of Wiener process degradation models, many scholars have proposed nonlinear Wiener process degradation models. Si et al. [21] addressed nonlinear issues by presenting two common forms of nonlinear degradation models—exponential and power functions—and derived analytical expressions for lifetime and remaining useful life PDFs. Tang et al. [22] developed a nonlinear model with measurement errors, building on existing nonlinear degradation models to address measurement error issues in degradation data. Peng et al. [23] proposed a novel nonlinear degradation model that combines power function degradation with linear degradation models for predicting the RUL of laser generators, based on existing linear and power function degradation model. Yu et al. [24] established a general nonlinear Wiener process model considering three sources of uncertainty, deriving the remaining useful life PDF and calculating estimates of RUL. Long et al. [25] created a state-space model for nonlinear Wiener processes and proposed a stochastic mixed system approach, improving the accuracy of RUL prediction. Lin et al. [26] proposed a two-stage nonlinear Wiener process degradation modeling method, considering that the degradation rate of equipment may vary across different time periods, thereby enhancing the accuracy of lifetime prediction. Hu et al. [27] proposed a general form of the two-stage nonlinear Wiener process degradation modeling method and validated its effectiveness using data from high-pressure pulse capacitors.

In predicting the RUL of equipment, current research primarily focuses on utilizing a single performance indicator of

the equipment for such predictions. However, for most equipment, relying solely on a single performance indicator makes it difficult to fully and accurately reflect the state of health status and degradation process of the equipment. Therefore, in order to reflect the state of health of the equipment as fully as possible, it is essential to fully utilize multiple performance indicators of the equipment. Among them, utilizing two performance indicators for predicting the RUL forms the foundation for research on predicting the RUL of equipment on the basis of multiple performance indicators. Therefore, scholars have already investigated methods for predicting the RUL of equipment based on bivariate stochastic processes, assuming a certain correlation exists between the degradation processes of the two performance indicators of the equipment. They introduce Copula functions to describe the correlation characteristics between indicators and establish degradation models on the basis of bivariate stochastic processes. Copula functions are tools used to characterize the correlation between variables, known for their simplicity in modeling, flexible application, and wide range of uses [28-29].

For multi-dimensional linear degradation equipment, Jin et al. [30] established a corresponding linear Wiener process degradation model for bearing's binary performance indicators and the marginal distribution of RUL. Then, using the Copula function, they combined the marginal distributions to obtain the joint distribution function of the equipment, achieving the prediction of the bearing's RUL. Similarly, Dai et al. [31] established a binary linear Wiener process degradation model based on the Copula function for the RUL prediction of nickel-cadmium batteries. Qi et al. [32] proposed a binary linear Wiener degradation model with two correlated performance indicators based on the Copula function and applied Bayesian theory to implement the online prediction of the RUL of onboard transformer oil-paper insulation in high-speed trains. For multi-dimensional nonlinear degradation equipment, Dong et al. [33] proposed a nonlinear Wiener process based on binary time-scale transformations, using the Frank Copula function to combine the marginal distributions and obtain the joint failure distribution function, which was used for the failure prediction of dry-type hollow reactor encapsulation materials. Zhao et al. [34] proposed two common binary nonlinear Wiener random process models, one based on power function and the other on exponential function, for the RUL prediction of transformer oil-paper insulation using the Copula function.

Current research indicates that existing methods for predicting the RUL of multi-degradation equipment predominantly rely on single Copula functions to characterize correlations between different features. However, a single Copula function can only represent a single type of dependency (e.g., symmetric, upper-tail, or lower-tail correlation), while complex dependencies exist among degradation data of different performance metrics in practical equipment. The exclusive use of a single Copula function in real-world applications may lead to mischaracterization of the dependency structure between different performance degradations, thereby increasing RUL prediction errors. To address these limitations, this paper innovatively proposes a method employing mixed Copula functions to characterize dependencies among different equipment performance metrics. A Wiener process-based degradation model incorporating multiple degradation modes is established, where mixed Copula functions are utilized to describe inter-performance dependencies. Leveraging the properties of Wiener processes and the definition of first hitting time (FHT), analytical expressions for lifetime and RUL probability density functions are derived for joint distributions constructed with different mixed Copula functions. A two-step maximum likelihood estimation method is implemented to estimate the unknown parameters of the model. The effectiveness and practicality of the proposed methodology are validated through simulated degradation data, LED lighting system datasets, and metal crack degradation data.

2. Degradation modeling

2.1. Single-performance degradation model

The Wiener process has been used widely in RUL prediction studies due to its incorporation of Brownian motion (BM) for effectively handling non-monotonic processes. Let $X(t)$ denote the monitored degradation value at time t, the degradation process can be modeled as follows [35]:

$$X(t) = X(0) + a\phi_i(t,b) + \delta_B B(t) \quad (1)$$

In this context, $X(0)$ represents the initial state of the degradation process, and for computational simplicity, it is commonly hypothesized that the initial state $X(0) = 0$.$B(t)$denotes the standard Brownian motion. $a\phi_i(t,b)$stands

for the drift term of degradation, a represents the drift coefficient. Due to variations in usage environments and processing materials among similar equipment, there exist certain differences in the degradation trajectories of each equipment. Therefore, in modeling performance degradation, the drift coefficient a is regarded as a random variable, satisfying $a \sim N(\mu_a, \delta_a^2)$, to account for individual differences among equipment. b is a fixed parameter describing the commonalities among similar equipment. δ_B represents the diffusion coefficient, with the assumption that the parameters a, b and δ_B are mutually independent to simplify analysis.

Eq. (1) represents a common form based on the Wiener degradation model, and different degradation patterns can be described by different drift terms. For instance, if the drift term is represented as $\phi(t,b) = t$, Eq. (1) becomes a linear degradation model, widely applied in RUL prediction studies [14-20]. In this paper, a RUL prediction method based on the Wiener process is proposed, which contains multiple degradation models, mainly including three typical degradation models, namely, linear function(M_1), power function(M_2) and exponential function (M_3), i.e., $\phi_i(t,b) = \big(\phi_1(t,b), \phi_2(t,b), \phi_3(t,b)\big) = (t, t^b, exp(bt))$ .Specific Wiener process degradation models can be expressed as: M_1 : $X(t) = at + \delta_B B(t)$, M_2 : $X(t) = at^b + \delta_B B(t)$,$M_3$:$X(t) = a\,exp(bt) + \delta_B B(t)$.

2.2. Copula function theory

Copula functions are a class of functions that connect the distribution functions of multiple random variables with their respective marginal distribution functions, and are therefore also referred to as connection functions. Taking binary variables as an example, its practical significance lies in connecting the marginal distribution and joint distribution of two random variables, establishing a mapping relationship between marginal and joint distributions, and separating the study of marginal and joint distributions. Sklar's theorem is an existence theorem for Copula functions. Its basic content is: if $H(x,y)$ is a bivariate joint distribution function with continuous marginal distributions $F(x)$ and $G(y)$, then a unique Copula function $C(\ )$ exists such that $H(x,y) = C\big(F(x), G(y)\big)$. Instead, if $C(\ )$ is a Copula function ,$F(x)$ and $G(y)$ are two arbitrary CDFs, then the function $H(x,y)$defined by the above equation must be a joint distribution function, and the corresponding marginal distributions are precisely $F(x)$ and $G(y)$ [36]. Assuming random variables$X$ and $Y$are correlated, let the joint distribution function of the two-dimensional random variable (X,Y) be represented as $H(x,y)$, with marginal distributions $F(x)$ and $G(y)$ respectively. According to Sklar's theorem, a Copula function $C(\ )$ exists such that

$$H(x,y) = C\big(F(x), G(y)\big) \tag{2}$$

If $F(x)$ and $G(y)$ are continuous, then $C(\ )$ is uniquely determined. The PDFs of $H(x,y)$obtained through the Copula function is given by:

$$h(x,y) = c\big(F(x), G(y)\big) f(x) g(x) \tag{3}$$

where $c(u,v) = \frac{\partial C(u,v)}{\partial u \partial v}$, $u = F(x)$, $v = G(y)$. Here, $c(\ )$ represents the PDF of the Copula function $C(\ )$, $f(x)$ and $g(y)$ are the PDFs of the marginal distributions $F(x)$and$G(y)$, respectively. The Archimedean Copula function family is an important component of many types of Copula functions. Due to its simple construction and strong variability, it has been widely used. Three common Archimedean binary Copula functions are shown in the following Table 1.

Table 1. Three common Archimedean binary Copula functions.

Function name	Probability density function $c(u,v;\alpha)$	Distribution function $C(u,v;\alpha)$	Parameter range
Frank Copula	$\frac{\alpha(1-e^{-\alpha})e^{-\alpha(u+v)}}{[(e^{-\alpha u}-1)(e^{-\alpha v}-1)-(1-e^{-\alpha})]^2}$	$-\frac{1}{\alpha} ln\left(1+\frac{(e^{-\alpha u}-1)(e^{-\alpha v}-1)}{(e^{-\alpha}-1)}\right)$	$\alpha \in R\backslash\{0\}$
Clayton Copula	$(1+\alpha)(uv)^{-\alpha-1}(u^{-\alpha}+v^{-\alpha}-1)^{-2-\frac{1}{\alpha}}$	$(u^{-\alpha}+v^{-\alpha}-1)^{-\frac{1}{\alpha}}$	$\alpha \in (1,\infty)$
Function name	Probability density function $c(u,v;\alpha)$	Distribution function $C(u,v;\alpha)$	Parameter range
Gumbel Copula	$\frac{exp\left\{-[(-ln\,u)^{\alpha}+(-ln\,v)^{\alpha}]^{\frac{1}{\alpha}}\right\}(ln\,u\,.\,ln\,v)^{\alpha-1}}{uv[(-ln\,u)^{\alpha}+(-ln\,v)^{\alpha}]^{2-\frac{1}{\alpha}}} \times\left\{[(-ln\,u)^{\alpha}+(-ln\,v)^{\alpha}]^{\frac{1}{\alpha}}+\alpha-1\right\}$	$exp\left\{-[(-ln\,u)^{\alpha}+(-ln\,v)^{\alpha}]^{\frac{1}{\alpha}}\right\}$	$\alpha \in [1,\infty)$

Among them, α represents the parameter of the correlation dependence direction. When $\alpha > 0$, it indicates that there is a positive correlation between variables; when $\alpha < 0$, it means there is a negative correlation between variables; when $\alpha \to 0$, it means the variables tend to be independent. In order to illustrate the difference between the three Archimedean binary Copula functions, the paper takes $\alpha = 2$ and plots the PDF of each of the three Copula functions as shown in Fig.1.

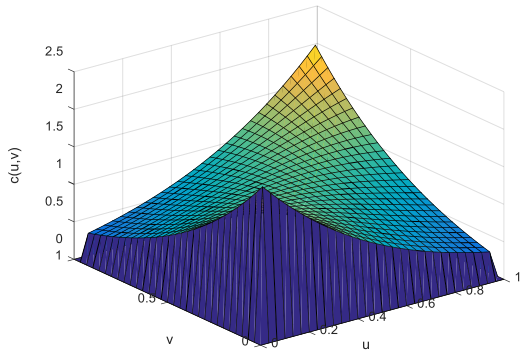

(a) Frank Copula's PDF

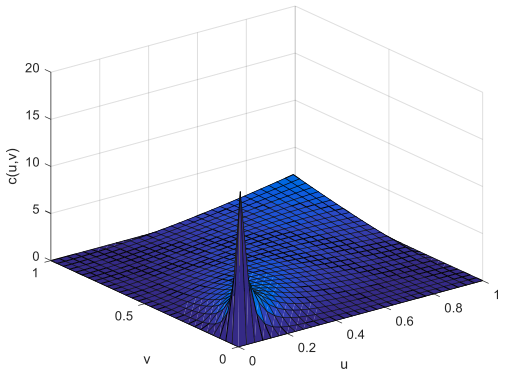

(b) Clayton Copula's PDF

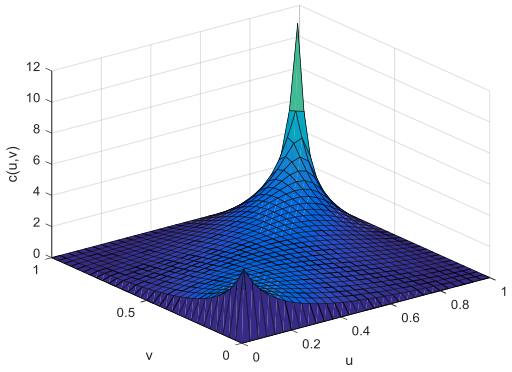

(c) Gumbel Copula's PDF

Fig.1. PDF graphs of three Copula functions.

From the PDF graphs of the aforementioned Copula functions, it can be observed that different Copula functions depict correlation differently. The Frank Copula is suitable for modeling symmetric dependence structures between variables, while the Clayton Copula effectively characterizes asymmetric lower-tail dependence, and the Gumbel Copula excels in describing asymmetric upper-tail dependence. Therefore, relying solely on a single Copula function to integrate data in practical applications may lead to distorted or inaccurate representations of the true dependency structure, particularly when the data exhibit complex or multi-modal dependence patterns. To address this, considering a mixture of multiple Copula functions becomes necessary. Such a mixed Copula function can better describe the dependence in the data and fuse the data more effectively.

The model of the binary mixed Copula function is as follows:

$$C(u_1, u_2) = \sum_{i=1}^{s} k_i C_i(u_1, u_2; \alpha_i) \quad (4)$$

where $C_i(u_1, u_2; \alpha_i)$ is a known Copula function, α_i is the corresponding parameter, $k_i$is the weight coefficient, and $0 \leq k_i \leq 1$, $\sum_{i=1}^{s} k_i = 1$. Research indicates that mixed Copula functions remain Copula functions [37].

3. Lifetime prediction

3.1. Lifetime prediction of single performance degradation data

This paper adopts the concept of FHT to define the equipment lifetime, which means that when the equipment's performance degradation process $\{X(t), t \geq 0\}$ first equals or exceeds the preset failure threshold ω, the equipment is considered to have failed [38,39], and the corresponding time is then considered as the equipment's lifetime. Based on the concept of FHT, lifetime T can be defined as

$$T = inf\{t: X(t) \geq \omega | X(0) < \omega\} \quad (5)$$

Without loss of generality, let the failure threshold $\omega > 0$. According to references [21] and [34], the lifetime PDF and distribution function of M_1,M_2,and M_3 are as follows:

(1) The PDF and distribution function of the lifetime corresponding to the degradation model M_1 are as follows:

$$f_T(t) \cong \frac{\omega}{\sqrt{2\pi t^3(\delta_a^2 t+\delta_B^2)}} exp\left\{-\frac{(\omega-\mu_a t)^2}{2t(\delta_a^2 t+\delta_B^2)}\right\} \quad (6)$$

$$F_T(t) = \Phi\left(\frac{\mu_a t-\omega}{\sqrt{\delta_a^2 t^2+\delta_B^2 t}}\right) + exp\left\{\frac{2\mu_a\omega}{\delta_B^2}+\frac{2\delta_a^2\omega^2}{\delta_B^4}\right\}\Phi\left(-\frac{2\delta_a^2\omega t+\delta_B^2(\mu_a t+\omega)}{\delta_B^2\sqrt{\delta_a^2 t^2+\delta_B^2 t}}\right) \quad (7)$$

(2) The PDF and distribution function of the lifetime corresponding to the degradation model M_2 are as follows:

$$f_T(t) \cong \frac{1}{\sqrt{2\pi t^3(\delta_a^2 t^{2b-1}+\delta_B^2)}}\left(\omega-(t^b-bt^b)\frac{\omega\delta_a^2 t^{2b-1}+\mu_a\delta_B^2}{\delta_a^2 t^{2b-1}+\delta_B^2}\right) exp\left\{-\frac{(\omega-\mu_a t^b)^2}{2t(\delta_a^2 t^{2b-1}+\delta_B^2)}\right\} \quad (8)$$

$$F_T(t) = 1-\Phi\left(\frac{\omega-\mu_a t^b}{\sqrt{\delta_a^2 t^{2b}+\delta_B^2 t}}\right) + exp\left\{\frac{2\mu_a\omega t^b}{\delta_B^2 t}+\frac{2\delta_a^2\omega^2 t^{2b}}{\delta_B^4 t^2}\right\}\Phi\left(-\frac{2\delta_a^2\omega t^{2b}+\delta_B^2 t(\mu_a t^b+\omega)}{\delta_B^2 t\sqrt{\delta_a^2 t^{2b}+\delta_B^2 t}}\right) \quad (9)$$

(3) The PDF and distribution function of the lifetime corresponding to the degradation model M_3 are as follows:

$$f_T(t) \cong \frac{1}{\sqrt{2\pi t^2(\delta_a^2(exp(bt)-1)^2+\delta_B^2 t)}}\left(\omega-\beta(t)\frac{\omega\delta_a^2(exp(bt)-1)+\mu_a\delta_B^2 t}{\delta_a^2(exp(bt)-1)^2+\delta_B^2 t}\right)\times exp\left\{-\frac{(\omega-\mu_a(exp(bt)-1))^2}{2(\delta_a^2(exp(bt)-1)^2+\delta_B^2 t)}\right\} \quad (10)$$

with$\beta(t) = exp(bt) - bt\,exp(bt) - 1$.

$$F_T(t) = 1-\Phi\left(\frac{\omega-\mu_a\,exp(bt)}{\sqrt{\delta_a^2(exp(bt))^2+\delta_B^2 t}}\right) + exp\left\{\frac{2\mu_a\omega\,exp(bt)}{\delta_B^2 t}+\frac{2\delta_a^2\omega^2(exp(bt))^2}{\delta_B^4 t^2}\right\}\times\Phi\left(-\frac{2\delta_a^2\omega(exp(bt))^2+\delta_B^2 t(\mu_a\,exp(bt)+\omega)}{\delta_B^2 t\sqrt{\delta_a^2(exp(bt))^2+\delta_B^2 t}}\right) \quad (11)$$

In the above equations, $\Phi(.)$ denotes the cumulative distribution function of the standard normal distribution. $\mu_a$and δ_a^2represent the mean and variance of the drift coefficient a, which follows a normal distribution. The proof process for Eqs. (7), (9), and (11) is shown in Appendix A.

For the current time t_i, according to the concept of FHT, the RUL of the equipment can be defined as

$$L_{t_i} = inf\{l_{t_i} > 0: X(l_{t_i}+t_i) \geq \omega\} \quad (12)$$

where l_{t_i} represents the RUL of the equipment at time t_i. Similarly, according to the literature [21], the remaining useful life PDFs of M_1, M_2, and M_3 can be obtained, and RUL probability distribution functions of the three models are also deduced as shown below:

(1) The PDF and distribution function of the RUL corresponding to the degradation model M_1 are as follows:

$$f(l_{t_i}) \cong \frac{\omega-X(t_i)}{\sqrt{2\pi l_{t_i}^3(\delta_B^2+l_{t_i}\delta_a^2)}} exp\left(-\frac{(\omega-X(t_i)-\mu_a l_{t_i})^2}{2l_{t_i}(\delta_B^2+l_{t_i}\delta_a^2)}\right) \quad (13)$$

$$F(l_{t_i}) = 1-\Phi\left(\frac{\omega-X(t_i)-\mu_a l_{t_i}}{\sqrt{l_{t_i}\delta_B^2+l_{t_i}^2\delta_a^2}}\right) + exp\left\{\frac{2\mu_a(\omega-X(t_i))}{\delta_B^2}+\frac{2\delta_a^2(\omega-X(t_i))^2}{\delta_B^4}\right\}\times\Phi\left(-\frac{2\delta_a^2(\omega-X(t_i))l_{t_i}+\delta_B^2(\mu_a l_{t_i}+\omega-X(t_i))}{\delta_B^2\sqrt{\delta_a^2 l_{t_i}^2+\delta_B^2 l_{t_i}}}\right) \quad (14)$$

(2) The PDF and distribution function of the RUL corresponding to the degradation model M_2 are as follows:

$$f(l_{t_i}) = \frac{1}{\sqrt{2\pi l_{t_i}^3(\delta_B^2 l_{t_i}+\delta_a^2(\gamma(l_{t_i}))^2)}}\left(\omega_{t_i}-(\gamma(l_{t_i})-bl_{t_i}(l_{t_i}+t_i)^{b-1})\right)\frac{\delta_a^2\gamma(l_{t_i})\omega_{t_i}+\mu_a\delta_B^2 l_{t_i}}{\delta_a^2(\gamma(l_{t_i}))^2+\delta_B^2 l_{t_i}}\times exp\left(-\frac{(\omega_{t_i}-\mu_a\gamma(l_{t_i}))^2}{2(\delta_B^2 l_{t_i}+(\gamma(l_{t_i}))^2\delta_a^2)}\right) \quad (15)$$

with$\omega_{t_i} = \omega - X(t_i)$,$\gamma(l_{t_i}) = (l_{t_i}+t_i)^b - t_i^b$.

$$F(l_{t_i}) = 1 - \Phi\left(\frac{\omega - X(t_i) - \mu_a l_{t_i}^b}{\sqrt{l_{t_i}\delta_B^2 + l_{t_i}^{2b}\delta_a^2}}\right) + exp\left\{\frac{2\mu_a(\omega - X(t_i))l_{t_i}^b}{\delta_B^2 l_{t_i}} + \frac{2\delta_a^2(\omega - X(t_i))^2 l_{t_i}^{2b}}{\delta_B^4 l_{t_i}^2}\right\} \times \Phi\left(-\frac{2\delta_a^2(\omega - X(t_i))l_{t_i}^{2b} + \delta_B^2 l_{t_i}\left(\mu_a l_{t_i}^b + \omega - X(t_i)\right)}{\delta_B^2 l_{t_i}\sqrt{\delta_a^2 l_{t_i}^{2b} + \delta_B^2 l_{t_i}}}\right) \quad (16)$$

(3) The PDF and distribution function of the RUL corresponding to the degradation model M_3 are as follows:

$$f(l_{t_i}) = \frac{1}{\sqrt{2\pi l_{t_i}^2\left(\delta_B^2 l_{t_i} + \delta_a^2\left(\gamma(l_{t_i})\right)^2\right)}}\left(\omega_{t_i} - \beta(l_{t_i})\right)\frac{\delta_a^2\gamma(l_{t_i})\omega_{t_i} + \mu_a\delta_B^2 l_{t_i}}{\delta_a^2\left(\gamma(l_{t_i})\right)^2 + \delta_B^2 l_{t_i}} exp\left(-\frac{\left(\omega_{t_i} - \mu_a\gamma(l_{t_i})\right)^2}{2\left(\delta_B^2 l_{t_i} + \left(\gamma(l_{t_i})\right)^2\delta_a^2\right)}\right) \quad (17)$$

with $\omega_{t_i} = \omega - X(t_i)$,$\gamma(l_{t_i}) = exp\left(b(l_{t_i} + t_i)\right) - exp(bt_i)$,$\beta(l_{t_i}) = (1 - bl_{t_i})\,exp\left(b(l_{t_i} + t_i)\right) - exp(bt_i)$.

$$F(l_{t_i}) = 1 - \Phi\left(\frac{(\omega - X(t_i)) - \mu_a\, exp(bl_{t_i})}{\sqrt{\delta_a^2\left(exp(bl_{t_i})\right)^2 + \delta_B^2 l_{t_i}}}\right) + exp\left\{\frac{2\mu_a(\omega - X(t_i))\, exp(bl_{t_i})}{\delta_B^2 l_{t_i}} + \frac{2\delta_a^2(\omega - X(t_i))^2\left(exp(bl_{t_i})\right)^2}{\delta_B^4 l_{t_i}^2}\right\} \times$$

$$\Phi\left(-\frac{2\delta_a^2(\omega - X(t_i))\left(exp(bl_{t_i})\right)^2 + \delta_B^2 l_{t_i}\left(\mu_a\left(exp(bl_{t_i})\right) + \omega - X(t_i)\right)}{\delta_B^2 l_{t_i}\sqrt{\delta_a^2\left(exp(bl_{t_i})\right)^2 + \delta_B^2 l_{t_i}^2}}\right) \quad (18)$$

The method of proving the RUL probability distribution function for models M_1,M_2,and M_3 is shown in Appendix B.

3.2. Lifetime prediction of dual performance degradation data

This section focuses on equipment with two performance indicators and investigates methods for predicting equipment lifetime based on a bivariate Wiener process degradation model. It is initially required that the performance indicators of the equipment meet the following assumptions:

Assumption 1: The degradation processes of the two performance indicators of the equipment can be modeled using Wiener processes with linear or nonlinear.

Assumption 2: For the same equipment, the monitoring time and intervals of the two performance indicators remain synchronous.

Assumption 3: There exists correlation in the degradation of the two performance indicators, and this correlation can be reasonably described using a certain bivariate Copula function.

To predict the lifetime of equipment with dual performance degradation, let $X(t) = \{X^1(t), X^2(t)\}$denote the degradation values of the two performance indicators of the equipment at time t, and let the failure threshold be denoted by $\omega = (\omega_1, \omega_2)$ .When either of the performance indicators in $X(t)$ exceeds its corresponding failure threshold, the equipment is considered to have failed. Therefore, the lifetime of the equipment with two performance indicators can be defined as:

$$T = inf\{t: X^1(t) \geq \omega_1 or X^2(t) \geq \omega_2\} \quad (19)$$

After obtaining the PDFs of lifetime for the two performance indicators of the equipment separately, according to Sklar's theorem, there must exist a Copula function that can be used to analyze the correlation between the two performance indicators. The joint PDF of the lifetime of the two performance indicators can be obtained through the following equation:

$$f_T^{union}(t) = f_T^1(t) + f_T^2(t) - c(F_T^1(t), F_T^2(t); \alpha) f_T^1(t) f_T^2(t) \quad (20)$$

where $f_T^1(t)$ and $f_T^2(t)$ are the PDFs of lifetime of the two performance indicators. $F_T^1(t)$ and $F_T^2(t)$ are the distribution functions of lifetime of the two performance indicators, respectively. $f_T^{union}(t)$represents the joint PDF of lifetime, and $c(F_T^1(t), F_T^2(t); \alpha)$ is the PDF of $C(F_T^1(t), F_T^2(t); \alpha)$.

Similarly, according to the concept of FHT, the RUL of equipment with two performance indicators can be defined as:

$$L_{t_i} = inf\{l_{t_i} > 0: X^1(l_{t_i} + t_i) \geq \omega^1 or X^2(l_{t_i} + t_i) \geq \omega^2\} \quad (21)$$

where l_{t_i} is the RUL of equipment at time t_i , when the PDFs of RUL of the two performance indicators of equipment are obtained separately, the joint PDF of RUL of the two performance indicators can be obtained through the following equation:

$$f^{union}(l_{t_i}) = f^1(l_{t_i}) + f^2(l_{t_i}) - c(F^1(l_{t_i}), F^2(l_{t_i}); \alpha) f^1(l_{t_i}) f^2(l_{t_i}) \quad (22)$$

In the equation, $f^1(l_{t_i})$and $f^2(l_{t_i})$are the PDFs of the RUL of the two performance indicators. $F^1(l_{t_i})$and$F^2(l_{t_i})$ are the distribution functions of CDFs of the RUL of the two performance indicators, respectively. $f^{union}(l_{t_i})$represents the

joint PDF of RUL.

4. Parameter estimation

Due to the large number of parameters to be estimated, the stepwise maximum likelihood estimation method has the advantages of simple calculation and clear process, so the stepwise maximum likelihood estimation method is used to estimate the parameters in the model [40]. From the aforementioned degradation model, it can be seen that the parameters to be estimated are two performance indicators corresponding to the parameters $\Theta = (\mu_a, \delta_a, \delta_B, b)$ in the degradation model and α in the Copula function, respectively. It can be inferred that all parameters to be estimated can be divided into two parts for stepwise estimation. The first part consists of the drift coefficient a and the diffusion coefficient $\delta_B$within the degradation model. The second part comprises the parameter αwithin the Copula function. $\Theta = (\mu_a, \delta_a, \delta_B, b)$ can be estimated by utilizing the measured values of their respective performance indicators combined with the maximum likelihood method. Suppose $X_i(t_j)$represents the performance degradation value measured by equipment i at time t_j, then the degradation trajectory can be expressed as follows:

$$X_i(t_j) = a_i\phi(t_j, b) + \delta_B B(t_j) \tag{23}$$

where $1 < i \le n, 1 < j \le m$, let $X_i = (X_i(t_1), X_i(t_2), \cdots, X_i(t_m))'$, $X = (X_1', X_2', \cdots, X_n')'$, and $t = (t_1, t_2, \cdots, t_m)'$. X_i follows a multivariate normal distribution, with its mean and variance being:

$$\mu_0 = \mu_a t, \Sigma = \delta_a^2 tt' + \Omega \tag{24}$$

with

$$\Omega = \delta_B^2 Q \tag{25}$$

$$Q = \begin{bmatrix} t_1 & t_1 & t_1 & \cdots & t_1 \\ t_1 & t_2 & t_2 & \cdots & t_2 \\ t_1 & t_2 & t_3 & \cdots & t_3 \\ \vdots & \vdots & \vdots & \ddots & \vdots \\ t_1 & t_2 & t_3 & \cdots & t_m \end{bmatrix} \tag{26}$$

Estimation of the unknown parameters $(\mu_a, \delta_a, \delta_B, b)$ in the degradation model using the maximum likelihood method, based on the assumption of independence between degradation measurements of different equipment, the log-likelihood function is:

$$l(Y) = -\frac{mn\,ln(2\pi)}{2} - \frac{n}{2} ln|\Sigma| - \frac{1}{2}\sum_{i=1}^{n}(X_i - \mu_a t)'\Sigma^{-1}(X_i - \mu_a t) \tag{27}$$

with

$$|\Sigma| = |\Omega|(1 + \delta_a^2 t'\Omega^{-1}t), \Sigma^{-1} = \Omega^{-1} - \frac{\delta_a^2}{1+\delta_a^2 t'\Omega^{-1}t}\Omega^{-1}tt'\Omega^{-1} \tag{28}$$

Taking the first-order partial derivatives of the above equation with respect to μ_a and δ_a respectively, and setting them equal to zero, we can obtain:

$$\hat{\mu_a} = \frac{\sum_{i=1}^{n} t'\Omega^{-1}X_i}{nt'\Omega^{-1}t} \tag{29}$$

$$\hat{\delta_a^2} = \frac{1}{n(t'\Omega^{-1}t)^2}\sum_{i=1}^{n}\left(X_i - \hat{\mu_a} t\right)'\Omega^{-1}tt'\left(X_i - \hat{\mu_a} t\right) - \frac{1}{t'\Omega^{-1}t} \tag{30}$$

Substituting Eqs. (29) and (30) into Eq. (27), we get:

$$l(b, \delta_B) = -\frac{mn\,ln(2\pi)}{2} - \frac{n}{2} - \frac{n}{2} ln|\Omega| - \frac{1}{2}\left[\sum_{i=1}^{n} X_i'\Omega X_i - \frac{\sum_{i=1}^{n}(t'\Omega^{-1}X_i)^2}{t'\Omega^{-1}t}\right] - \frac{n}{2} ln\left[\frac{\sum_{i=1}^{n}(t'\Omega^{-1}X_i)^2}{nt'\Omega^{-1}t} - \frac{\sum_{i=1}^{n}(t'\Omega^{-1}X_i)^2}{n^2 t'\Omega^{-1}t}\right] \tag{31}$$

By maximizing Eq. (31), we can obtain estimates for δ_B and b, and then substituting them into Eqs. (29) and (30) allows us to compute estimates for μ_a and δ_a .To estimate the parameters α in the Copula function, assuming there are N equipment, each undergoing M measurements. Let $X_{ki}(t_{ij})$represent the measurement of the i-th equipment at time t_{ij}, where $i = 1,2, \cdots N$, $j = 1,2, \cdots M$,and $k = 1,2$ .Then the experimental data for the k-th performance degradation value can be represented as:

$$X_k(t) = \begin{bmatrix} X_{k1}(t_{11}) & X_{k1}(t_{12}) & \cdots & X_{k1}(t_{1M}) \\ X_{k2}(t_{21}) & X_{k2}(t_{22}) & \cdots & X_{k2}(t_{2M}) \\ \vdots & \vdots & \vdots & \vdots \\ X_{kN}(t_{N1}) & X_{kN}(t_{N2}) & \cdots & X_{kN}(t_{NM}) \end{bmatrix} \tag{32}$$

The increment of the k-th performance degradation value of the i-th equipment in the time interval $[t_{ij-1}, t_{ij}]$ is $\Delta X_{ki} = X_{ki}(t_{ij}) - X_{ki}(t_{ij-1})$. $\Delta\phi_k(t_{ij}) = \Delta\phi_k(t_{ij}) - \Delta\phi_k(t_{ij-1})$, $\Delta t_{ij} = \Delta t_{ij} - \Delta t_{ij-1}$, $\Delta x_{ki} = x_{ki}(t_{ij}) - x_{ki}(t_{ij-1})$. By the nature of the Wiener process, it follows that $\Delta X_{ki} \sim N(a_k\Delta\phi_k(t_{ij}), \delta_{Bk}^2\Delta t_{ij})$.Therefore, the PDF of the increment of the performance degradation value ΔX_{ki} is:

$$f(\Delta x_{ki}|a_k) = \frac{1}{\sqrt{2\pi\delta_{Bk}^2\Delta t_{ij}}} exp\left(-\frac{\left(\Delta x_{ki} - a_k\Delta\phi_k(t_{ij})\right)^2}{2\delta_{Bk}^2\Delta t_{ij}}\right) \tag{33}$$

When $a_k$is a random variable and follows$a_k \sim N(\mu_{ak}, \delta_{ak}^2)$, its corresponding PDF is

$$f(a_k) = \frac{1}{\sqrt{2\pi\delta_{ak}^2}} exp\left(-\frac{(a_k - \mu_{ak})^2}{2\delta_{ak}^2}\right) \tag{34}$$

Using the law of total probability for continuous random variables, we can get:

$$f(\Delta x_{ki}) = \int_{-\infty}^{+\infty} f(\Delta x_{ki}|a_k)\, f(a_k) da_k = \frac{1}{\sqrt{\delta_{Bk}^2 \Delta t_{ij} + \delta_{ak}^2 \Delta \phi_k^2(t_{ij})}} exp\left(- \frac{\left(\Delta x_{ki} - \mu_k \Delta \phi_k(t_{ij})\right)^2}{2\left(\delta_{Bk}^2 \Delta t_{ij} + \delta_{ak}^2 \Delta \phi_k^2(t_{ij})\right)} \right) \quad (35)$$

Meanwhile, the PDF of the degradation increment value ΔX_{ki} can be represented by its cumulative distribution function

$$F(\Delta x_{ki}) = \Phi\left(\frac{\Delta x_{ki} - \mu_{ak} \Delta t_{ij}}{\delta_{Bk}^2 \Delta t_{ij} + \delta_{ak}^2 \Delta \phi_k^2(t_{ij})} \right) \quad (36)$$

When considering two performance degradation characteristics of the equipment, according to Sklar's theorem, there exists a Copula function $C(.)$ such that:

$$H(\Delta X_{1i}, \Delta X_{2i}) = C\big(F(\Delta x_{1i}), F(\Delta x_{2i})\big) \quad (37)$$

Thus, the maximum likelihood function of the performance degradation data can be obtained as:

$$L(\alpha) = \Pi_{i=1}^{N} \quad \Pi_{j=1}^{M} \quad c\big(F(\Delta x_{1i}), F(\Delta x_{2i})\big)\, \Pi_{k=1}^{2} \quad f(\Delta x_k) =$$

$$\Pi_{i=1}^{N} \quad \Pi_{j=1}^{M} \quad c\left(\Phi\left(\frac{\Delta x_{1i} - \mu_{a1} \Delta t_{ij}}{\delta_{B1}^2 \Delta t_{ij} + \delta_{a1}^2 \Delta \phi_1^2(t_{ij})} \right), \Phi\left(\frac{\Delta x_{2i} - \mu_{a2} \Delta t_{ij}}{\delta_{B2}^2 \Delta t_{ij} + \delta_{a2}^2 \Delta \phi_2^2(t_{ij})} \right) \right) - \Pi_{k=1}^{2} \quad \frac{1}{\sqrt{\delta_{Bk}^2 \Delta t_{ij} + \delta_{ak}^2 \Delta \phi_k^2(t_{ij})}} exp\left(- \frac{\left(\Delta x_{ki} - \mu_k \Delta \phi_k(t_{ij})\right)^2}{2\left(\delta_{Bk}^2 \Delta t_{ij} + \delta_{ak}^2 \Delta \phi_k^2(t_{ij})\right)} \right) \quad (38)$$

Taking the logarithm of Eq. (38) on both sides yields:

$$log\big(L(\alpha)\big) = \sum_{i=1}^{N} \sum_{j=1}^{M} log\, c\left(\Phi\left(\frac{\Delta x_{1i} - \mu_{a1} \Delta t_{ij}}{\delta_{B1}^2 \Delta t_{ij} + \delta_{a1}^2 \Delta \phi_1^2(t_{ij})} \right), \Phi\left(\frac{\Delta x_{2i} - \mu_{a2} \Delta t_{ij}}{\delta_{B2}^2 \Delta t_{ij} + \delta_{a2}^2 \Delta \phi_2^2(t_{ij})} \right) \right) - \frac{1}{2} \sum_{i=1}^{N} \sum_{j=1}^{M} \sum_{k=1}^{2} log\left(\delta_{Bk}^2 \Delta t_{ij} + \delta_{ak}^2 \Delta \phi_k^2(t_{ij}) \right) - \sum_{i=1}^{N} \sum_{j=1}^{M} \sum_{k=1}^{2} log\left(\frac{\left(\Delta x_{ki} - \mu_k \Delta \phi_k(t_{ij})\right)^2}{2\left(\delta_{Bk}^2 \Delta t_{ij} + \delta_{ak}^2 \Delta \phi_k^2(t_{ij})\right)} \right) \quad (39)$$

The unknown parameter α in the model is estimated by maximizing Eq. (39). In this paper, the "Fminsearch" function in Matlab, which is a multidimensional search method, is used to achieve this.

5. Simulation experiment study

This section will validate the practicality and effectiveness of the proposed method using simulated data, real LED lighting system data, and crack degradation data from metal equipment. Since different Copula functions used in modeling will yield different prediction results, selecting a Copula function with good goodness of fit is crucial based on practical scenarios. This paper employs the Akaike Information Criterion (AIC), a widely applicable standard for measuring the goodness of fit of statistical models, for Copula function selection. Thus, the AIC can be used to choose an appropriate Copula function [41].

$$AIC = -2\, ln\, L + 2m \quad (40)$$

where $ln\, L$ is the logarithmic maximum likelihood function value corresponding to the model, m is the number of parameters in the model. A smaller AIC value indicates a better fit, meaning that the Copula function with the lowest AIC value is considered the best choice.

In order to more intuitively demonstrate the predictive performance of the degradation model, the total mean square error (TMSE), root mean square error (RMSE) and mean absolute error (MAE) are further calculated for different degradation models using different prediction methods [26]. The TMSE can be calculated from the mean square error.

$$MSE_k = \int_0^{\infty} \big(l_k - \tilde{l_k}\big)^2 f_{L_k|X_{1:k}}(L_k|X_{1:k}) dl_k \quad (41)$$

where l_k and $\tilde{l_k}$ represent the actual and predicted RUL of the equipment at time t_k, respectively. $f_{L_k|X_{1:k}}(L_k|X_{1:k})$ represents the PDF of RUL of the equipment . From this, we can calculate the TMSE.

$$TMSE = \frac{\sum_{k=1}^{n} MSE_k}{n} \quad (42)$$

where n is the total number of predicted points. N represents the total number of experimental samples. TMSE is widely used in the field of degradation modeling to evaluate the fitting accuracy of models. The minimum TMSE value corresponds to the best fitting accuracy and is therefore commonly used as a criterion for model selection [42]. RMSE is one of the common metrics used to assess the accuracy of predictive models. It measures the degree of deviation between the predicted value and the true value, and is calculated as the square root of the sum of the squares of the differences between the predicted value and the true value. The smaller the value of RMSE is, the smaller the prediction error of the model is, and the better the predictive ability of the model, which is calculated as follows:

$$RMSE = \sqrt{\frac{1}{n}\sum_{k=1}^{n}\left(l_k - \tilde{l_k}\right)^2} \quad (43)$$

MAE is a metric used to assess the accuracy of prediction models. It is the average of the absolute differences between predicted values and actual values. The specific calculation formula is:

$$MAE = \frac{1}{n}\sum_{k=1}^{n}\left|l_k - \tilde{l_k}\right| \quad (44)$$

The smaller the MAE, the closer the predicted values are to the true values, indicating higher predictive accuracy of the model.

5.1. Simulation experiment data

To verify the RUL prediction effectiveness of the method proposed in this paper, we discretized model M_1 and simulated 30 sets of degradation data. We assumed the parameters in the degradation model to be $\mu_a = 0.1$, $\delta_a = 0.01$, and $\delta_b = 0.5$ .Each sample is observed 24 times, with observation intervals of 5 hours. The simulation data are shown in Fig.2. To illustrate that the equipment has two performance degradation characteristics, we divide the simulated degradation data into two groups, each representing one type of performance degradation data for the equipment.

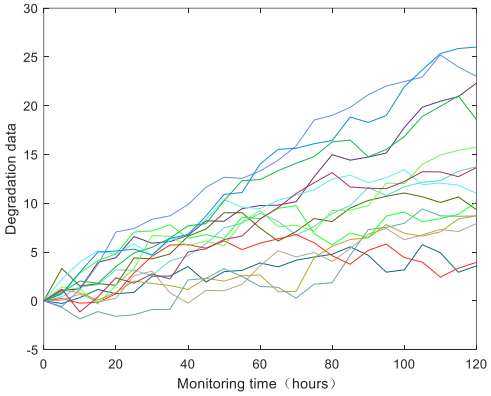

(a) Degradation data of performance I

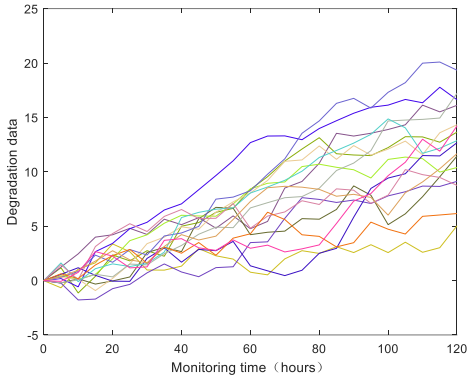

(b) Degradation data of performance II

Fig. 2. Simulation degradation data of M_1.

To compare the differences in RUL prediction between single-performance and dual-performance degradation data, this study also simulates and analyzes RUL prediction results using two single-performance degradation datasets, designated as Method I and Method II, respectively. The dual-performance degradation models constructed using a single Frank Copula function, Clayton Copula function, and Gumbel Copula function are labeled as Method III, Method IV, and Method V, respectively. For the mixed Copula function approaches:

The model integrating Frank Copula function and Clayton Copula function is denoted as Method VI;

The model combining Frank Copula function and Gumbel Copula function is designated as Method VII;

The model merging Clayton Copula function and Gumbel Copula function is labeled as Method VIII;

The mixed model incorporating Frank Copula function, Clayton Copula function, and Gumbel Copula function is identified as Method IX.

By applying the degradation data to the aforementioned methods, the unknown parameters in each model are estimated using a two-step maximum likelihood estimation method, with results summarized in Table 2.

Table 2. Parameter estimates for different Copula functions

Copula	α	k_1	k_2	k_3	ln$L$	AIC
Frank	0.0001	1	-	-	-814.8203	1631.6410
Clayton	1.0500e-05	-	1	-	-814.8206	1631.6412
Gumbel	1.09895	-	-	1	-814.8330	1631.6660
k_1Frank+ k_2Clayton	5.0000e-11	0.0200	0.9800	-	-20.4287	46.8574
k_1Frank+ k_3Gumbel	1.0000	3.9098e-04	-	0.9996	-493.1649	992.3298
k_2Clayton+ k_3Gumbel	1.0000	-	2.1441e-16	1.0000	-783.9734	1573.9468
k_1Frank+ k_2Clayton+ k_3Gumbel	1.0000	8.9873e-05	0.0018	0.9981	-784.1568	1576.3136

Based on Table 2, it can be observed that the parameter values estimated using different Copula functions vary significantly. The log-likelihood values obtained from using a single Copula function are all lower than those derived from any mixed Copula function. Furthermore, the AIC values estimated with a single Copula function are greater than those estimated using any mixed Copula function. Therefore, the mixed Copula function model should be prioritized for predicting the RUL of equipment. The estimated parameters are substituted into their corresponding remaining useful life PDFs, and the resulting curves are plotted as shown below.

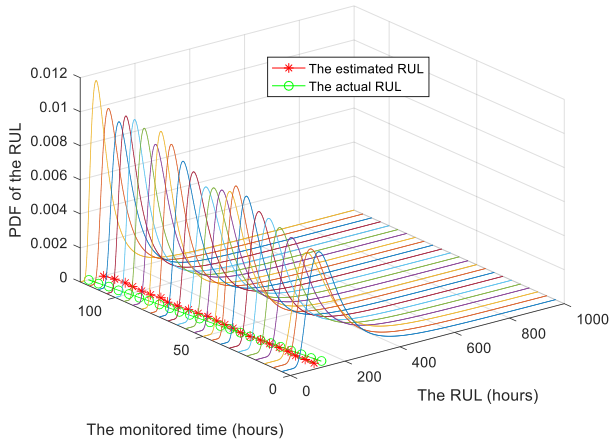

(a) PDF curves of RUL predicted by method I

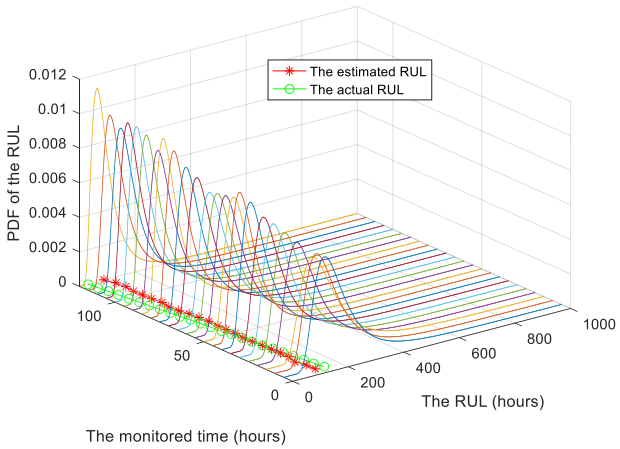

(b) PDF curves of RUL predicted by method II

Fig.3. PDF curves of RUL predicted by the single performance degradation data.

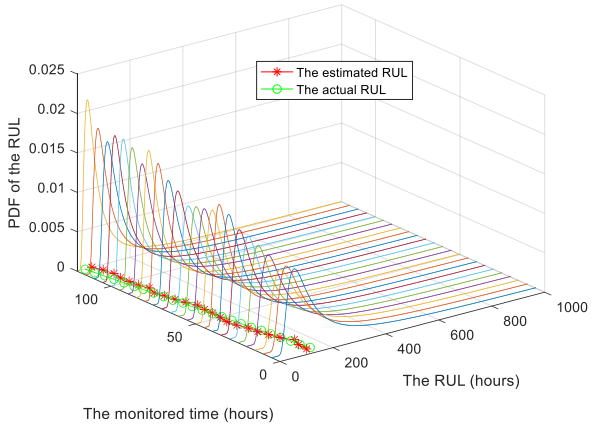

(a) PDF curves of RUL predicted by method III

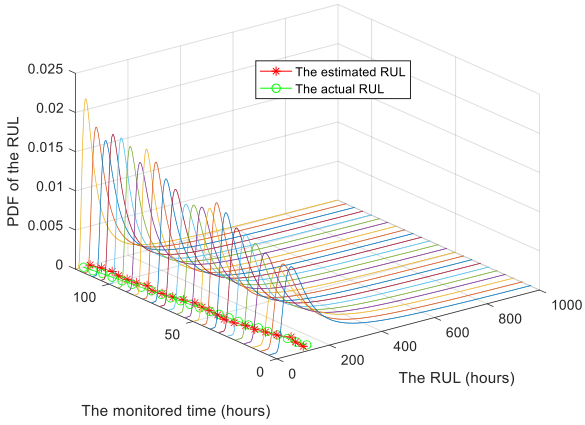

(b) PDF curves of RUL predicted by method IV

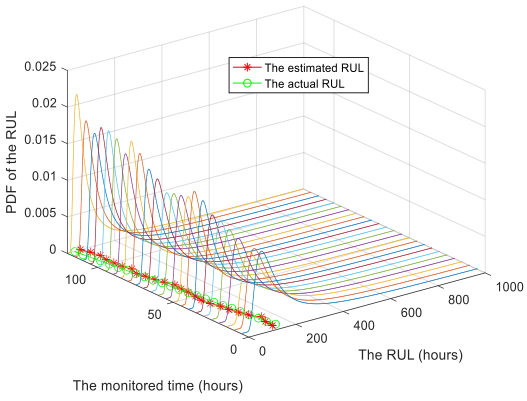

(c) PDF curves of RUL predicted by method V

Fig. 4. PDF curves of RUL predicted by single Copula functions.

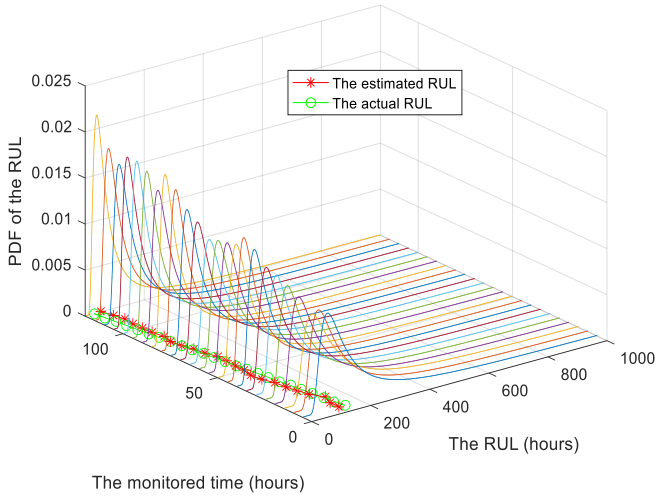

(a) PDF curves of RUL predicted by method VI

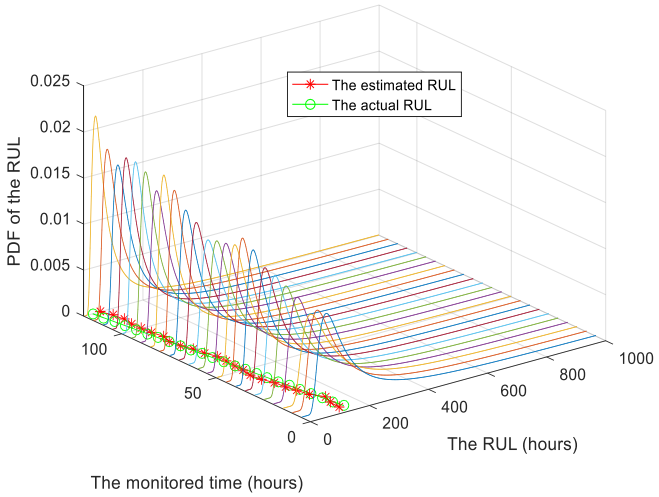

(b) PDF curves of RUL predicted by method VII

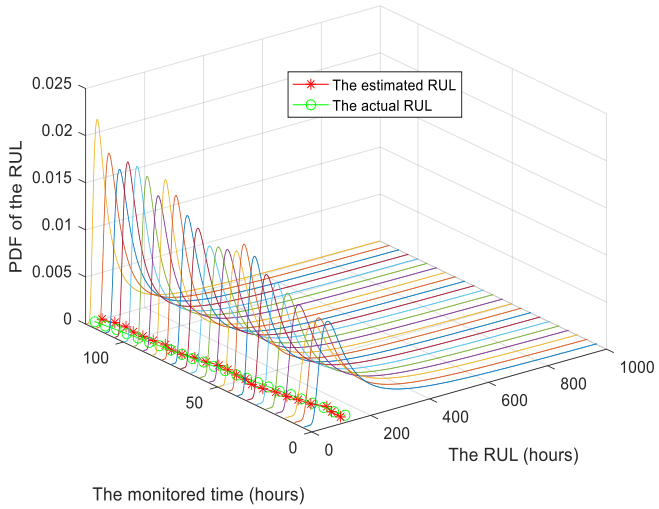

(c) PDF curves of RUL predicted by method VIII

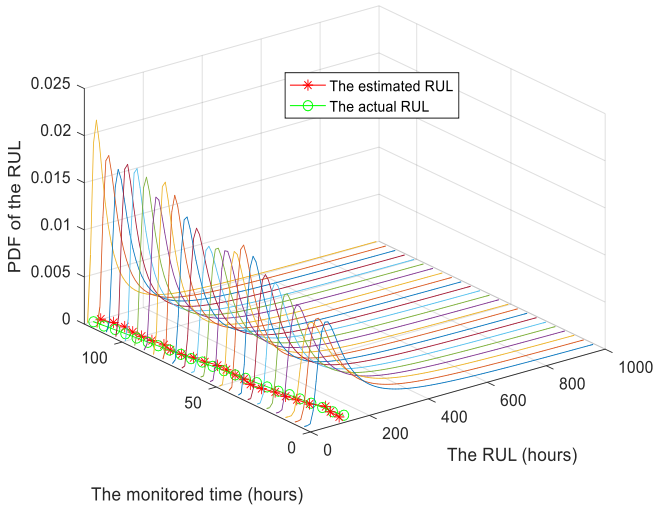

(d) PDF curves of RUL predicted by method IX

Fig.5. PDF curves of RUL predicted by mixed Copula functions.

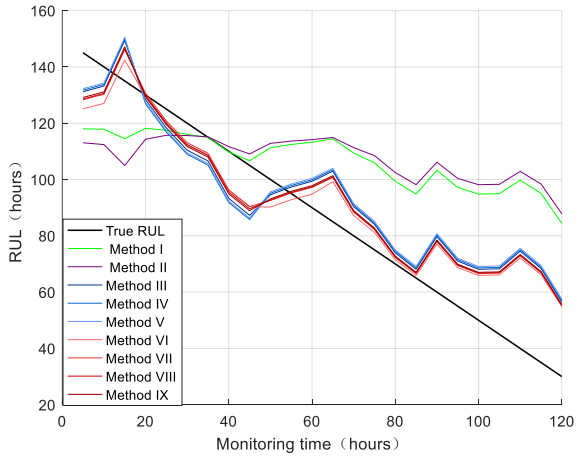

Fig.6. RUL curves predicted by different methods.

As illustrated in Figs. 3, 4, and 5, the RUL of the equipment can be predicted using single performance degradation data, two performance degradation data based on a single Copula function, or a mixed Copula function, yet the outcomes vary distinctly, the PDF curves of RUL predicted by single Copula functions and mixed Copula functions (with two performance degradation datasets) are notably higher and sharper than those from single degradation data, reflecting reduced prediction uncertainty due to more comprehensive utilization of degradation information for enhanced accuracy. While the PDF curves from single and mixed Copula functions appear visually similar, their key divergence lies in the error between predicted and actual RUL. As can be seen from Fig. 6, compared to RUL prediction methods using single performance degradation data or a single Copula function, the hybrid Copula function-based method proposed in this paper yields predicted RUL values closer to the actual values. To quantitatively evaluate prediction errors, this study calculates TMSE, RMSE, and MAE values, as detailed in Table 3.

Table 3. Errors of different prediction methods.

Method	TMSE	RMSE	MAE
Performance I (I)	8.2360e+03	1.0651e+03	27.0926
Performance II (II)	8.7205e+03	1.2485e+03	29.9124
Frank (III)	4.4263e+03	279.3134	14.2076
Clayton (IV)	4.4289e+03	279.5082	14.2091
Gumbel (V)	4.4290e+03	279.5096	14.2092
k_1Frank+ k_2Clayton (VI)	2.7058e+03	264.8426	13.8784
k_1Frank+ k_3Gumbel (VII)	3.6891e+03	267.5347	13.9660
k_2Clayton+ k_3Gumbel (VIII)	4.0515e+03	268.2546	13.9884
k_1Frank+k_2Clayton+k_3Gumbel (IX)	4.1632e+03	269.9203	14.0330

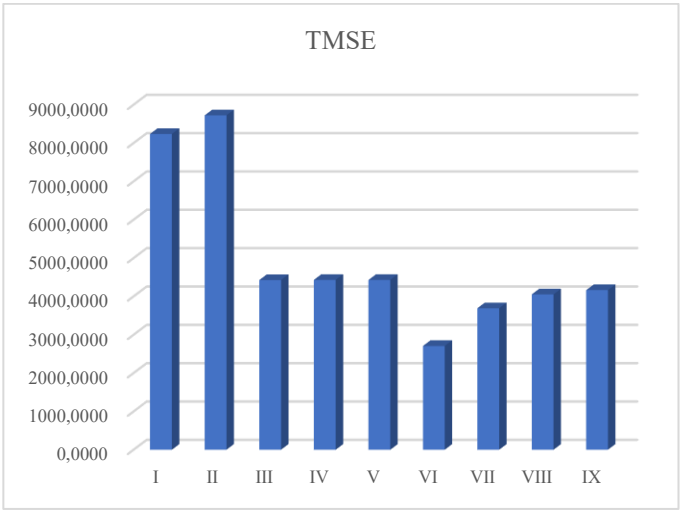

(a) TMSE values for different methods

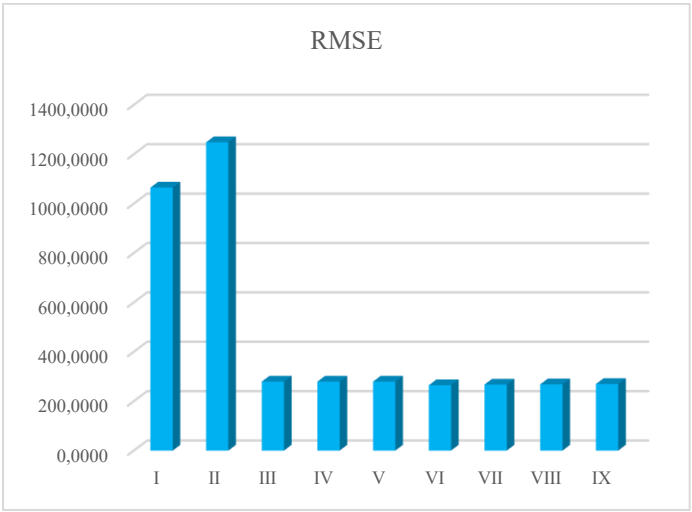

(b) RMSE values for different methods

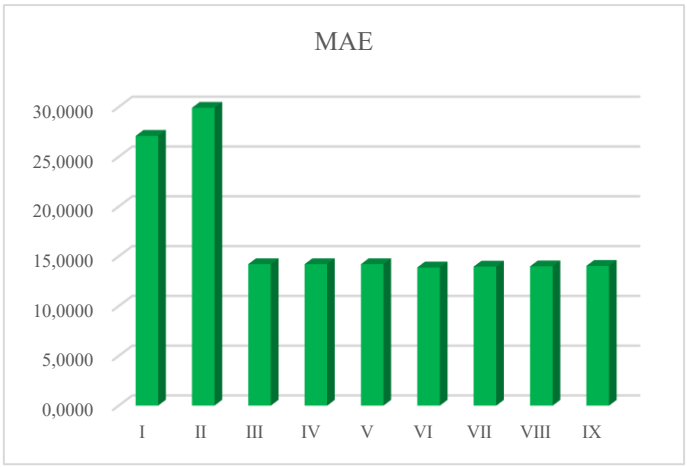

(c) MAE values for different methods

Fig. 7. Comparison of prediction errors across different methods.

From Table 3 and Fig.7, it can be seen that the prediction errors vary according to the method used. The RUL prediction errors based on the two performance degradation data using single Copula and mixed Copula functions are smaller than those based on single performance degradation data, and the RUL prediction errors based on the mixed Copula functions are lower than those based on the single Copula functions. Among the nine RUL prediction methods, predictions based on the mixed Copula function combines Frank Copula and Clayton Copula yield the smallest TMSE, RMSE, and MAE values, indicating that this method is particularly suitable for the degradation data, resulting in minimal prediction errors and the most accurate outcomes. This method can be selected based on the AIC value. Additionally, Table 3 shows that the TMSE,

RMSE, and MAE values predicted by the mixed Copula function of Frank Copula, Clayton Copula, and Gumbel Copula are greater than those predicted by any other two mixed Copula functions, suggesting that having a larger variety of mixed Copula functions in practical applications does not necessarily lead to better results, but rather that specific selections should be made based on requirements.

After discretizing model M_2, 30 sets of degradation data are generated through simulation. Assuming that the parameters in the degraded model are $\mu_a = 0.1, \delta_a = 0.01, \delta_b = 0.05$, and $b = 0.02$, respectively. Each sample is observed 24 times with a time interval of 5 hours, the simulation data are shown in Fig. 7. In order to illustrate that the equipment has two performance degradation characteristics, the simulated degradation data are divided into two groups, which represent the two performance degradation data of the equipment.

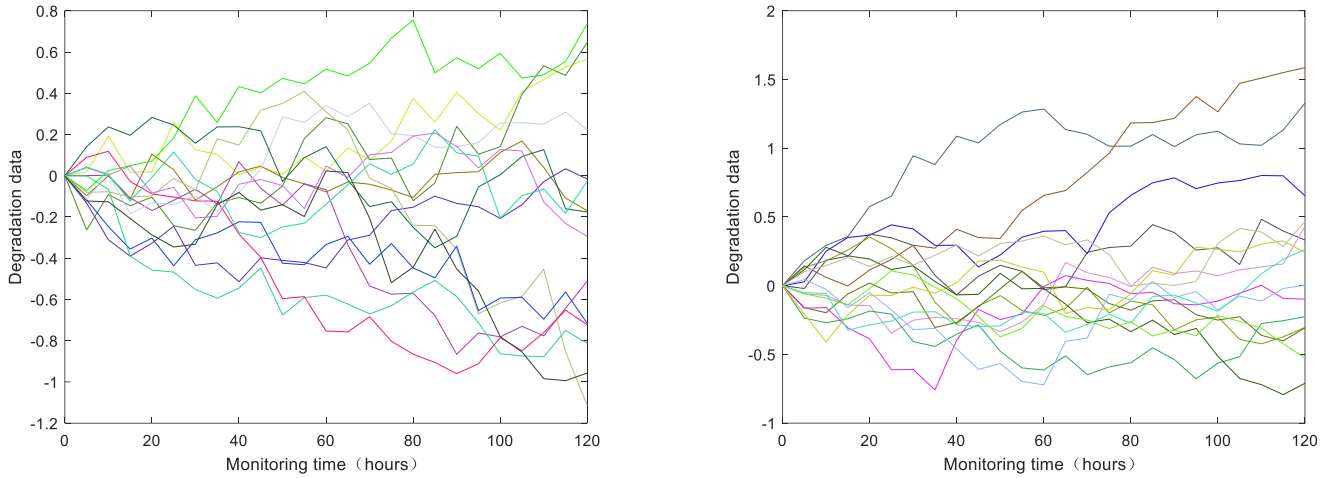

(a) Degradation data of performance I (b) Degradation data of performance II

Fig. 8. Simulation degradation data of M_2

The parameters in the degradation model are estimated by substituting the above two performance degradation data into different methods using the stepwise maximum likelihood method, as shown in Table 4.

Table 4. Parameter estimates for different Copula functions.

Copula	α	k_1	k_2	k_3	ln$L$	AIC
Frank	1.6653e-16	1	-	-	243.6016	-485.2032
Clayton	1.0996e-15	-	1	-	240.7715	-479.5430
Gumbel	1.9975	-	-	1	227.7007	-453.4014
k_1Frank+ k_2Clayton	1.7764e-15	0.9984	0.0016	-	252.8338	-499.6676
k_1Frank+ k_3Gumbel	1.0000	0.9424	-	0.0576	256.7494	-507.4988
k_2Clayton+ k_3Gumbel	1.0000	-	0.9424	0.0576	264.0263	-522.0526
k_1Frank+ k_2Clayton+ k_3Gumbel	1.0000	0.0000	0.8824	0.1176	261.3849	-514.7698

From Table 4, it can be observed that the log-likelihood values estimated using single Copula functions are lower than those estimated by any mixed Copula function. Furthermore, the AIC and BIC values estimated by the single Copula function are consistently higher than those for mixed Copula functions. Therefore, mixed Copula function models should be prioritized for predicting the RUL of the equipment. The estimated parameters are substituted into the corresponding PDFs of RUL for different methods, and the resulting graphs are shown below.

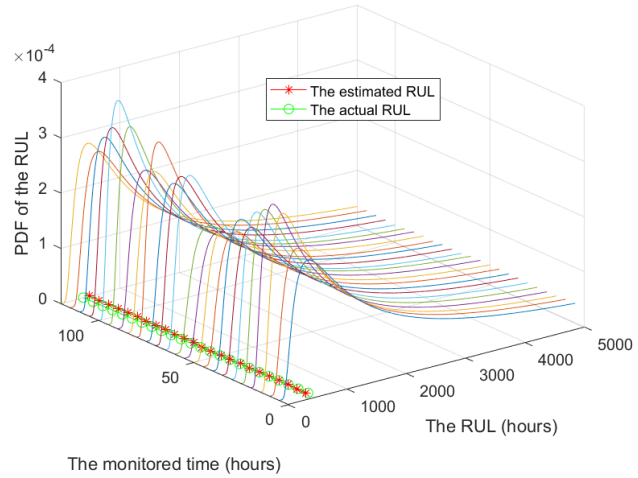

(a) PDF curves of RUL predicted by performance I

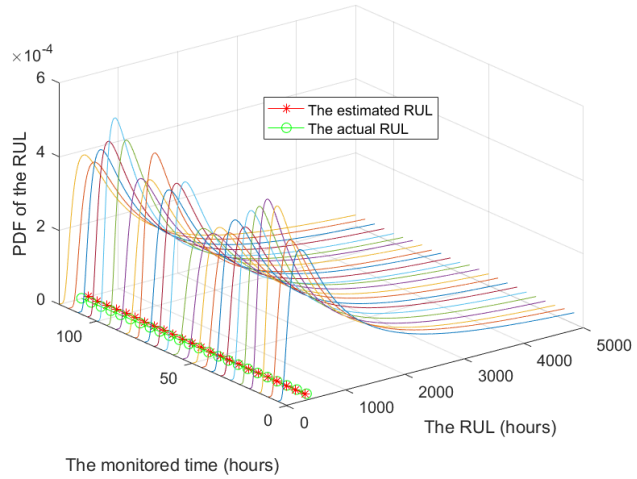

(b) PDF curves of RUL predicted by performance II

Fig.9. PDF curves of RUL predicted by the single performance degradation data.

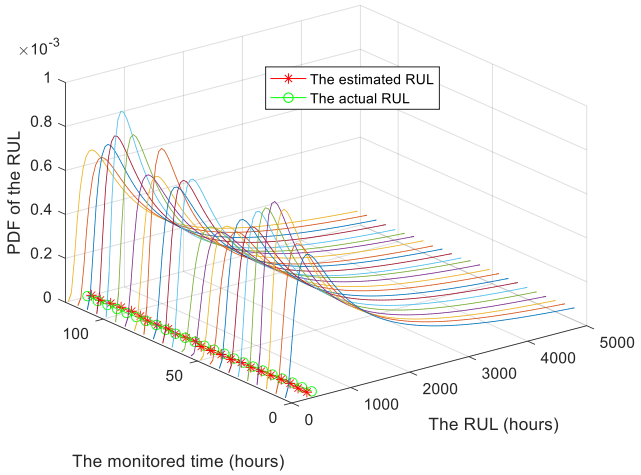

(a) PDF curves of RUL predicted by method III

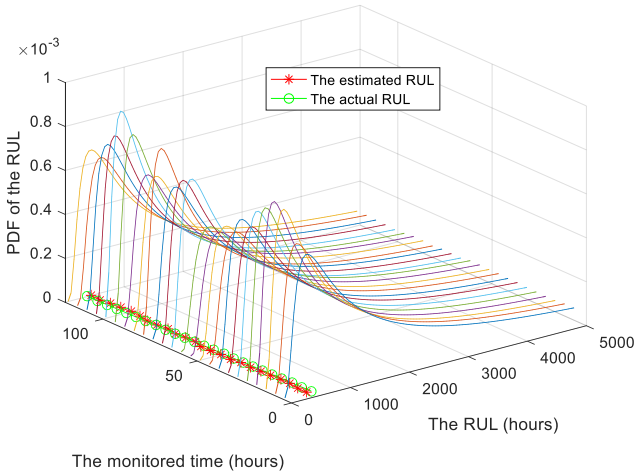

(b) PDF curves of RUL predicted by method IV

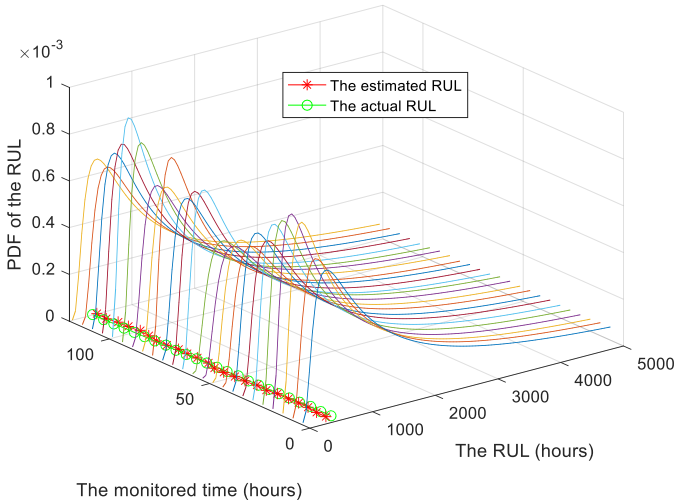

(c) PDF curves of RUL predicted by method V

Fig. 10. PDF curves of RUL predicted by single Copula functions.

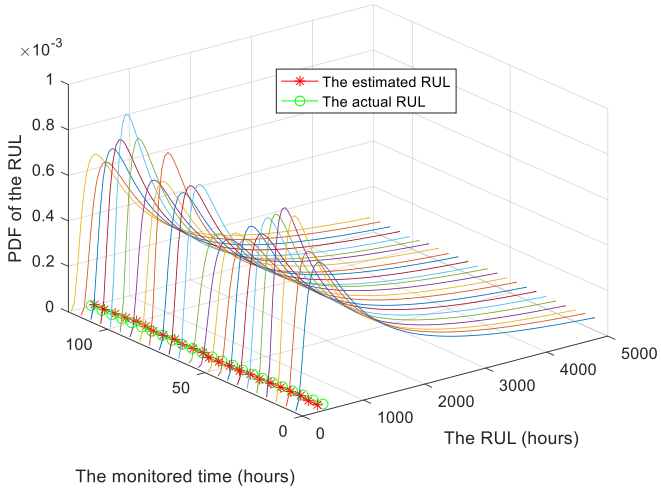

(a) PDF curves of RUL predicted by method VI

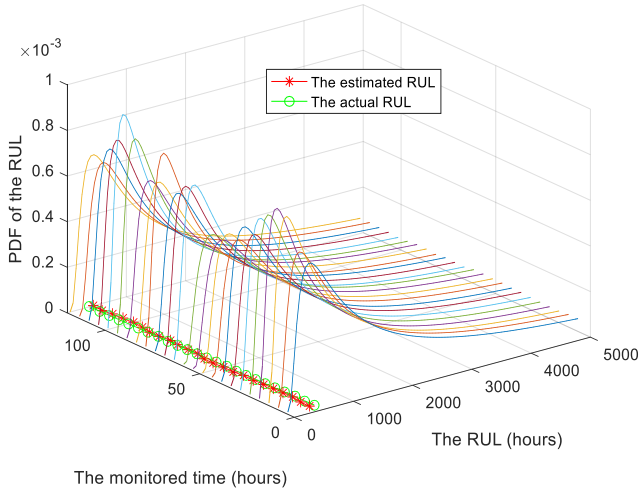

(b) PDF curves of RUL predicted by method VII

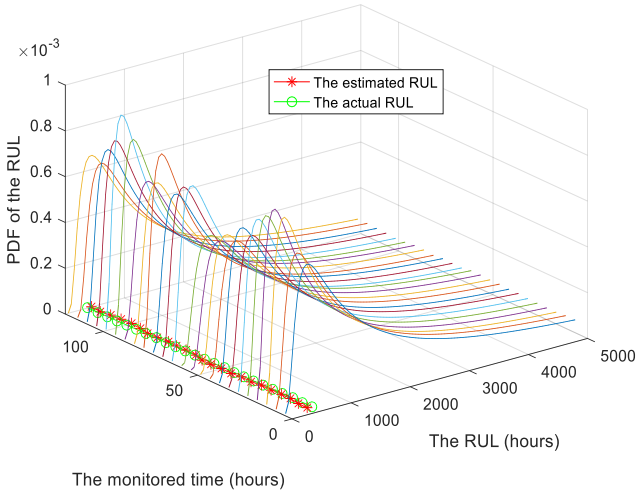

(c) PDF curves of RUL predicted by method VIII

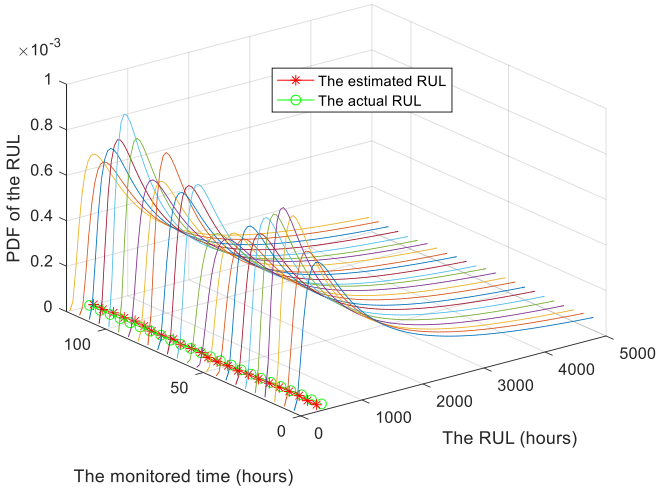

(d) PDF curves of RUL predicted by method IX

Fig.11. PDF curves of RUL predicted by mixed Copula functions.

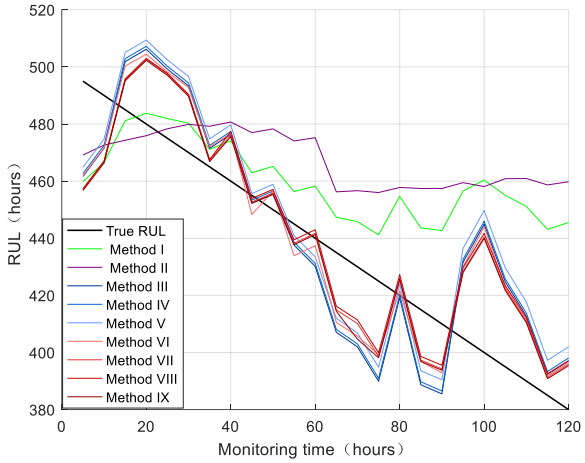

Fig.12. RUL curves predicted by different methods.

From Figs. 9, 10, and 11, it can be seen that both single performance degradation data and the two performance degradation datasets based on single Copula and mixed Copula functions can predict the RUL of equipment. As the number of measurement points increases, the curves of remaining useful life PDFs become higher and sharper, indicating a gradual decrease in prediction uncertainty. Notably, the remaining useful life PDF curves predicted using single Copula and mixed Copula functions are higher and sharper than those predicted using single performance degradation data, suggesting that the predictions made using single Copula and mixed Copula functions exhibit lower uncertainty. The differences between the PDF curves predicted using single Copula and mixed Copula functions remain small, with the main distinction being the varying errors between the predicted and actual RUL. It can be seen from Fig.12 that compared with the RUL prediction methods using single performance degradation data and a single Copula function, the RUL values predicted by the proposed

RUL prediction method based on the hybrid Copula function in this paper are still closer to the actual RUL values. The TMSE, RMSE, and MAE values corresponding to different methods are shown in Table 5.

Table 5. Errors of different prediction methods.

Method	TMSE	RMSE	MAE
Performance I (I)	7.4495e+04	3.6250e+03	47.2338
Performance II (II)	8.0899e+04	3.6528e+03	49.5831
Frank (III)	6.8977e+04	2.3963e+03	44.2321
Clayton (IV)	6.8984e+04	2.3967e+03	44.2350
Gumbel (V)	7.1108e+04	2.4022e+03	44.2827
k_1Frank+ k_2Clayton (VI)	6.8981e+04	2.3803e+03	44.0514
k_1Frank+ k_3Gumbel (VII)	6.8980e+04	2.3601e+03	43.9850
k_2Clayton+ k_3Gumbel (VIII)	6.8976e+04	2.3518e+03	43.9722
k_1Frank+k_2Clayton+k_3Gumbel (IX)	6.8978e+04	2.3557e+03	43.9817

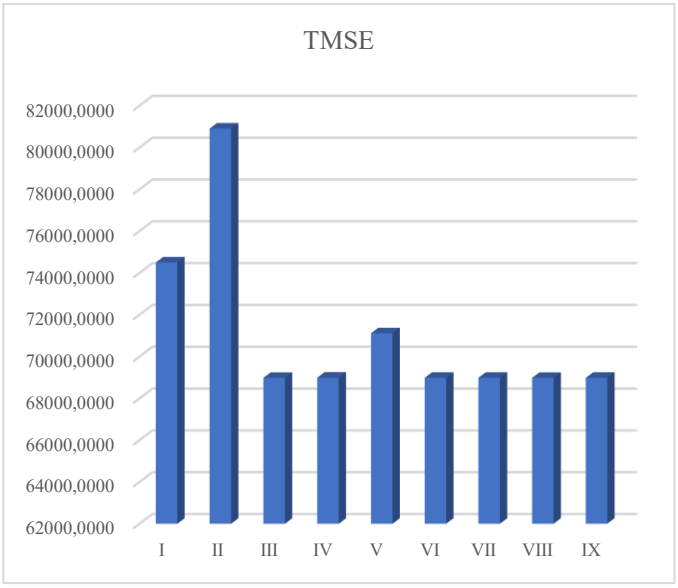

(a) TMSE values for different methods

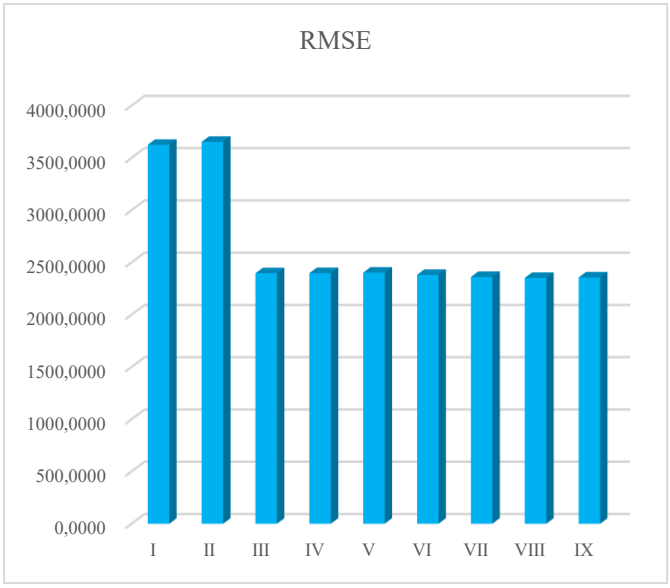

(b) RMSE values for different methods

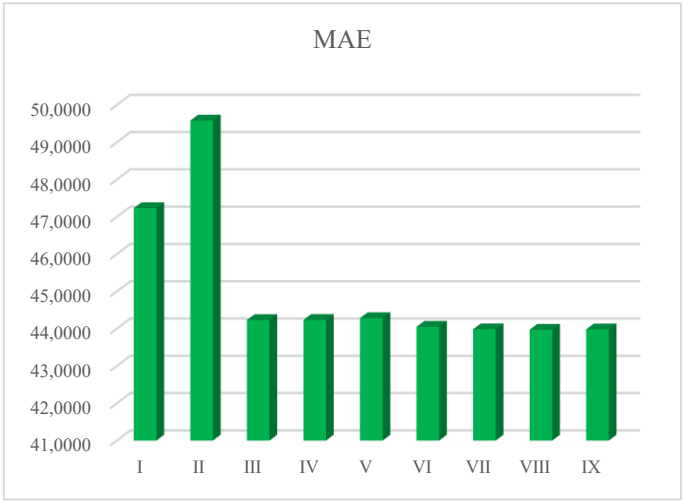

(c) MAE values for different methods

Fig. 13. Comparison of prediction errors across different methods.

From Table 5 and Fig.13, it is evident that the RUL errors predicted based on both single Copula and mixed Copula functions for two performance degradation datasets are lower than those predicted using single performance degradation data. Among these, the TMSE, RMSE, and MAE values predicted using the mixed Copula function are all lower than those

predicted using the single Copula function and single performance degradation data. Among the above nine RUL prediction methods, the method based on the mixed Copula function composed of Clayton Copula and Gumbel Copula has the smallest values of TMSE, RMSE, and MAE, and also has the smallest corresponding AIC value, indicating. its optimal suitability for the analyzed degradation data. The values of TMSE, RMSE, and MAE predicted by the mixed Copula function composed of Frank Copula, Clayton Copula, and Gumbel Copula are larger than those predicted by the mixed Copula function composed of Clayton Copula and Gumbel Copula. This again demonstrates that in practical RUL predictions, having more types of mixed Copula functions is not necessarily better; specific selection is required.

After discretizing model M_3, 30 sets of degradation data are generated through simulation. It is assumed that the parameters in the degradation model are $\mu_a = 1, \delta_a = 20, \delta_b = 1$, and $b = 0.01$. Each sample is observed 24 times, with a time interval of 5 hours, and the simulation data are shown in Fig.14. Similarly, the simulated degradation data are divided into two groups, representing two types of performance degradation data for the equipment.

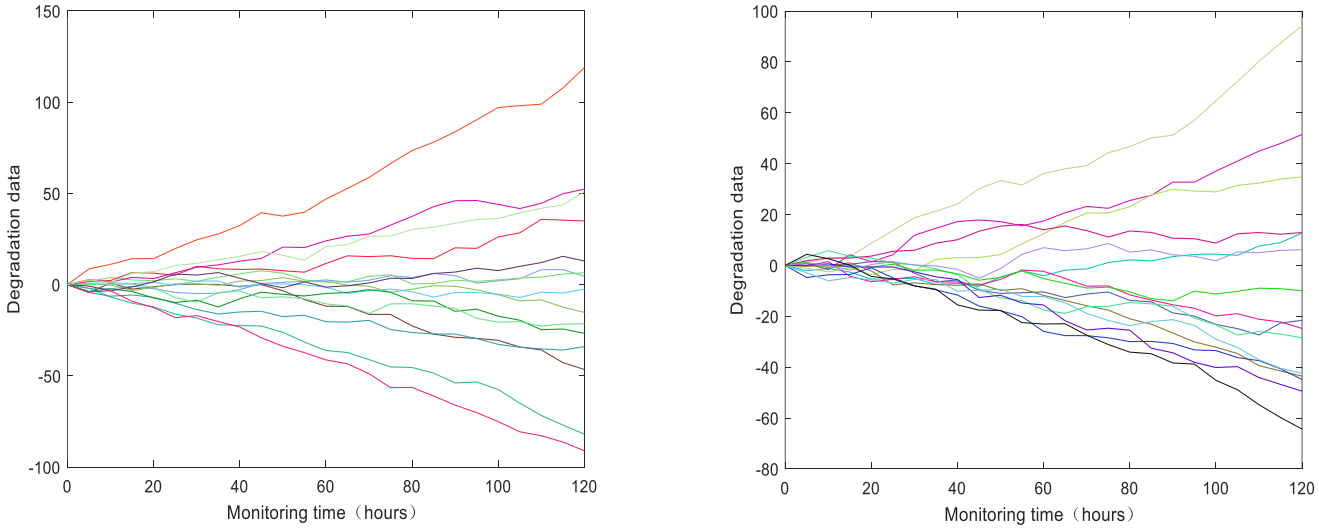

(a) Degradation data of performance I (b) Degradation data of performance II

Fig. 14. Simulation degradation data of M_3

The simulated degradation data for M_3 are substituted into different predictive methods, using the stepwise maximum likelihood method to estimate the parameters in the model, as shown in Table 6.

Table 6. Parameter estimates for different Copula functions.

Copula	α	k_1	k_2	k_3	ln$L$	AIC
Frank	7.7696	1	-	-	-730.5116	1463.0232
Clayton	3.1831	-	1	-	-743.2890	1488.5780
Gumbel	2.6636	-	-	1	-741.9119	1485.8238
k_1Frank+ k_2Clayton	5.0000e-11	0.2000	0.8000	-	-658.8697	1323.7394
k_1Frank+ k_3Gumbel	1.0000	0.1681	-	0.8319	-411.4020	828.8040
k_2Clayton+ k_3Gumbel	2.9716	-	0.3951	0.6049	-684.1968	1374.3936
k_1Frank+k_2Clayton+k_3Gumbel	4.8943	6.5979e-16	0.9999	5.3373e-16	-719.6916	1447.3832

From Table 6, it can be seen that the log-likelihood values estimated by a mixed Copula function are higher than those estimated by a single Copula function. The AIC values for any mixed Copula function are lower than those for any single Copula function. Therefore, the mixed Copula function method is preferred for predicting the RUL of equipment. The estimated parameters are substituted into the corresponding remaining useful life PDFs for different methods, and their graphs are shown below.

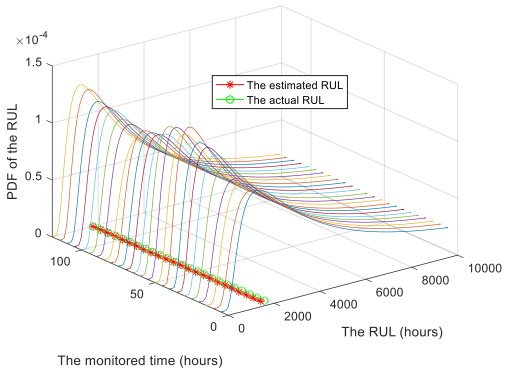

(a) PDF curves for RUL predicted by performance I

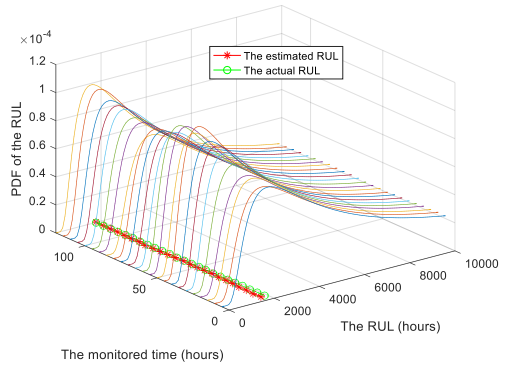

(b) PDF curves of RUL predicted by performance II

Fig.15. PDF curves of RUL predicted by the single performance degradation data.

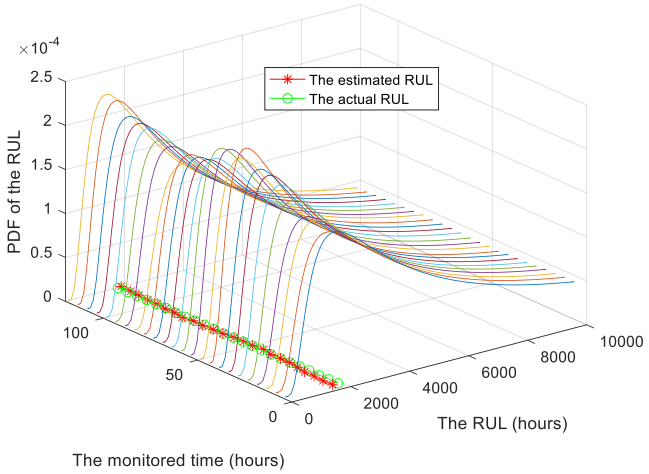

(a) PDF curves of RUL predicted by method III

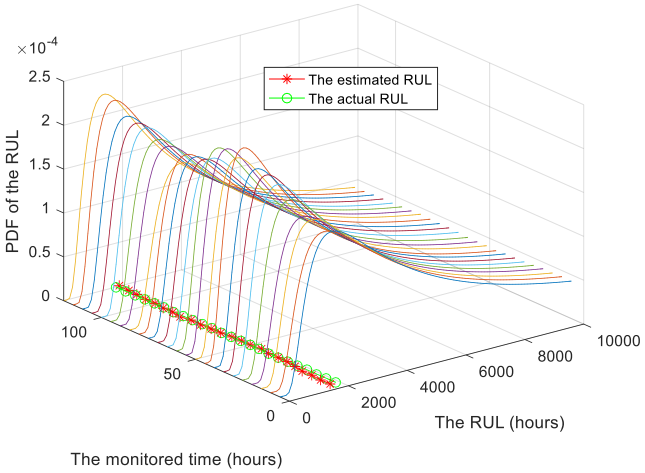

(b) PDF curves of RUL predicted by method IV

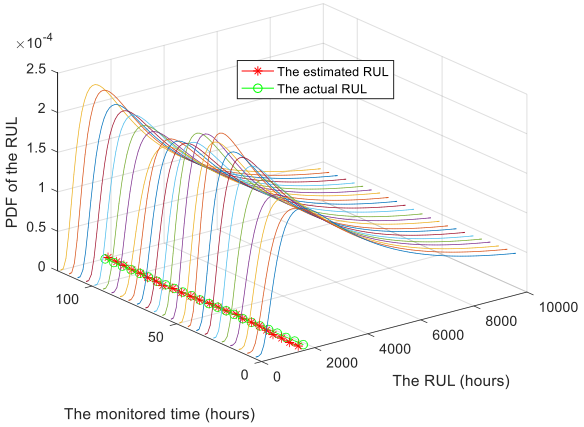

(c) PDF curves of RUL predicted by method V

Fig. 16. PDF curves of RUL predicted by single Copula functions.

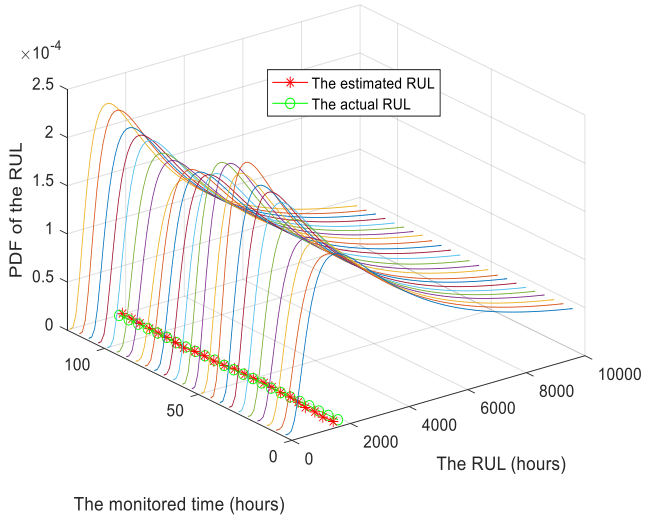

(a) PDF curves of RUL predicted by method VI

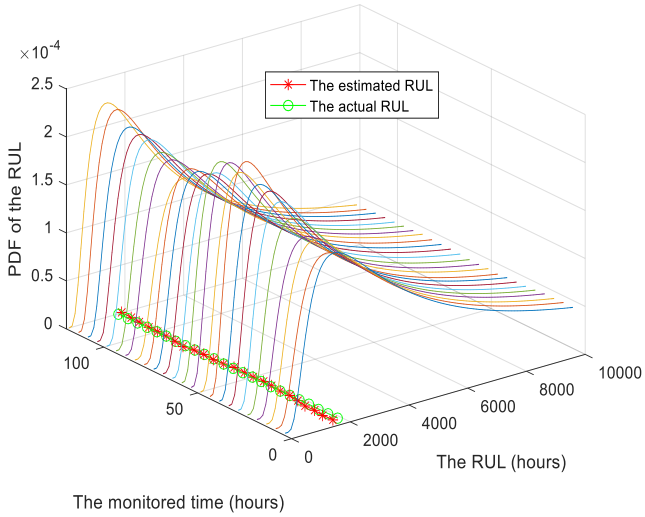

(b) PDF curves of RUL predicted by method VII

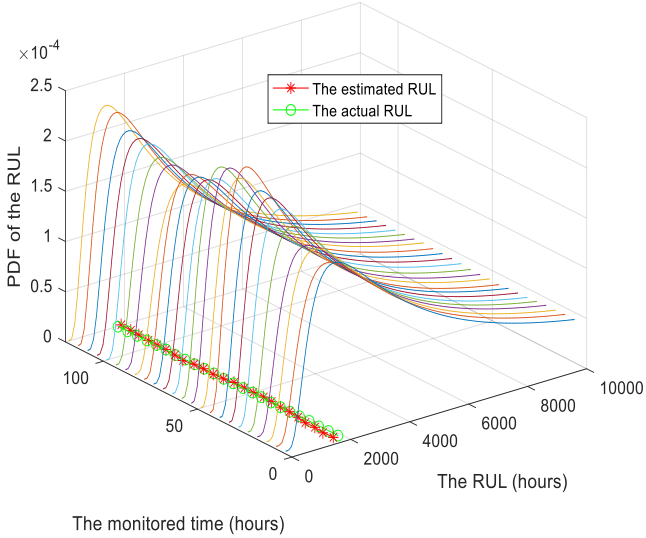

(c) PDF curves of RUL predicted by method VIII

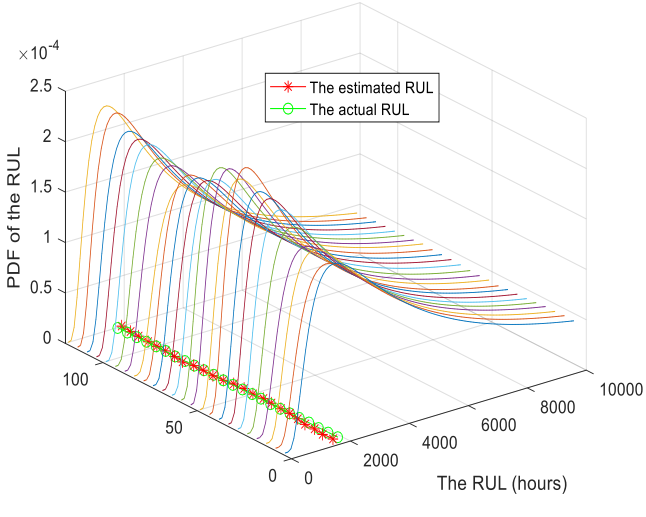

(d) PDF curves of RUL predicted by method IX

Fig.17. PDF curves of RUL predicted by mixed Copula functions.

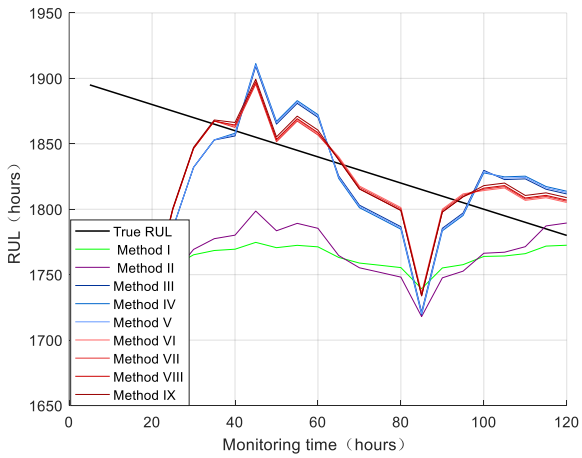

Fig.18. RUL curves predicted by different methods.

From the above graphs, it is evident that the remaining useful life PDF curves based on single Copula and mixed Copula functions for the two performance degradation data are higher and sharper than those based on single performance degradation data, indicating that the predictions made using single Copula and mixed Copula functions have lower uncertainty regarding the RUL. As can be seen from Fig.18, the RUL values predicted by the hybrid Copula function-based method proposed in this paper are closer to the actual values. The TMSE, RMSE, and MAE values predicted by different methods are presented in Table 7

.

Table 7. Errors of different prediction methods.

Method	TMSE	RMSE	MAE
Performance I (I)	9.2496e+04	7.8617e+03	78.1786
Performance II (II)	9.4665e+04	8.8624e+03	79.6017
Frank (III)	7.9411e+04	7.5816e+03	65.1711
Clayton (IV)	8.5164e+04	7.5858e+03	65.1848
Gumbel (V)	8.0594e+04	7.5818e+03	65.1720
k_1Frank+ k_2Clayton (VI)	7.0932e+04	6.9956e+03	63.0637
k_1Frank+ k_3Gumbel (VII)	7.0533e+04	6.9955e+03	63.0635
k_2Clayton+ k_3Gumbel (VIII)	7.1832e+04	6.9991e+03	63.0832
k_1Frank+k_2Clayton+k_3Gumbel (IX)	7.3125e+04	6.9998e+03	63.1159

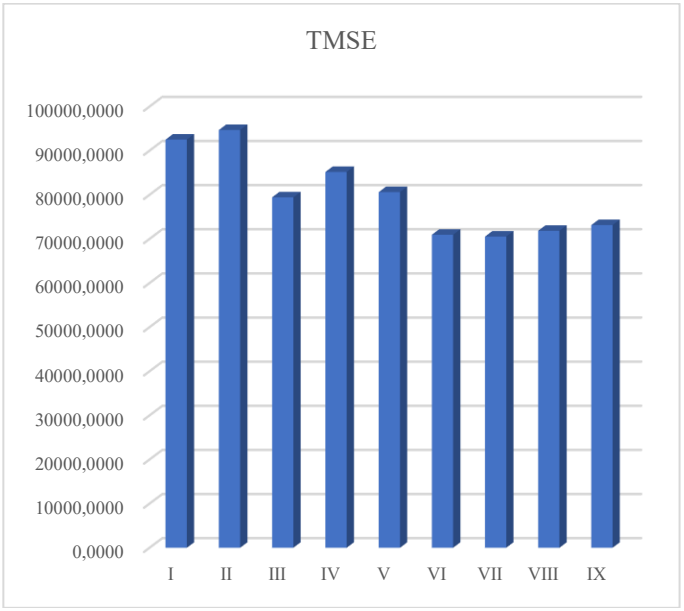

(a) TMSE values for different methods

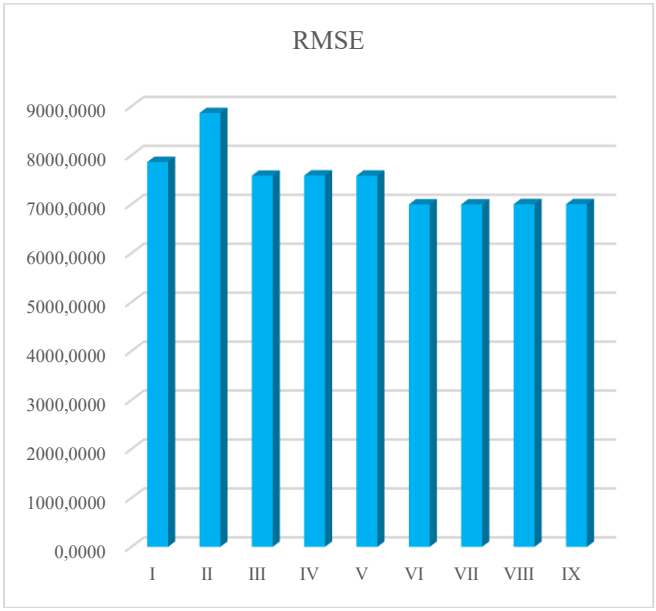

(b) RMSE values for different methods

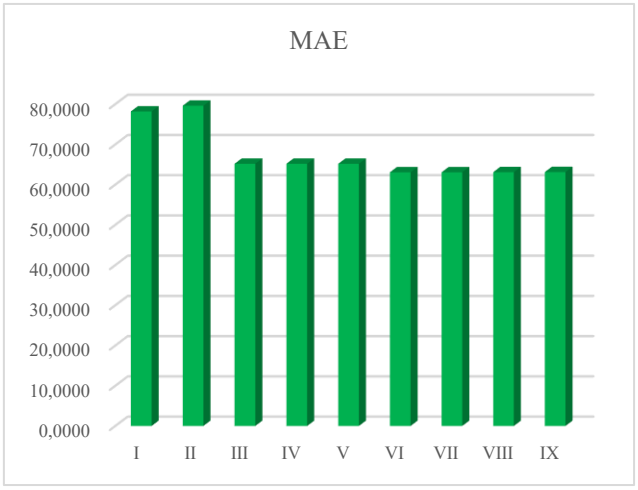

(c) MAE values for different methods

Fig. 19. Comparison of prediction errors across different methods.

From Table 7 and Fig.19, it is observed that the TMSE, RMSE, and MAE values predicted by the mixed Copula function method are lower than those predicted by the single Copula function and single performance degradation data. Among the aforementioned RUL prediction methods, the TMSE, RMSE, and MAE values predicted by the mixed Copula

function composed of Frank Copula and Gumbel Copula are the smallest. This indicates that this degradation data is better suited for this method, resulting in smaller prediction errors and greater accuracy.

5.2. LED lighting system data

Recently, LED lighting systems have attracted widespread attention due to their high efficiency, low energy consumption and long lifetime. Considering different usage functions such as lighting and color change, LED lighting systems may exhibit multiple distinct performance degradation characteristics. Since these characteristics are influenced by the same stress factors (such as current), they are not independent of each other. Therefore, it is important to carry out the RUL prediction of LED lighting systems based on multiple performance degradation characteristics. This study conducts further research based on the data provided in reference [43], which primarily includes degradation data for two performance aspects: LED lighting and color conversion, as shown in Fig.20. The failure threshold for the illumination data is set at $\omega_1 = 50$, while that for the color conversion data is defined as $\omega_2 = 45$.

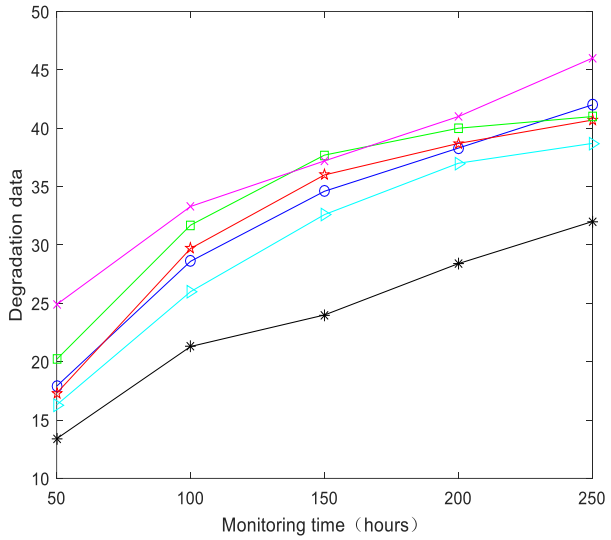

(a) Lighting data

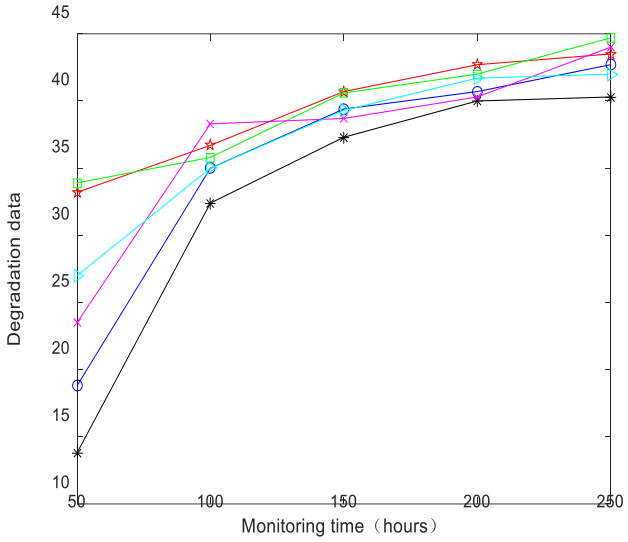

(b) Color conversion data

Fig.20. LED degradation data.

To validate the superiority of the proposed method, the aforementioned degradation data are applied to three degradation models: M_1, M_2, and M_3 for verification and analysis.

A. Degradation model M_1

The lighting data and color conversion data are incorporated into the RUL prediction methods corresponding to different Copula function forms based on degradation model M_1. The unknown parameters in the model are estimated using a stepwise maximum likelihood method, as shown in Table 8.

Table 8. Parameter estimates for different Copula functions.

Copula	α	k_1	k_2	k_3	ln$L$	AIC
Frank	1.6653e-16	1	-	-	-25.8643	53.7286
Clayton	1.0500e-05	-	1	-	-17.7551	37.5102
Gumbel	29.5789	-	-	1	-66.6140	135.2280
k_1Frank+ k_2Clayton	1.0000	4.0074e-04	0.9996	-	0.8671	4.2658
k_1Frank+ k_3Gumbel	1.0000	2.17477	-	0.9998	0.8766	4.2468
k_2Clayton+ k_3Gumbel	29.5797	-	0.9999	8.0078e-05	0.8139	4.3722
k_1Frank+ k_2Clayton+ k_3Gumbel	1.0000	0.9988	9.5678e-04	1.9780e-04	0.8458	6.3084

It can be seen from Table 8 that the values of the log - likelihood function estimated by single Copula functions are all smaller than those corresponding to any mixed Copula functions. Among them, the mixed Copula function composed of Frank Copula and Gumbel Copula has the largest log - likelihood function value. Moreover, the AIC values estimated

by any mixed Copula functions are all smaller than those estimated by single Copula functions. Specifically, the mixed Copula function composed of Frank Copula and Gumbel Copula has the smallest AIC value. Therefore, the method based on mixed Copula functions should be preferentially selected to predict the RUL of LEDs. In particular, the mixed Copula function composed of Frank Copula and Gumbel Copula should be chosen. Substitute the above - estimated parameters into their respective corresponding probability density functions of the RUL, and the graphs are shown as follows.

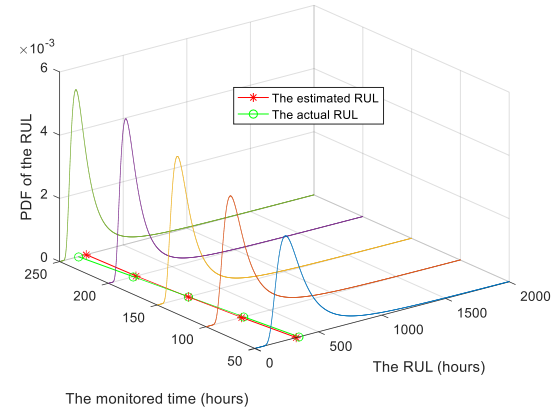

(a) PDF curves for RUL predicted by lighting data

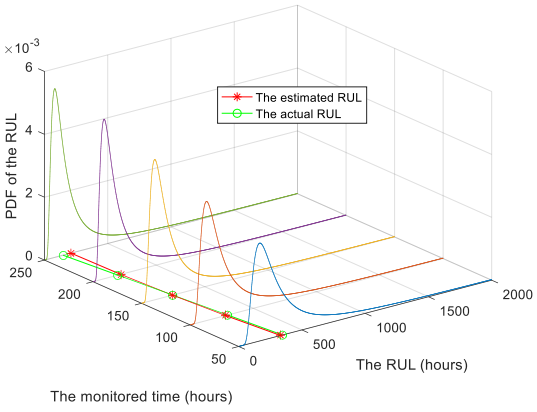

(b) PDF curves of RUL predicted by color conversion data

Fig.21. PDF curves of RUL predicted by the single performance degradation data.

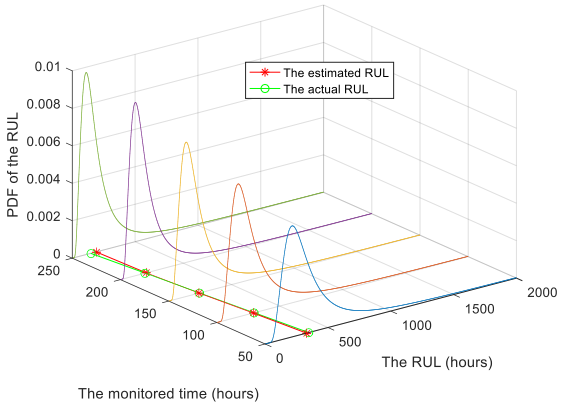

(a) PDF curves of RUL predicted by method III

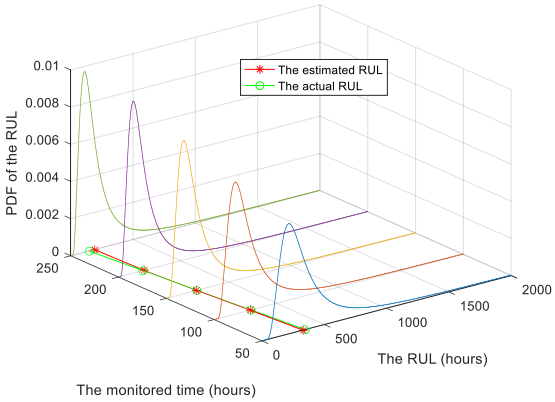

(b) PDF curves of RUL predicted by method IV

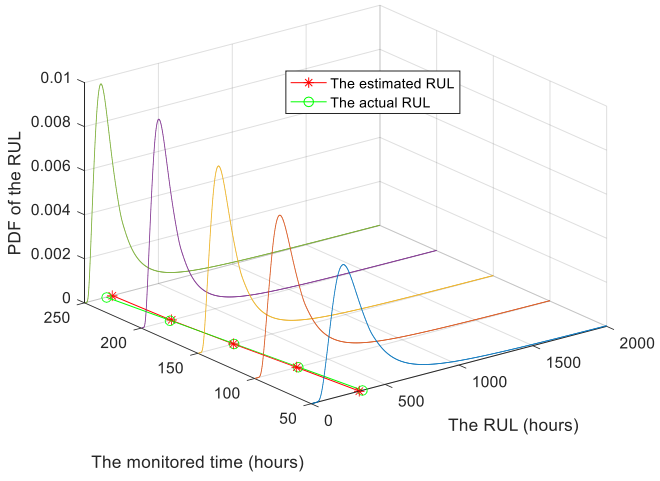

(c) PDF curves of RUL predicted by method V

Fig. 22. PDF curves of RUL predicted by single Copula functions.

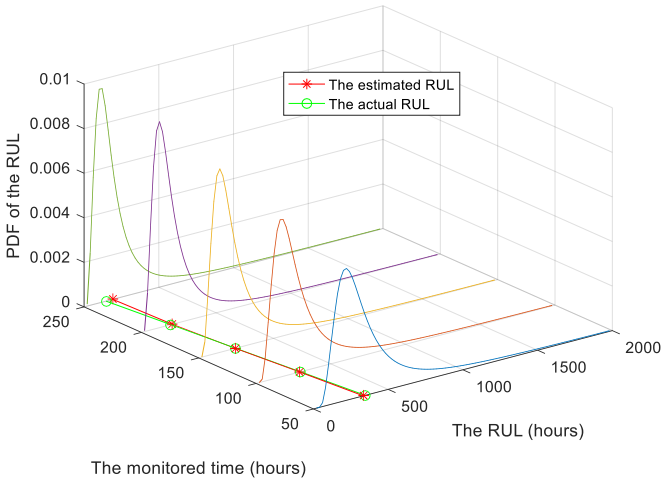

(a) PDF curves of RUL predicted by method VI

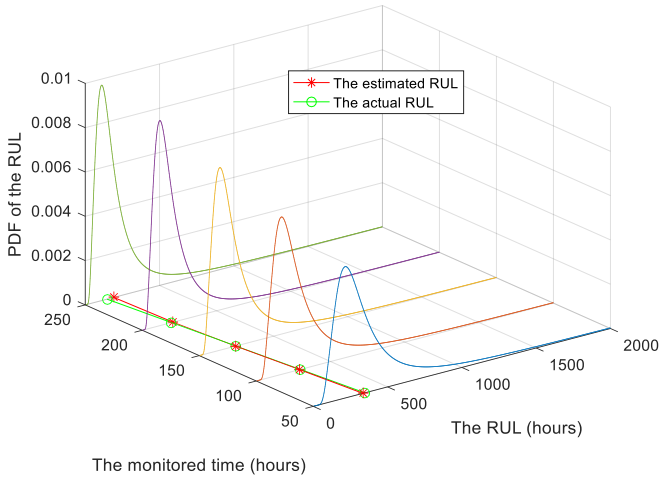

(b) PDF curves of RUL predicted by method VII

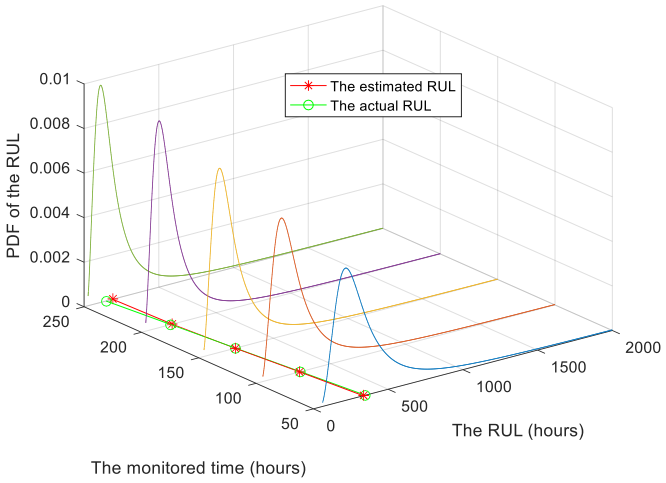

(c) PDF curves of RUL predicted by method VIII

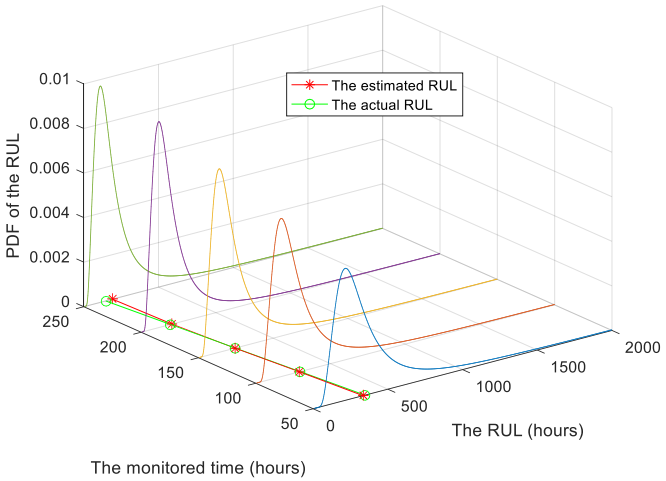

(d) PDF curves of RUL predicted by method IX

Fig.23. PDF curves of RUL predicted by mixed Copula functions.

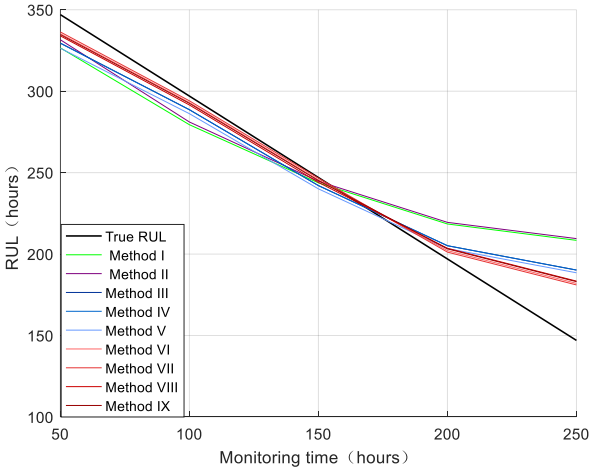

Fig.24. RUL curves predicted by different methods.

As illustrated in the figures above, RUL of LEDs can be predicted using single-performance degradation data as well as dual-performance degradation data modeled with either single Copula functions or mixed Copula functions. The RUL probability density function curves generated by dual-performance degradation data (employing single or mixed Copula functions) exhibit significantly higher and sharper peaks compared to those derived from single-performance degradation data, indicating reduced uncertainty and enhanced precision in RUL predictions when leveraging dual-performance frameworks. Notably, the RUL probability density function curves produced by single Copula and mixed Copula models show minimal visual divergence. The key distinction lies in the prediction errors between the predicted RUL of LEDs and the actual RUL. As can be seen from Fig. 24, compared to methods predicting the RUL of LEDs using single performance degradation data or a single Copula function, the hybrid Copula function-based method proposed in this paper yields predicted RUL values for LEDs that are closer to their actual values. To provide a more intuitive demonstration of prediction errors for

various methods, this paper calculates the TMSE, RMSE, and MAE values for different methods, as shown in Table 9.

Table 9. Errors of different prediction methods.

Method	TMSE	RMSE	MAE
Lighting data (I)	9.2023e+03	994.2004	24.8316
Color conversion data (II)	9.0090e+03	981.6278	23.7192
Frank (III)	4.9588e+03	466.1903	16.5037
Clayton (IV)	4.4387e+03	467.4019	16.4547
Gumbel (V)	5.1751e+03	471.1080	17.2589
k_1Frank+ k_2Clayton (VI)	3.9165e+03	464.8463	15.0555
k_1Frank+ k_3Gumbel (VII)	3.4041e+03	464. 4083	15.0344
k_2Clayton+ k_3Gumbel (VIII)	4.4362e+03	466.0343	15.0829
k_1Frank+k_2Clayton+k_3Gumbel (IX)	4.1233e+03	465.8463	15.0685

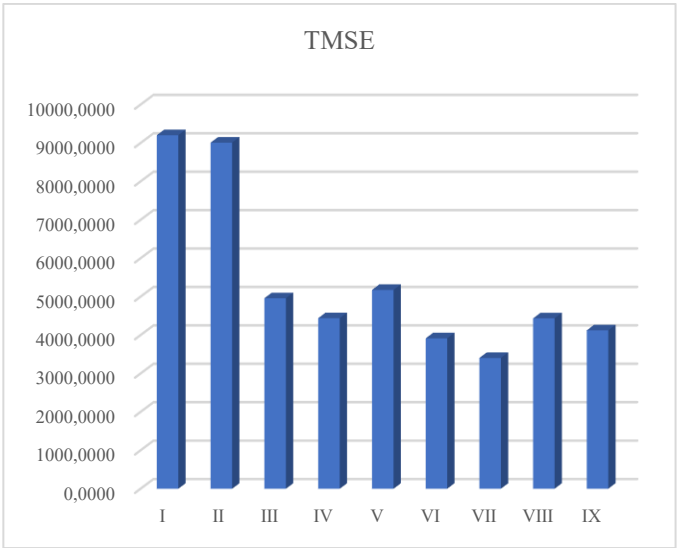

(a) TMSE values for different methods

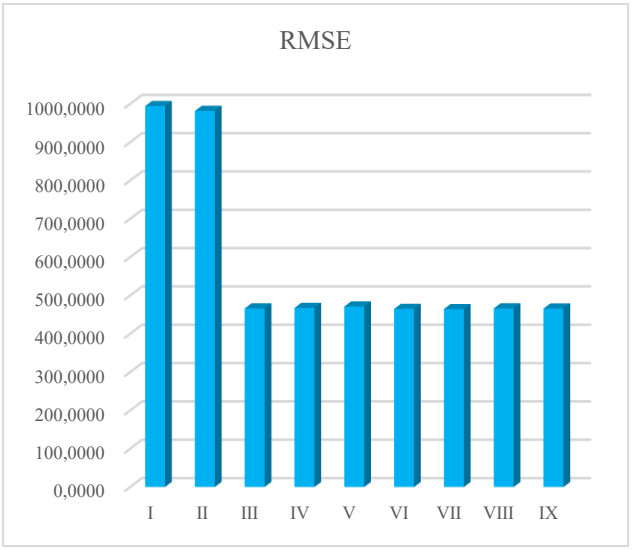

(b) RMSE values for different methods

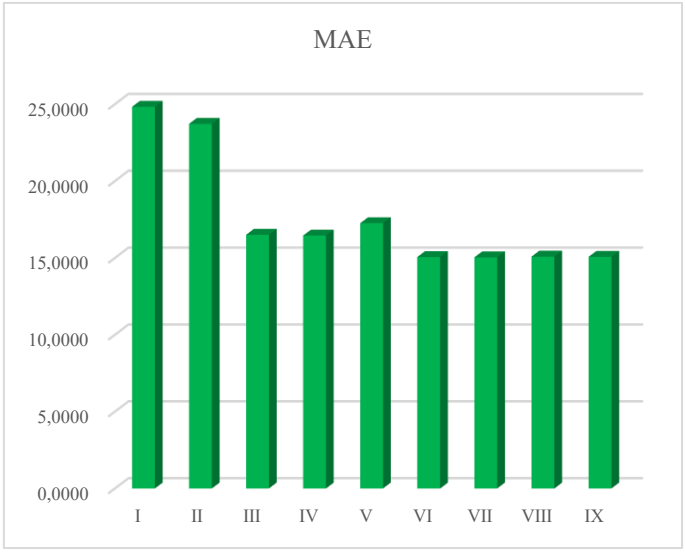

(c) MAE values for different methods

Fig. 25. Comparison of prediction errors across different methods.

The analysis of Table 9 and Fig. 25 reveals that the prediction errors for the RUL of LEDs, using data from both lighting and color degradation, are smaller than those predicted using single-performance degradation data. Furthermore, the RUL prediction errors based on the mixed Copula function are consistently lower than those derived from a single Copula

function. Among the nine RUL prediction methods analyzed, the mixed Copula function combining Frank Copula and Gumbel Copula exhibits the lowest TMSE, MAE, and RMSE values, indicating that LED degradation data is more suitable for this approach. This finding aligns with the earlier results based on the AIC value. Meanwhile, it can be seen from Table 9 that the values of TMSE, MAE, and RMSE predicted by the mixed Copula function composed of Frank Copula, Clayton Copula, and Gumbel Copula are larger than those predicted by any other two-component mixed Copula functions. This further demonstrates that in the RUL prediction of actual equipment, a greater number of mixed Copula functions does not necessarily lead to more accurate prediction results. Instead, the specific types of mixed Copula functions need to be selected according to the characteristics of the degradation data.

B. Degradation model M_2

The LED degradation data are incorporated into the RUL prediction methods based on degradation model M_2 with different Copula functions. The unknown parameters in the models are estimated using a two-step maximum likelihood estimation method, and the results are summarized in Table 10.

Table 10.Parameter estimates for different Copula functions.

Copula	α	k_1	k_2	k_3	ln$L$	AIC
Frank	1.0500e-06	1	-	-	-1186.2419	2374.4838
Clayton	0.0152	-	1	-	-1203.4046	2408.8092
Gumbel	3.0461	-	-	1	-1218.3193	2438.6386
k_1Frank+ k_2Clayton	0.6602	0.7884	0.2116	-	-404.6535	815.3070
k_1Frank+ k_3Gumbel	20.4432	0.1201	-	0.8799	-639.5522	1285.1044
k_2Clayton+ k_3Gumbel	1.0152	-	0.9998	0.0002	-1032.2012	2070.4024
k_1Frank+ k_2Clayton+ k_3Gumbel	1.6602	0.0045	7.6821e-06	0.9954	-228.2098	464.4196

The table indicates that the log-likelihood function values estimated by single Copula functions are lower than those corresponding to any mixed Copula function. The AIC values estimated from single Copula functions are also higher than those from any mixed Copula function. Therefore, mixed Copula functions should be prioritized for predicting the RUL of LEDs. By substituting the estimated parameters into the PDFs of the RUL corresponding to various methods, the resulting graphs are displayed below.

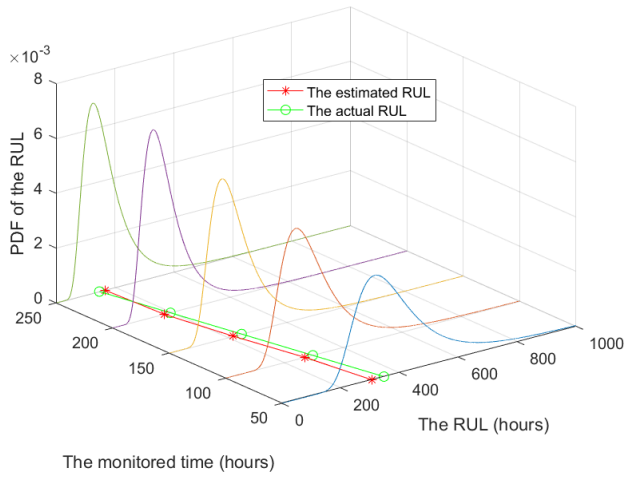

(a) PDF curves for RUL predicted by lighting data

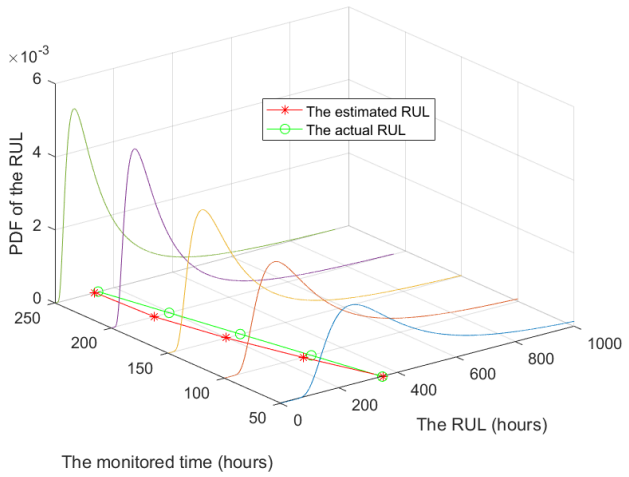

(b) PDF curves of RUL predicted by color conversion data

Fig.26. PDF curves of RUL predicted by the single performance degradation data.

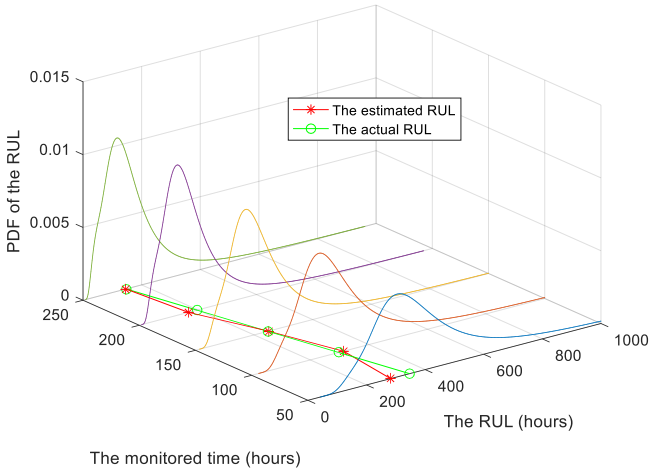

(a) PDF curves of RUL predicted by method III

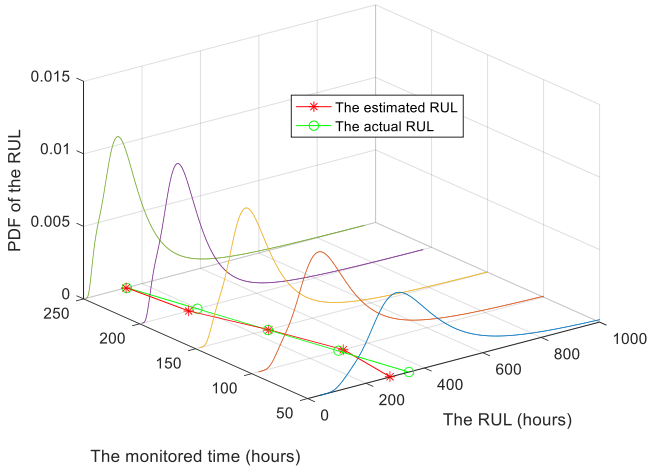

(b) PDF curves of RUL predicted by method IV

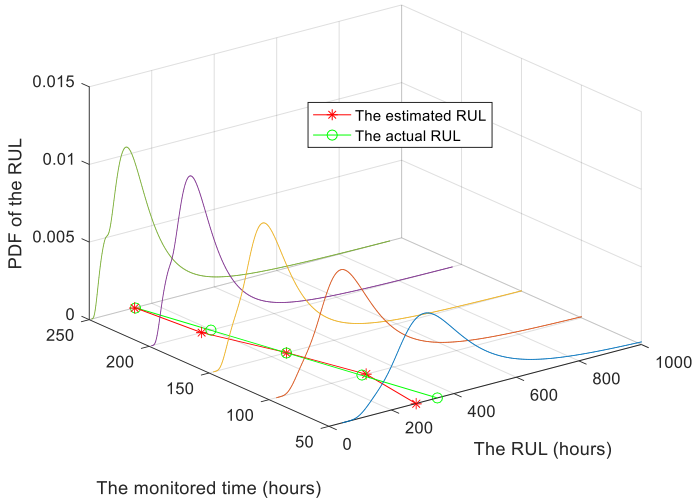

(c) PDF curves of RUL predicted by method V

Fig. 27. PDF curves of RUL predicted by single Copula functions.

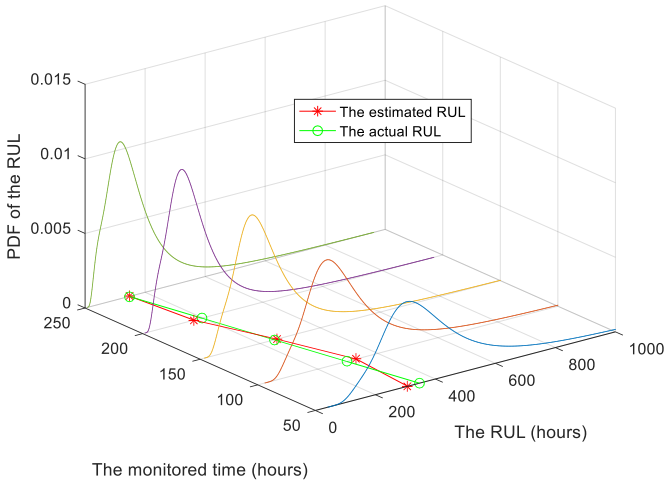

(a) PDF curves of RUL predicted by method VI

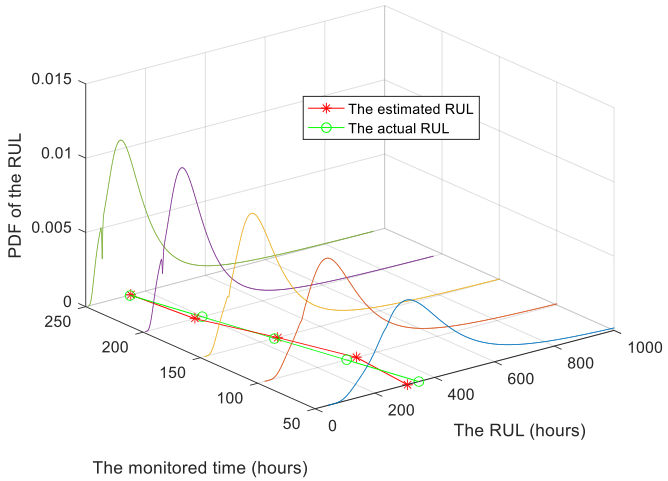

(b) PDF curves of RUL predicted by method VII

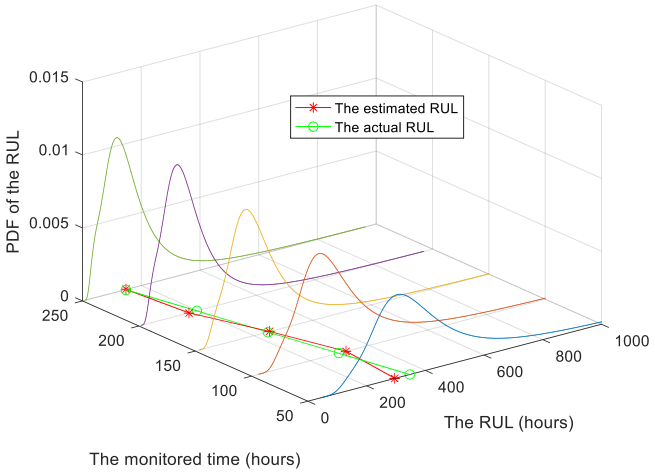

(c) PDF curves of RUL predicted by method VIII

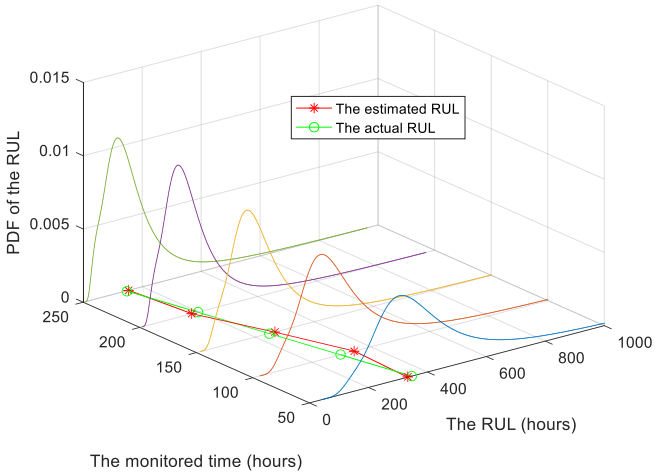

(d) PDF curves of RUL predicted by method IX

Fig.28. PDF curves of RUL predicted by mixed Copula functions.

Table 11.Errors of different prediction methods.

Method	TMSE	RMSE	MAE
Lighting data (I)	1.1074e+04	1.2987e+03	32.7539
Color conversion data (II)	1.0504e+04	1.1725e+03	28.4964
Frank (III)	9.2063e+03	1.0184e+03	22.4452
Clayton (IV)	9.5709e+03	1.0484e+03	22.6283
Gumbel (V)	9.9406e+03	1.1498e+03	22.8663
k_1Frank+ k_2Clayton (VI)	8.1568e+03	655.8787	21.5636
k_1Frank+ k_3Gumbel (VII)	8.6658e+03	666.7068	22.1501
k_2Clayton+ k_3Gumbel (VIII)	9.0533e+03	788.0997	22.1767
k_1Frank+k_2Clayton+k_3Gumbel (IX)	7.4652e+03	645.6840	21.3614

Figs. 26, 27, and 28 illustrate that as the number of measurement points increases, the PDF curves for the RUL become higher and sharper, indicating a gradual reduction in prediction uncertainty. Specifically, the PDF curves predicted by single Copula and mixed Copula functions are higher and sharper, suggesting lower uncertainty in predictions using these methods. From Fig. 29, we can see the RUL values for LEDs predicted using the hybrid Copula function-based method are closer to their actual values. The TMSE, RMSE, and MAE values corresponding to each prediction method are summarized in Table 11.

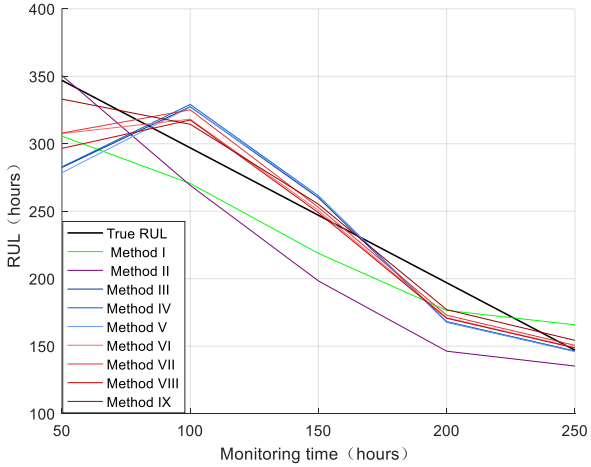

Fig.29. RUL curves predicted by different methods.

From Table 11 and Fig. 30, it is evident that the TMSE, RMSE, and MAE values predicted by the mixed Copula function method are lower than those predicted by a single Copula function and single-performance degradation data.

Among the nine LED remaining useful life prediction methods described above, the mixed Copula function composed of Frank Copula, Clayton Copula, and Gumbel Copula yields

the smallest TMSE, RMSE, and MAE values, indicating that this method has the smallest prediction error. Therefore, among the RUL prediction methods corresponding to different Copula functions associated with the degradation model M_2, the mixed Copula function composed of Frank Copula, Clayton Copula, and Gumbel Copula should be preferentially selected to predict the RUL of LEDs.

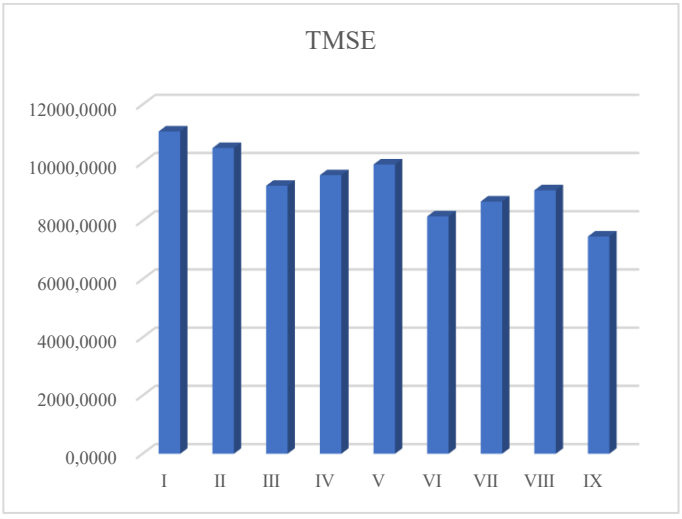

(a) TMSE values for different methods

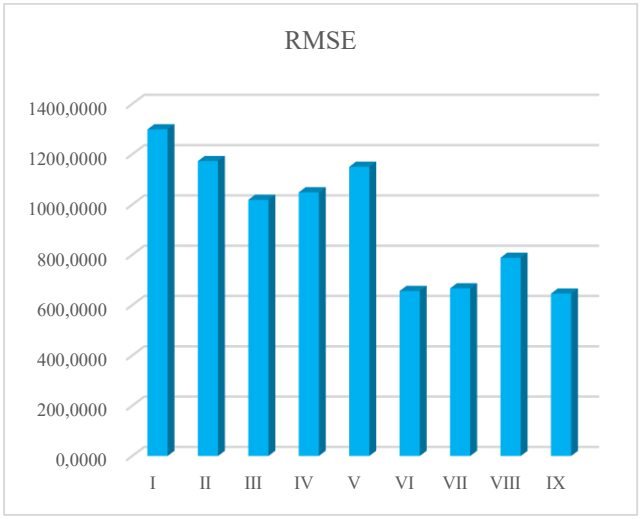

(b) RMSE values for different methods

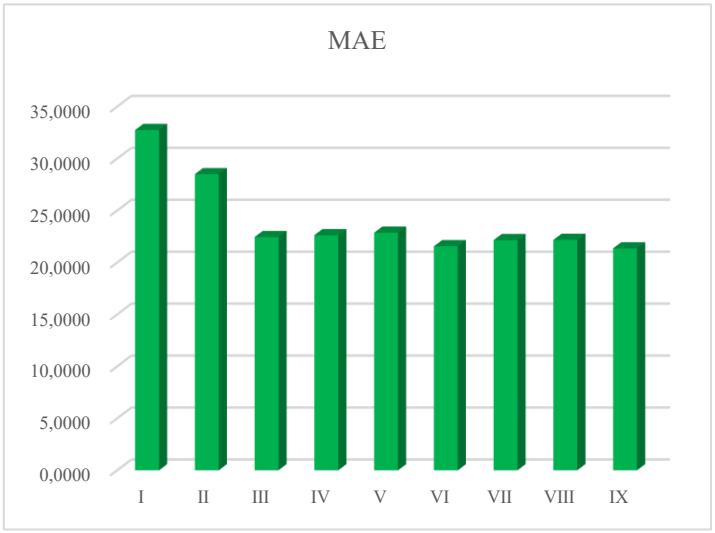

(c) MAE values for different methods

Fig. 30. Comparison of prediction errors across different methods.

C. Degradation model M_3

The LED degradation data are incorporated into the RUL prediction methods based on the degradation model M_3 with different Copula functions. The parameters in the model are estimated using the stepwise maximum likelihood method, as shown in Table 12.

Table 12.Parameter estimates for different Copula functions.

Copula	α	k_1	k_2	k_3	ln$L$	AIC
Frank	2.0500e-13	1	-	-	-3.4763	8.9526
Clayton	1.0500e-04	-	1	-	-2.2053	6.4106
Gumbel	10.0000	-	-	1	-3.4730	9.9460
k_1Frank+ k_2Clayton	3.9616e-10	0.0651	0.9349	-	5.4436	-4.8872
k_1Frank+ k_3Gumbel	1.0000	6.0939e-33	-	1.0000	23.7442	-41.4884
k_2Clayton+ k_3Gumbel	69.3083	-	0.4641	0.5359	10.9455	-15.8910
k_1Frank+ k_2Clayton+ k_3Gumbel	1.0000	0.1077	0.0157	0.8766	26.9640	-45.9280

From Table 12, it can be observed that the mixed Copula function composed of Frank Copula, Clayton Copula, and Gumbel Copula has the largest log-likelihood function value and the smallest AIC value estimated by this mixed Copula function. A comparison of Tables 8, 10, and 12 further shows that the mixed Copula function composed of these three Copula functions in Table 12 still yields the largest log-likelihood function value and the smallest AIC value. Therefore, among the three degradation models M_1,M_2, and M_3, the mixed Copula function composed of Frank Copula, Clayton Copula, and Gumbel Copula corresponding to model M_3 should be preferentially selected for predicting the RUL of LEDs. Substitute the above-estimated parameters into their respective RUL probability density functions, and the graphs are shown as follows.

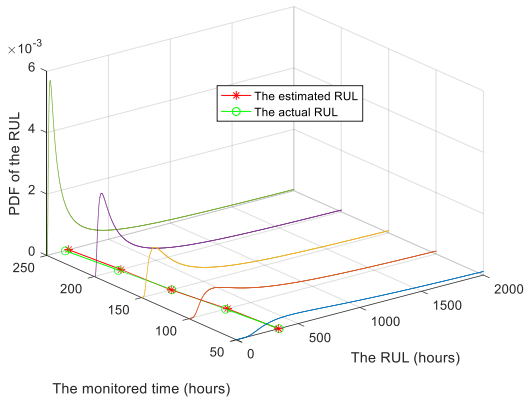

(a) PDF curves for RUL predicted by lighting data

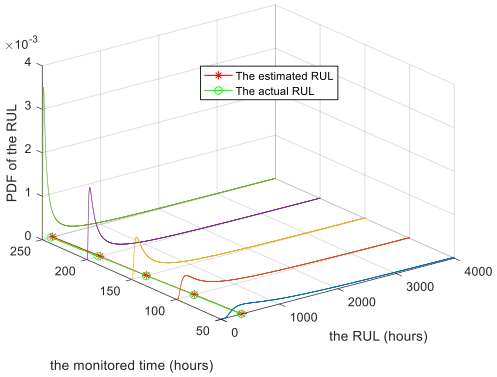

(b) PDF curves of RUL predicted by color conversion data

Fig.31. PDF curves of RUL predicted by the single performance degradation data.

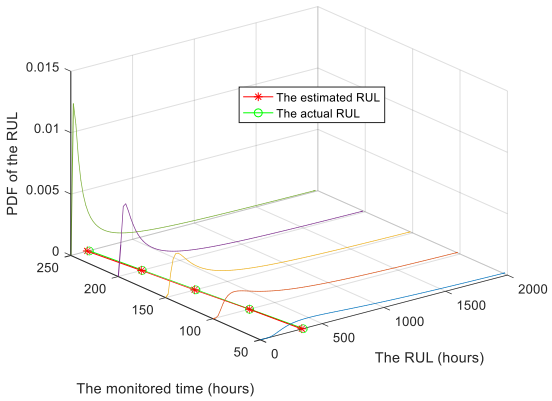

(a) PDF curves of RUL predicted by method III

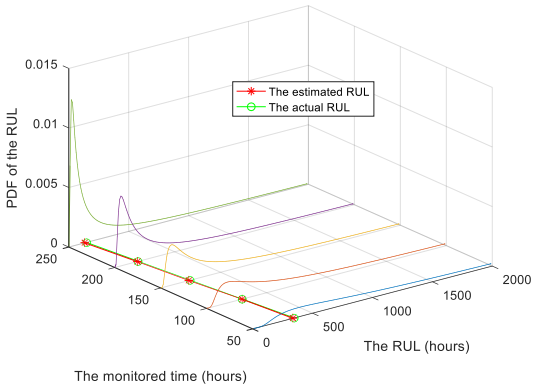

(b) PDF curves of RUL predicted by method IV

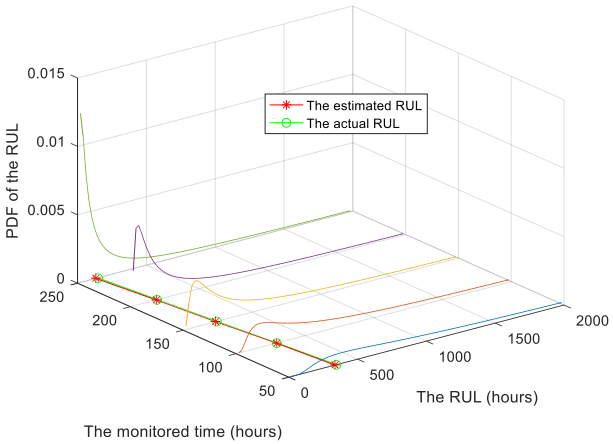

(c) PDF curves of RUL predicted by method V

Fig. 32. PDF curves of RUL predicted by single Copula functions.

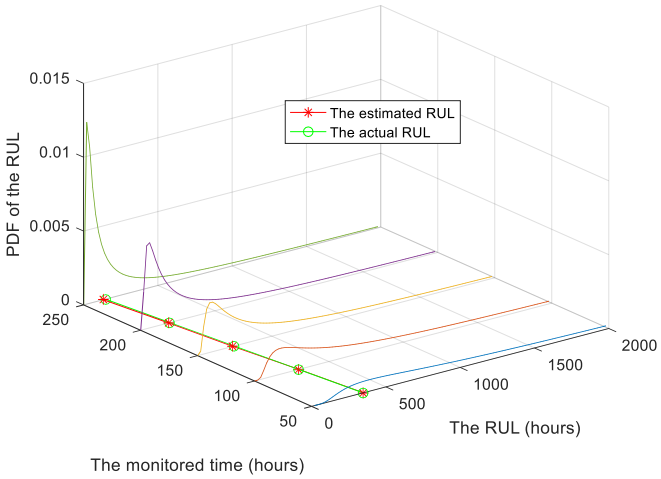

(a) PDF curves of RUL predicted by method VI

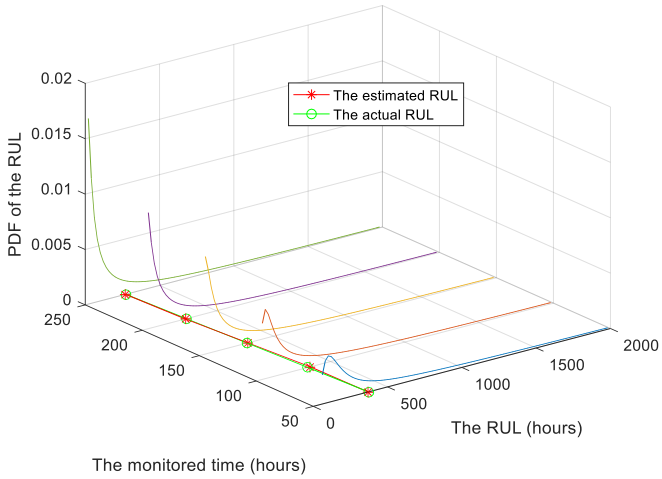

(b) PDF curves of RUL predicted by method VII

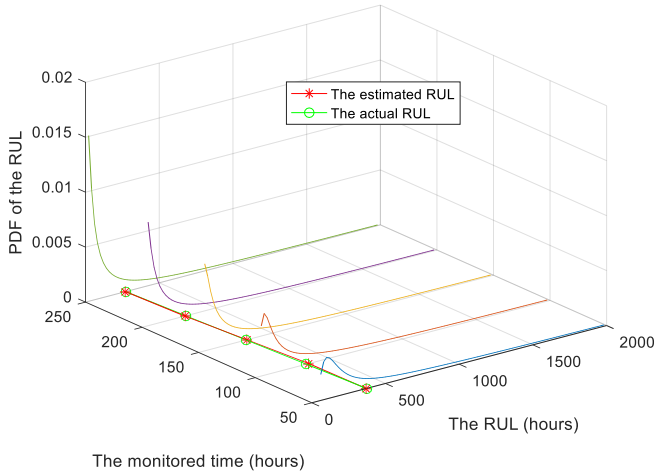

(c) PDF curves of RUL predicted by method VIII

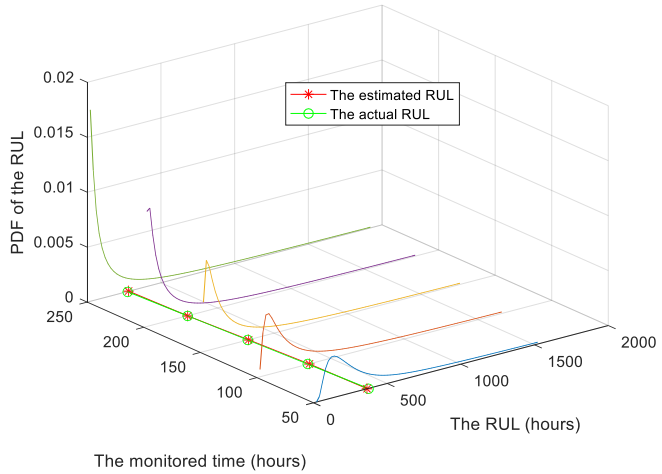

(d) PDF curves of RUL predicted by method IX

Fig.33. PDF curves of RUL predicted by mixed Copula functions.

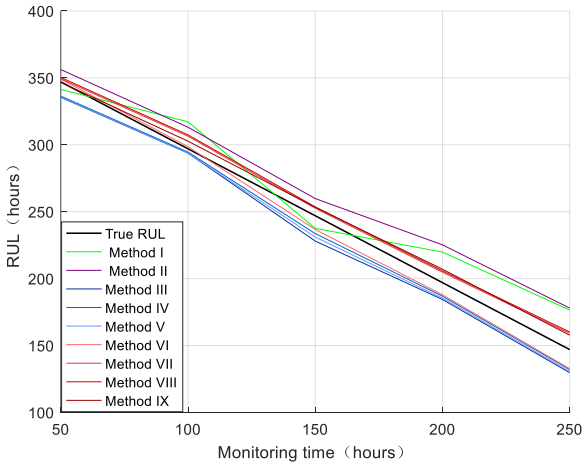

Fig.34. RUL curves predicted by different methods.

From the graphs above, it can be seen that the PDF curves for the RUL predicted by degradation model M_3 is higher and sharper than those predicted by models M_1 and M_2, indicating that the RUL predicted by model M_3 has less uncertainty. Among the different Copula functions corresponding to degradation model M_3, the PDF curves for the RUL predicted using single Copula and mixed Copula functions are higher and sharper than those predicted using single performance degradation data, suggesting that the predictions using single Copula and mixed Copula functions have lower uncertainty. The reduction of uncertainty in RUL estimation is crucial for equipment prognosis and health management, as it can lower maintenance costs and increase the confidence in decision-making results [44]. Meanwhile, as shown in Fig.34, the RUL values for LEDs predicted using the hybrid Copula function-based method are closer to their actual values. To compare the prediction errors of different methods, TMSE, RMSE, and MAE values corresponding to each method are calculated, as shown in Table 13.

Table 13.Errors of different prediction methods.

Method	TMSE	RMSE	MAE
Lighting data (I)	3.0309e+03	311.8699	15.5166
Color conversion data (II)	4.0419e+03	433.0662	18.4866
Frank (III)	2.5572e+03	116.2486	10.1074
Clayton (IV)	2.1644e+03	104.7042	9.4801
Gumbel (V)	2.3702e+03	115.9133	10.0892
k_1Frank+ k_2Clayton (VI)	1.5608e+03	79.6613	7.4456
k_1Frank+ k_3Gumbel (VII)	1.1048e+03	70.5354	6.5532
k_2Clayton+ k_3Gumbel (VIII)	1.3151e+03	72.0298	7.1667
k_1Frank+k_2Clayton+k_3Gumbel (IX)	1.0877e+03	49.8730	6.2508

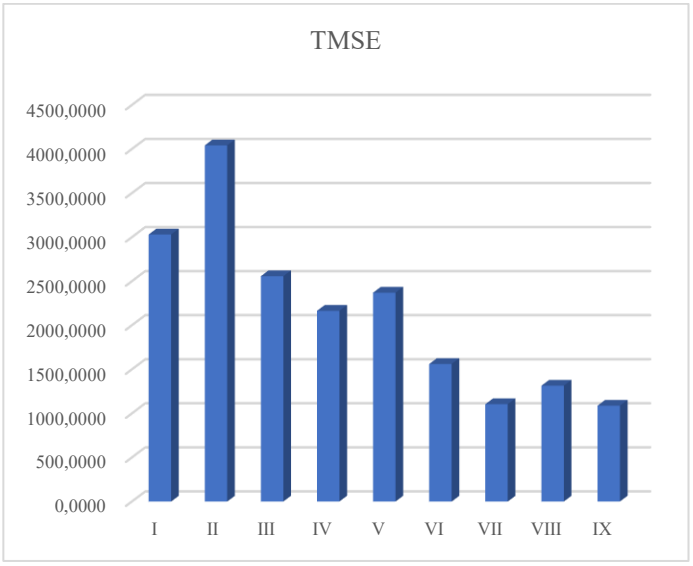

(a) TMSE values for different methods

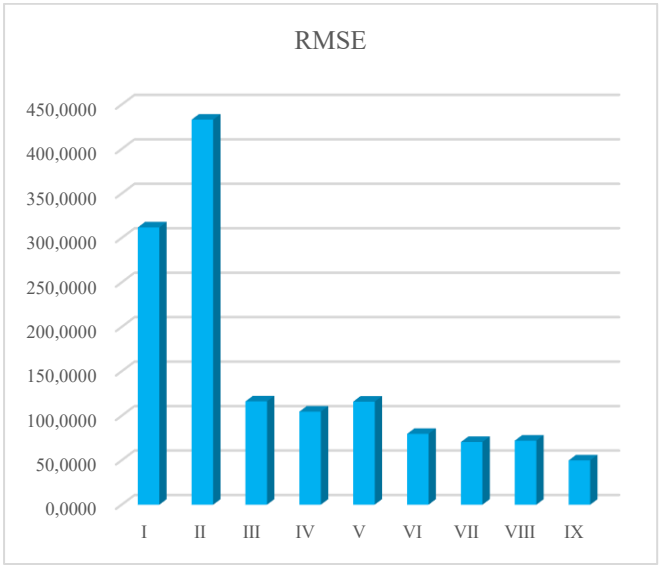

(b) RMSE values for different methods

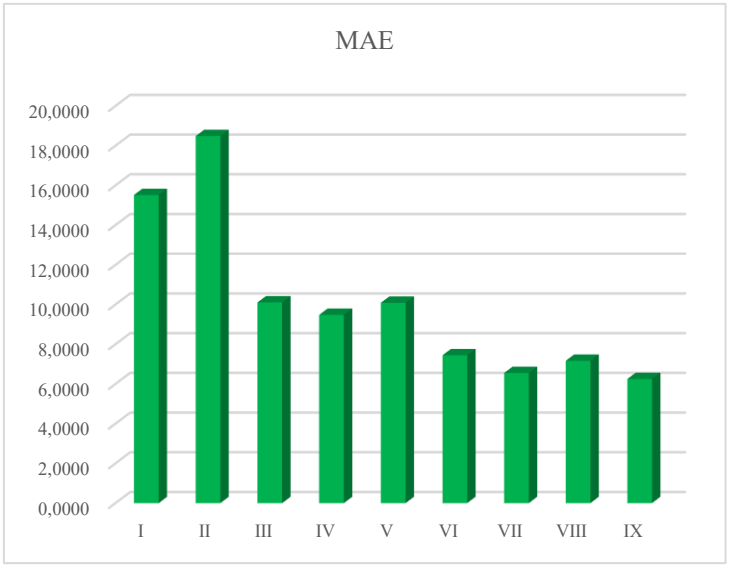

(c) MAE values for different methods

Fig. 35. Comparison of prediction errors across different methods.

From Table 13 and Fig. 35, it can be observed that the RUL prediction errors based on single Copula functions and mixed Copula functions for two-performance degradation data are both smaller than those based on single-performance degradation data. Moreover, the RUL prediction errors based on mixed Copula functions are smaller than those based on single Copula functions. Among them, the mixed Copula function composed of Frank Copula, Clayton Copula, and Gumbel

Copula yields the lowest TMSE, RMSE, and MAE values, indicating minimal prediction error. Meanwhile, a comparison with previous prediction results shows that the TMSE, RMSE, and MAE values predicted by degradation model M_3 are all smaller than those predicted by models M_1 and M_2. Therefore, the mixed Copula function composed of Frank Copula, Clayton Copula, and Gumbel Copula corresponding to degradation model M_3 should be preferentially selected for predicting the RUL of LEDs. This approach can thus obtain the most accurate prediction results and thereby reduce future equipment maintenance costs.

5.3. Metal crack degradation data

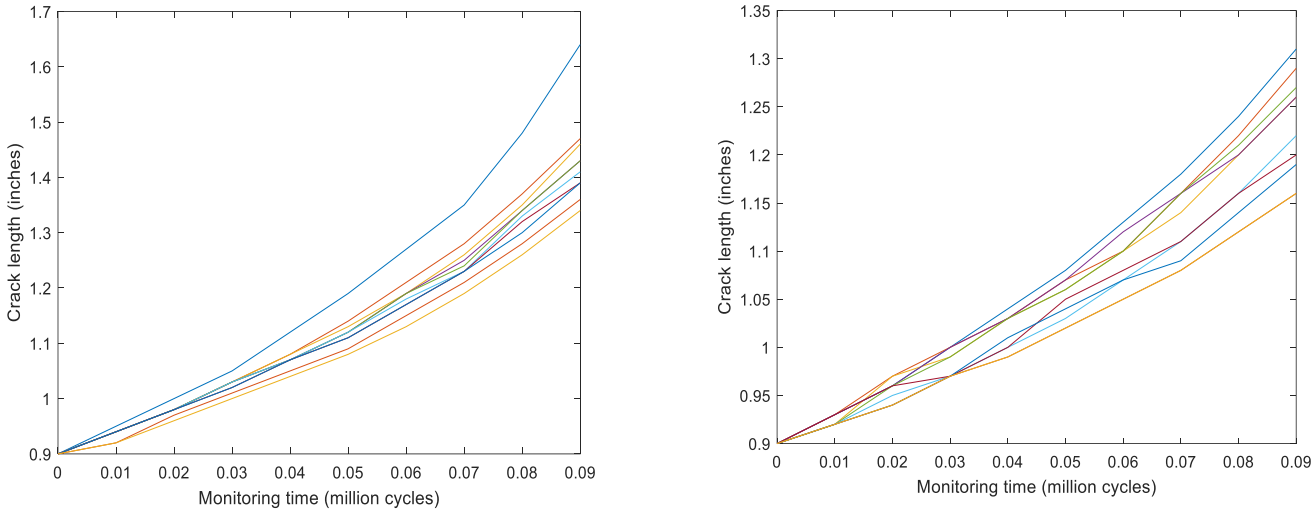

(a) Degradation data PC1 (b) Degradation data PC2

Fig. 36. Crack Degradation Data.

Metal materials are widely used in the equipment manufacturing industry due to their excellent corrosion resistance, machinability, and weldability. Under prolonged fatigue loading, stress concentration areas in metal components are prone to fatigue damage, leading to crack initiation. Early-stage cracks may further propagate under continuous service and cyclic loading conditions, ultimately resulting in structural fracture failures and significant safety risks. Therefore, employing rational technical approaches to predict the RUL of such components through fatigue crack performance parameters is critical for determining optimal maintenance schedules, enhancing reliability, and mitigating operational risks. This section utilizes crack growth data from platinum-based equipment for RUL prediction, with the original dataset sourced from Reference [45]. The dataset includes crack growth testing results from 21 identical equipment, measured at intervals of 0.01 million cycles, and testing is terminated at 0.09 million cycles. To validate the effectiveness of the proposed methodology, 20 equipment are selected and divided into two groups, representing crack lengths at two distinct points on the equipment (both with an initial crack length of 0.9 inches). For analytical purposes, these crack lengths are treated as two performance metrics of the equipment, labeled PC1 and PC2, respectively, as illustrated in Fig. 36. The equipment is deemed failed if PC1 exceeds 1.6 inches or PC2 exceeds 1.3 inches. Similar assumptions have been applied in reliability analysis and RUL prediction studies of dual-degradation equipment [46,47].

The two groups of degradation data are incorporated into three degradation models (M_1 , M_2 ,and M_3) for validation analysis.

A. Degradation model M_1

The two crack datasets are integrated into the degradation model M_1 with different Copula functions. The unknown parameters in the model are estimated using the two-step maximum likelihood estimation method, and the results are summarized in Table 14.

Table 14.Parameter estimates for different Copula functions.

Copula	α	k_1	k_2	k_3	ln$L$	AIC
Frank	6.3000e-04	1	-	-	-1.3281e+03	2.6582e+03
Clayton	2.0732	-	1	-	-1.3076e+03	2.6172e+03
Gumbel	10.5784	-	-	1	-1.2956e+03	2.5932e+03
k_1Frank+ k_2Clayton	5.7808	1.6229e-04	5.8572e-06	-	-1.2473e+03	2.5006e+03
k_1Frank+ k_3Gumbel	10.5785	1.0000	-	4.8012e-17	-1.2901e+03	2.5862e+03
k_2Clayton+ k_3Gumbel	5.7808	-	1.0444e-04	0.9999	-1.1312e+03	2.2684e+03
k_1Frank+ k_2Clayton+ k_3Gumbel	1.8272	1.2465e-18	1.0000	3.7901e-20	-1.1320e+03	2.2700e+03

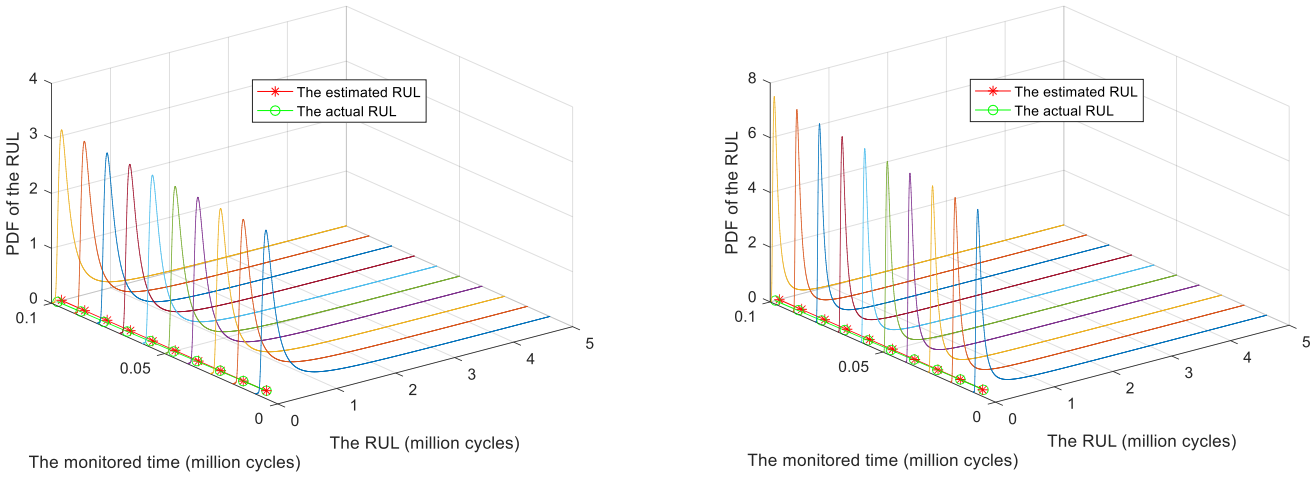

(a) PDF curves for RUL predicted by PC1

(b) PDF curves of RUL predicted by PC2

Fig.37. PDF curves of RUL predicted by the single performance degradation data.

From Table 14, it can be seen that the log-likelihood function values estimated by single Copula functions are still all smaller than those corresponding to any mixed Copula function. Among them, the mixed Copula function composed of Clayton Copula and Gumbel Copula has the largest log-likelihood function value. The AIC values estimated by any mixed Copula function are all smaller than those estimated by single Copula functions, with the mixed Copula function composed of Clayton Copula and Gumbel Copula yielding the smallest AIC value. Therefore, the method based on mixed Copula functions should be preferentially selected for predicting the RUL of metal equipment—specifically, the mixed Copula function composed of Frank Copula and Gumbel Copula. Substitute the above parameters into their respective PDFs of RUL, and the graphs are shown as follows.

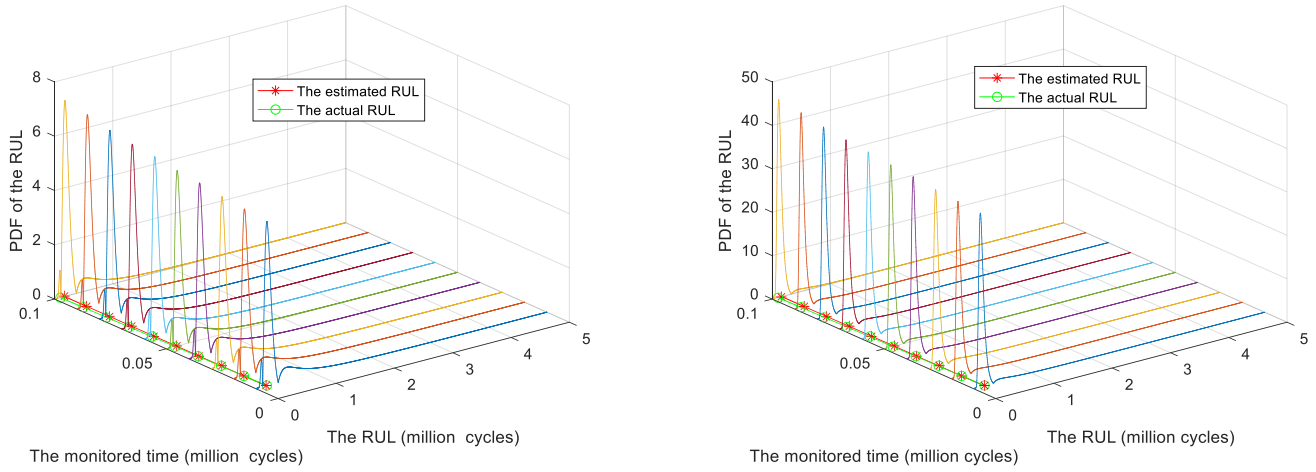

(a) PDF curves of RUL predicted by method III

(b) PDF curves of RUL predicted by method IV

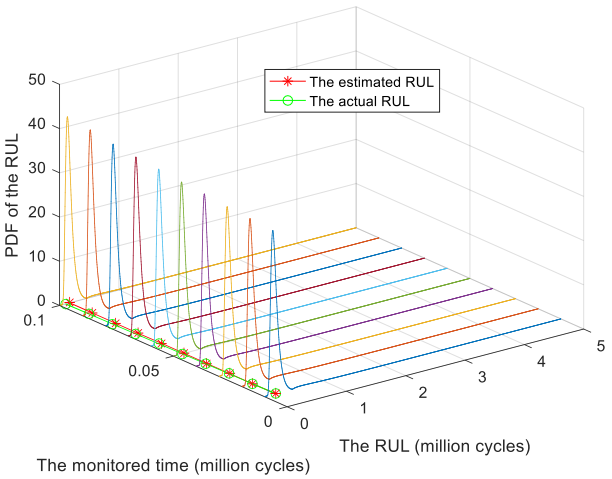

(c) PDF curves of RUL predicted by method V

Fig. 38. PDF curves of RUL predicted by single Copula functions.

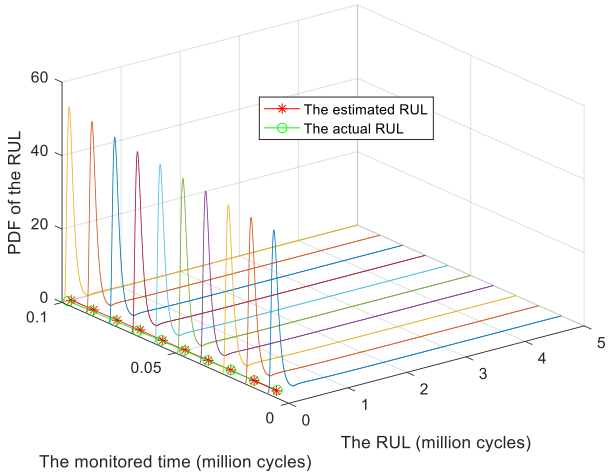

(a) PDF curves of RUL predicted by method VI

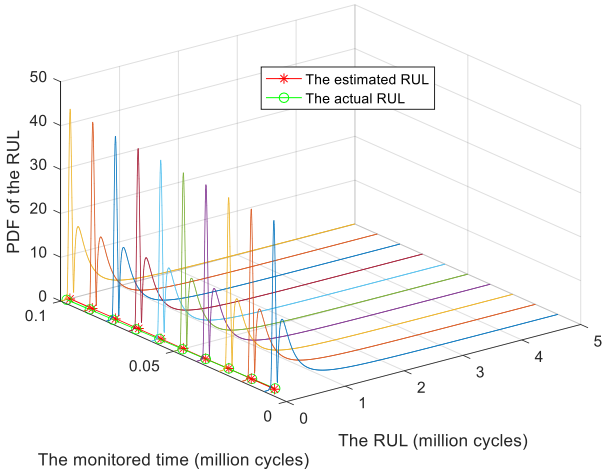

(b) PDF curves of RUL predicted by method VII

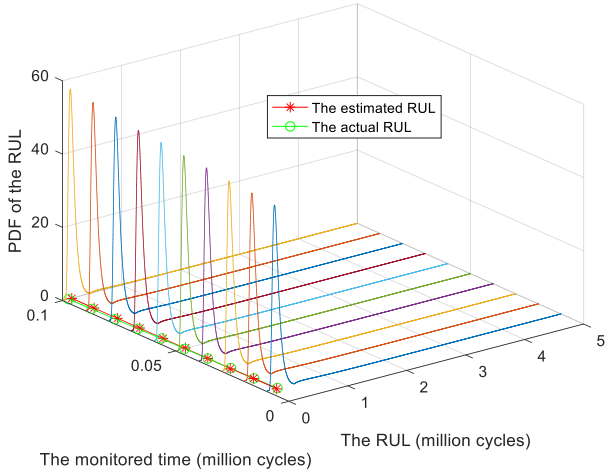

(c) PDF curves of RUL predicted by method VIII

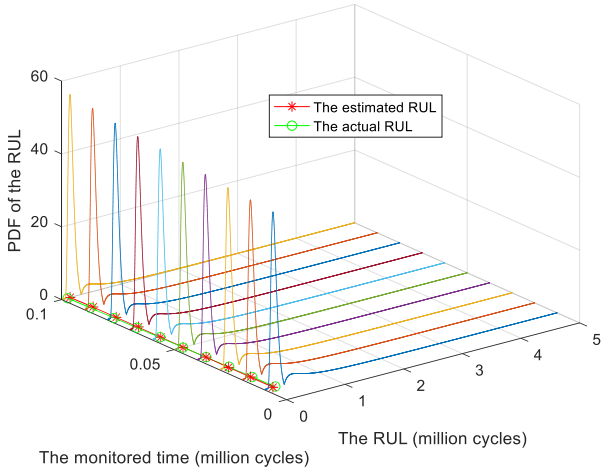

(d) PDF curves of RUL predicted by method IX

Fig.39. PDF curves of RUL predicted by mixed Copula functions.

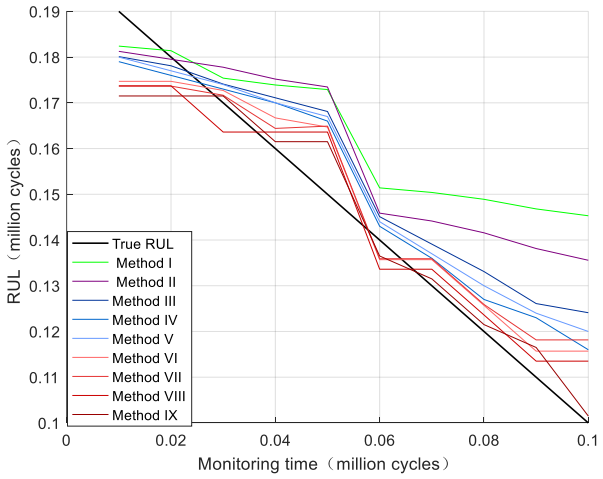

Fig.40. RUL curves predicted by different methods.

From the aforementioned graphs, it can be observed that the RUL of metallic equipment can be predicted using three approaches: single performance degradation data, dual performance degradation data based on single Copula functions, and dual performance degradation data based on mixed Copula functions. The PDF curves of RUL predicted by dual performance degradation data (using either single Copula or mixed Copula functions) exhibit higher peaks and narrower spreads compared to those derived from single performance degradation data. This indicates that predictions based on dual performance degradation data with Copula functions demonstrate reduced uncertainty and improved accuracy. Furthermore, the PDF curves generated by the mixed Copula function show even higher peaks and sharper concentration than those from the single Copula function approach, suggesting that the mixed Copula method achieves the lowest prediction uncertainty. Notably, the mixed Copula function combining Clayton Copula and Gumbel Copula yields the minimal uncertainty among all methods. As can be seen from Fig.40, the RUL values for metal equipment predicted using the hybrid Copula function-based method proposed in this paper are closer to its actual values. To quantitatively compare prediction errors across different approaches, this paper calculates the TMSE, RMSE, and MAE values for each method, as shown in Table 15.

Table 15. Errors of different prediction methods.

Method	TMSE	RMSE	MAE
PC1 (I)	0.0575	0.0020	0.0374
PC2(II)	0.0447	0.0017	0.0344
Frank (III)	0.0412	0.0015	0.0327
Clayton (IV)	0.0348	0.0014	0.0293
Gumbel (V)	0.0404	0.0016	0.0320
k_1Frank+ k_2Clayton (VI)	0.0315	9.9541e-04	0.0259
k_1Frank+ k_3Gumbel (VII)	0.0336	9.9629e-04	0.0264
k_2Clayton+ k_3Gumbel (VIII)	0.0302	8.1025e-04	0.0244
k_1Frank+k_2Clayton+k_3Gumbel (IX)	0.0310	8.8894e-04	0.0248

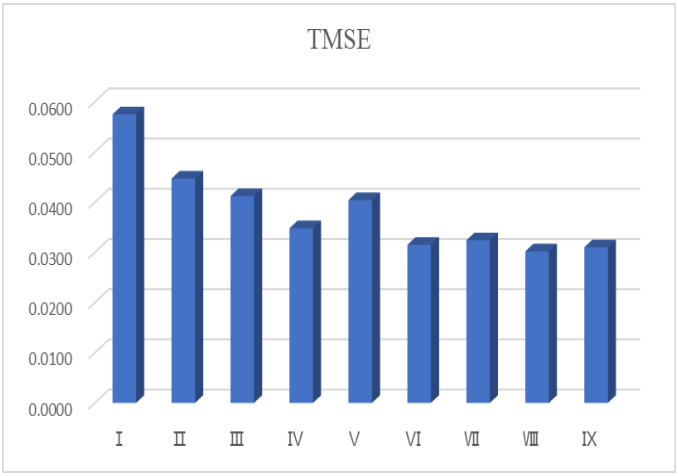

(a) TMSE values for different methods

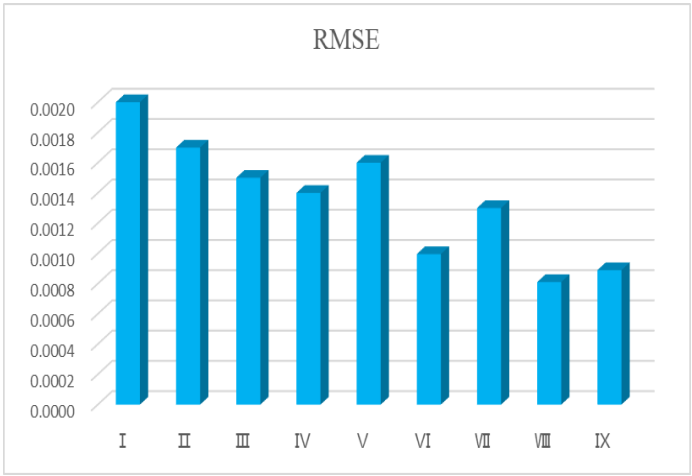

(b) RMSE values for different methods

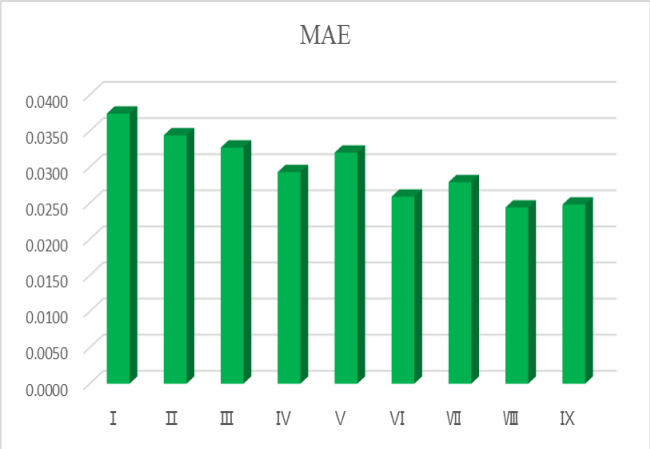

(c) MAE values for different methods

Fig. 41. Comparison of prediction errors across different methods.

As can be seen from Table 15 and Fig.41, among the nine RUL prediction methods described above, the mixed Copula function composed of the Frank Copula and Gumbel Copula yields the smallest TMSE, MAE, and RMSE values. This indicates that the degradation data is more suitable for this method, and the result is exactly consistent with the selection outcome of the AIC value mentioned earlier. Additionally, Table 14 shows that the TMSE, RMSE, and MAE values obtained using mixed Copula functions are all smaller than those from single Copula functions and single-performance predictions. This demonstrates that the mixed Copula function, by fully utilizing multiple performance degradation data of the equipment, can predict the RUL more accurately and improve the prediction precision of RUL.

B. Degradation model M_2

The two crack datasets are integrated into the degradation model M_2 with different Copula functions. The unknown parameters in the model are estimated using the two-step maximum likelihood estimation method, and the results are summarized in Table 16.

Table 16. Parameter estimates for different Copula functions.

Copula	α	k_1	k_2	k_3	ln$L$	AIC
Frank	1.5750e-05	1	-	-	-1.7943e+03	3.5906e+03
Clayton	1.0500e-06	-	1	-	-1.8475e+03	3.6970e+03
Gumbel	5.0000	-	-	1	1.7960e+03	3.5940e+03
k_1Frank+ k_2Clayton	67.7065	1.0000	9.5442e-07	-	-1.7914e+03	3.5848e+03
k_1Frank+ k_3Gumbel	2.2867	1.0000	-	1.0561e-07	-1.7902e+03	3.5824e+03
k_2Clayton+ k_3Gumbel	2.3625	-	0.0176	0.9824	-1.6377e+03	3.2774e+03
k_1Frank+ k_2Clayton+ k_3Gumbel	2.2866	0.9517	0.0473	0.0001	-1.7873e+03	3.5766e+03

As can be seen from Table 16, the log-likelihood function values estimated using single Copula functions are all smaller than those corresponding to any mixed Copula function. Consequently, the AIC values for single Copula functions are all greater than those for any mixed Copula function. Therefore, the mixed Copula functions should be prioritized for predicting the RUL of equipment. Substituting the aforementioned estimated parameters into the PDFs of RUL corresponding to different methods, the resulting graphs are plotted as shown below.

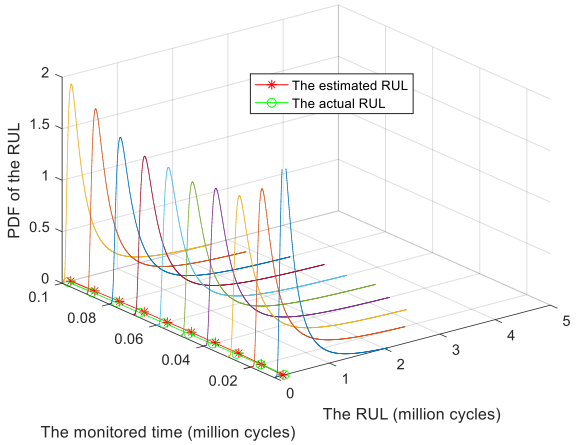

(a) PDF curves for RUL predicted by PC1

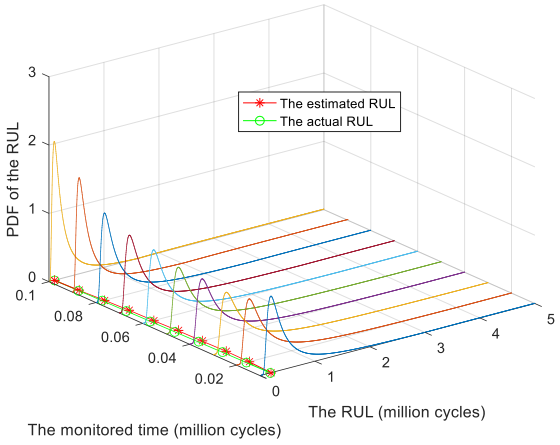

(b) PDF curves of RUL predicted by PC2

Fig.42. PDF curves of RUL predicted by the single performance degradation data.

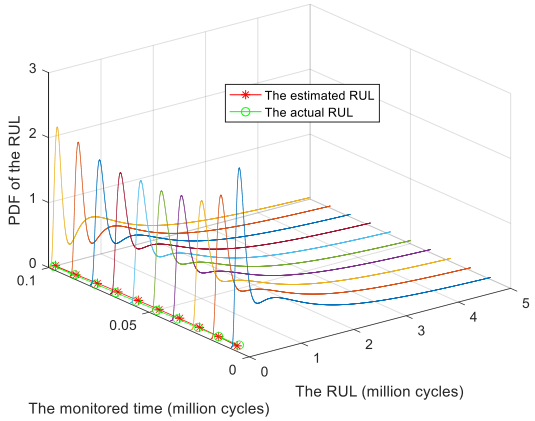

(a) PDF curves of RUL predicted by method III

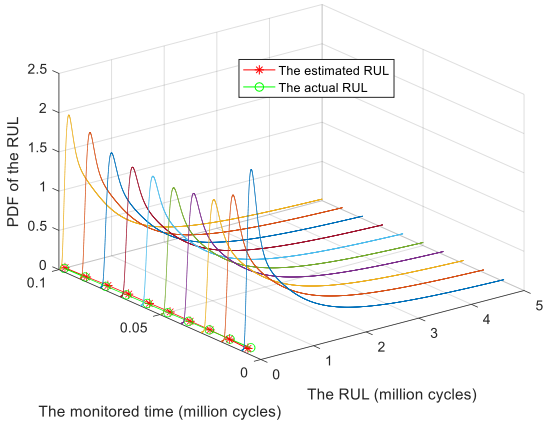

(b) PDF curves of RUL predicted by method IV

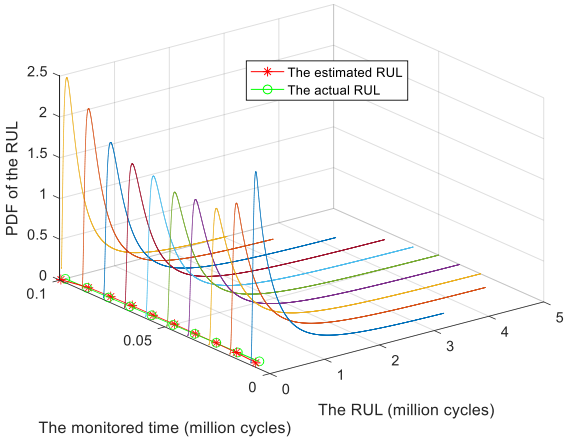

(c) PDF curves of RUL predicted by method V

Fig. 43. PDF curves of RUL predicted by single Copula functions.

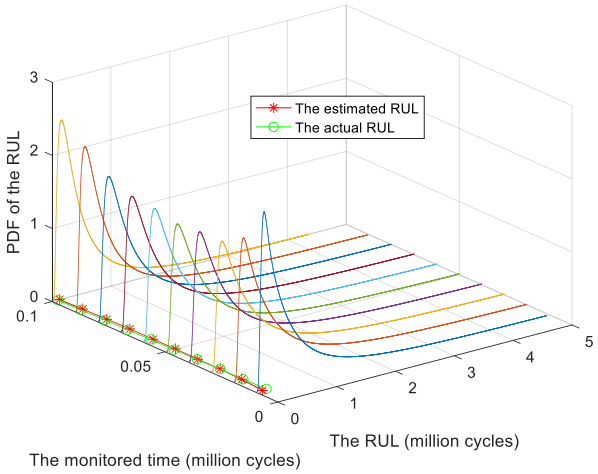

(a) PDF curves of RUL predicted by method VI

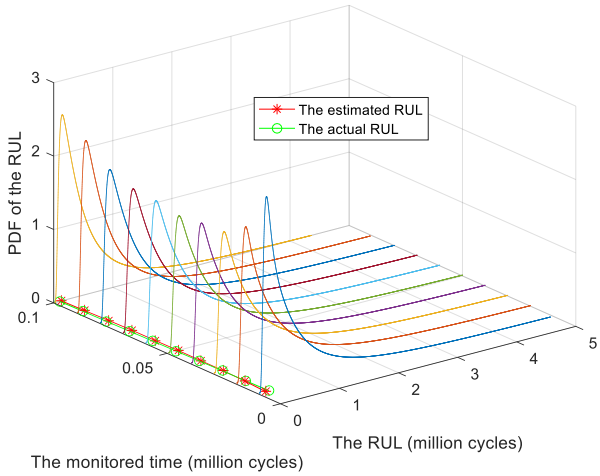

(b) PDF curves of RUL predicted by method VII

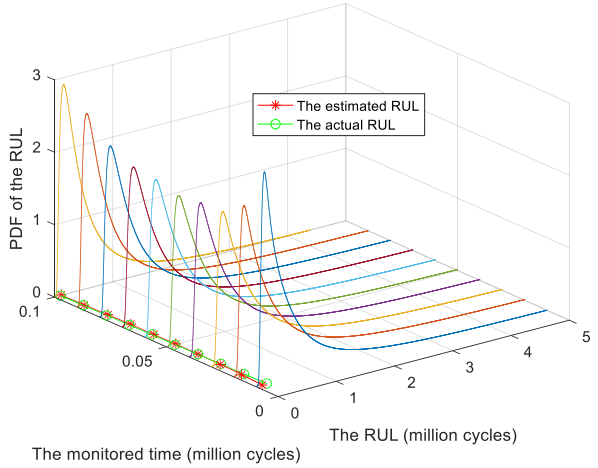

(c) PDF curves of RUL predicted by method VIII

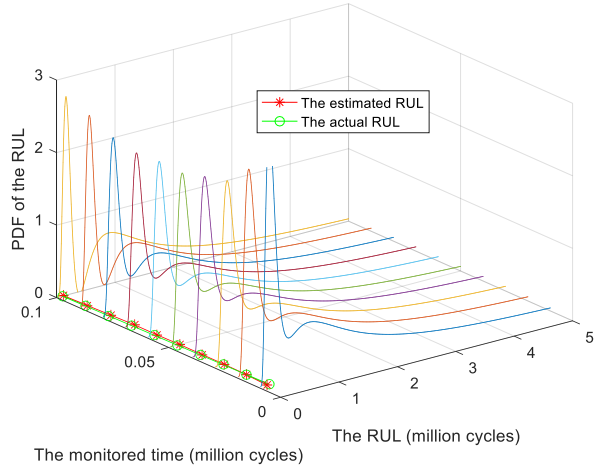

(d) PDF curves of RUL predicted by method IX

Fig.44. PDF curves of RUL predicted by mixed Copula functions.

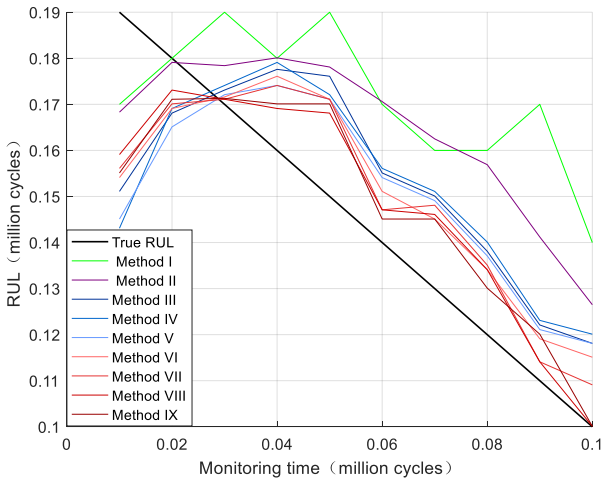

Fig.45. RUL curves predicted by different methods.

As illustrated in Figs. 42, 43, and 44, as the number of measurement points increases, the PDF curves of RUL become higher and sharper, indicating a gradual reduction in prediction uncertainty. The curves predicted using single Copula functions and mixed Copula functions exhibit even higher peaks and narrower spreads, demonstrating that these approaches yield lower uncertainty compared to other methods. Specifically, predictions using mixed Copula functions show even smaller uncertainty. A comparative analysis with the PDF curves predicted by model M_2 further reveals that the uncertainty associated with M_2 is greater than that of model M_1. Therefore, the degradation data is more suitable for model M_1 for RUL prediction, a conclusion also supported by comparative analysis of AIC values. Furthermore, as shown in Fig.45, the RUL values for metal equipment predicted using the hybrid Copula function-based method are closer to its actual values. For a quantitative evaluation, the TMSE, RMSE, and MAE values corresponding to each prediction method are calculated and summarized in Table 17.

Table 17. Errors of different prediction methods.

Method	TMSE	RMSE	MAE
PC1 (I)	0.0716	0.0031	0.0524
PC2(II)	0.0645	0.0023	0.0419
Frank (III)	0.0474	0.0015	0.0344
Clayton (IV)	0.0602	0.0020	0.0400
Gumbel (V)	0.0513	0.0014	0.0340
k_1Frank+ k_2Clayton (VI)	0.0459	0.0013	0.0335
k_1Frank+ k_3Gumbel (VII)	0.0451	0.0012	0.0332
k_2Clayton+ k_3Gumbel (VIII)	0.0301	0.0010	0.0285
k_1Frank+k_2Clayton+k_3Gumbel (IX)	0.0413	0.0011	0.0311

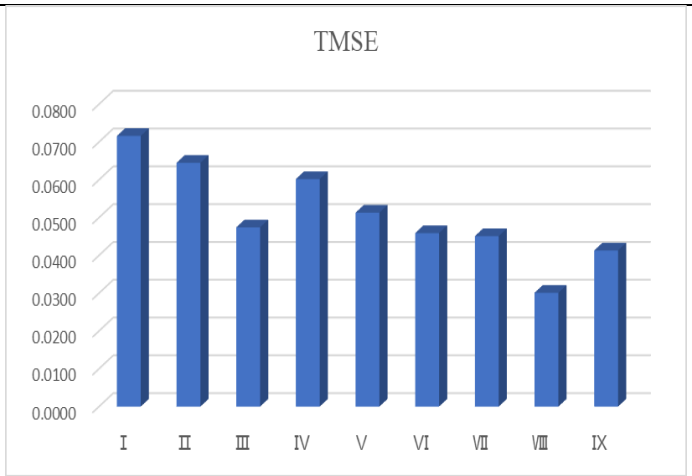

(a) TMSE values for different methods

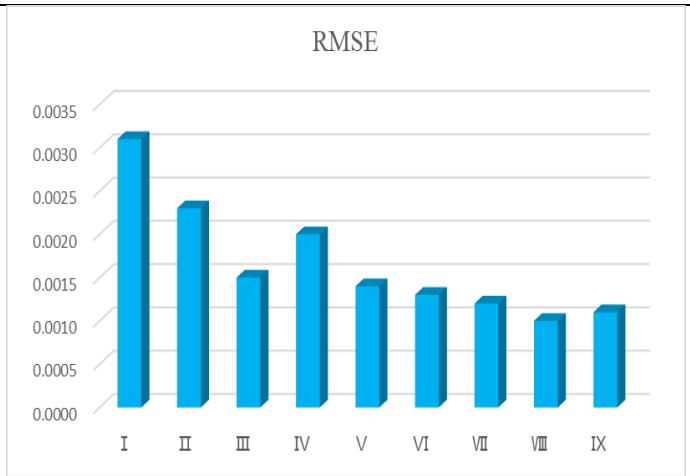

(b) RMSE values for different methods

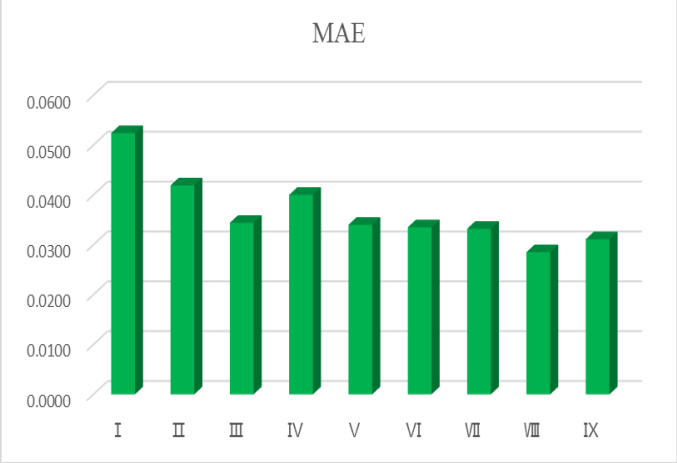

(c) MAE values for different methods

Fig. 46. Comparison of prediction errors across different methods.

As evident from Table 17 and Fig. 46, the TMSE, RMSE, and MAE values predicted by the mixed Copula function-based method are all smaller than those predicted using single Copula functions or single-performance degradation data. Among the nine RUL prediction methods evaluated, the mixed Copula function combining Clayton Copula and Gumbel Copula achieves the smallest TMSE, RMSE, and MAE values, indicating that this method yields the lowest prediction errors. Furthermore, a comparative analysis of the TMSE, RMSE, and MAE values in Table 15 and Table 17 reveals that model M_2 produces larger errors (higher TMSE, RMSE, and MAE values) compared to model M_1, demonstrating that model M_1 achieves superior prediction accuracy with smaller errors. This conclusion aligns with the earlier findings from the AIC value

comparison, reinforcing the consistency and reliability of the results.

C. Degradation model M_3

The two crack datasets are integrated into the degradation model M_3 with different Copula functions. The unknown parameters in the model are estimated using the two-step maximum likelihood estimation method, and the results are summarized in Table 18.

Table 18. Parameter estimates for different Copula functions.

Copula	α	k_1	k_2	k_3	ln$L$	AIC
Frank	2.0500	1	-	-	-1.4547e+03	2.9114e+03
Clayton	36.4974	-	1	-	-1.4495e+03	2.9010e+03
Gumbel	1.0966	-	-	1	-1.4692e+03	2.9404e+03
k_1Frank+ k_2Clayton	34.7648	0.2742	0.7258	-	-1.4019e+03	2.8098e+03
k_1Frank+ k_3Gumbel	1.2742	0.9778	-	0.0222	-1.3768e+03	2.7597e+03
k_2Clayton+ k_3Gumbel	39.8976	-	6.6657e-16	1.0000	-1.3677e+03	2.7414e+03
k_1Frank+ k_2Clayton+ k_3Gumbel	16.8392	0.1017	0.8983	3.8044e-19	-1.3403e+03	2.6867e+03

From Table 18, it can be observed that the mixed Copula function composed of Frank Copula, Clayton Copula, and Gumbel Copula achieves the largest log-likelihood function value and the smallest AIC value. Additionally, a comparative analysis of Tables 14, 16, and 18 reveals that the AIC values of model M_3 (for both single Copula and mixed Copula functions) are smaller than those of model M_2 but larger than those of model M_1. Therefore, among the three degradation models evaluated, the mixed Copula function corresponding to model M_1 should be prioritized for predicting the RUL of the metallic equipment. By substituting the aforementioned estimated parameters into their respective remaining useful life PDFs, the resulting graphs are plotted as shown below.

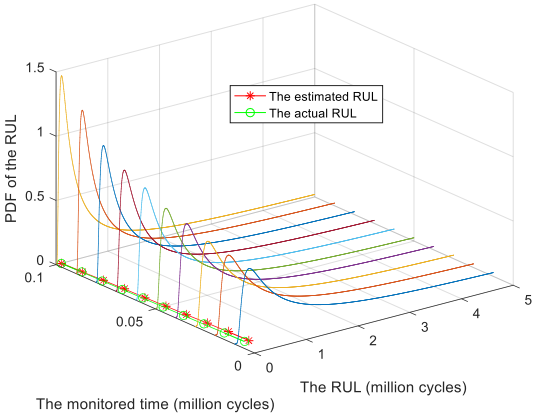

(a) PDF curves for RUL predicted by PC1

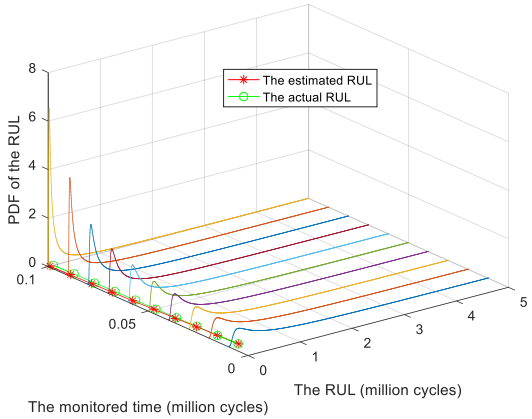

(b) PDF curves of RUL predicted by PC2

Fig.47. PDF curves of RUL predicted by the single performance degradation data.

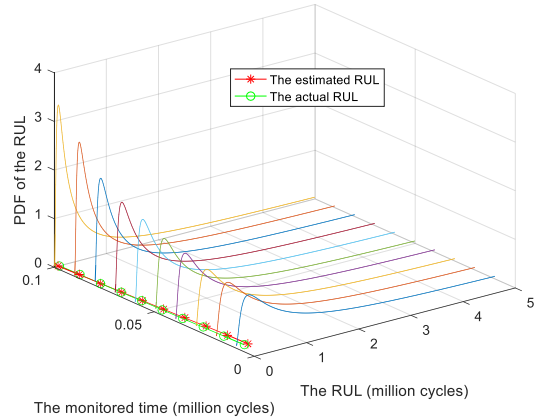

(a) PDF curves of RUL predicted by method III

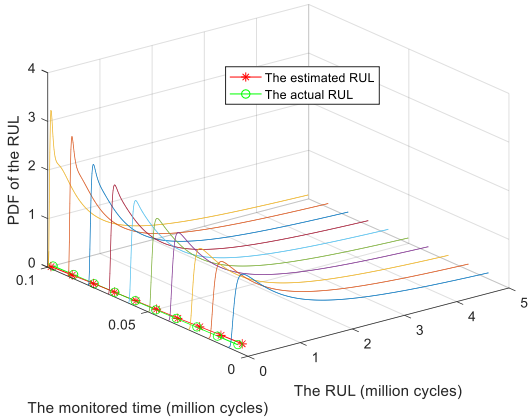

(b) PDF curves of RUL predicted by method IV

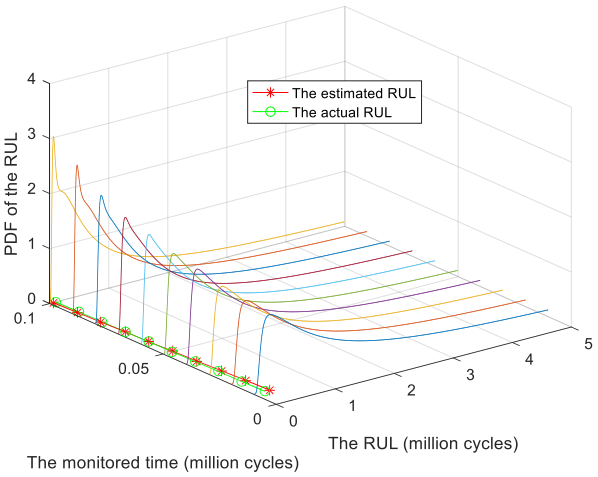

(c) PDF curves of RUL predicted by method V

Fig. 48. PDF curves of RUL predicted by single Copula functions.

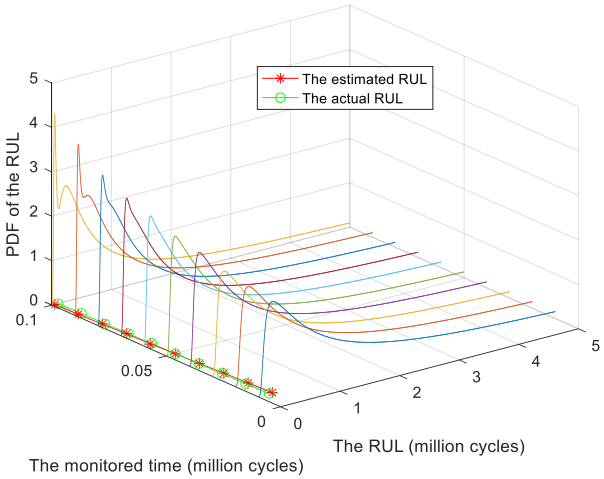

(a) PDF curves of RUL predicted by method VI

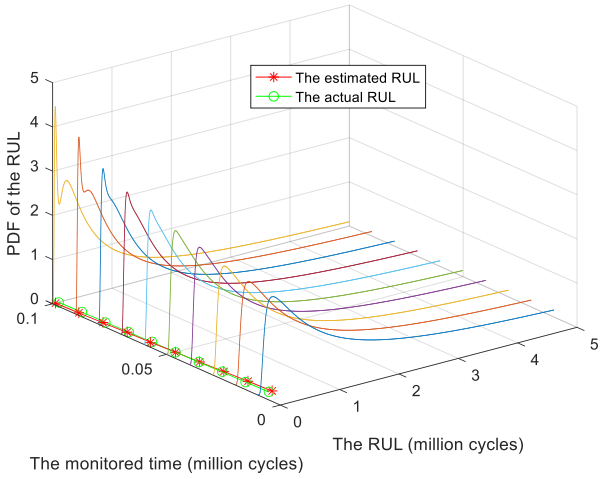

(b) PDF curves of RUL predicted by method VII

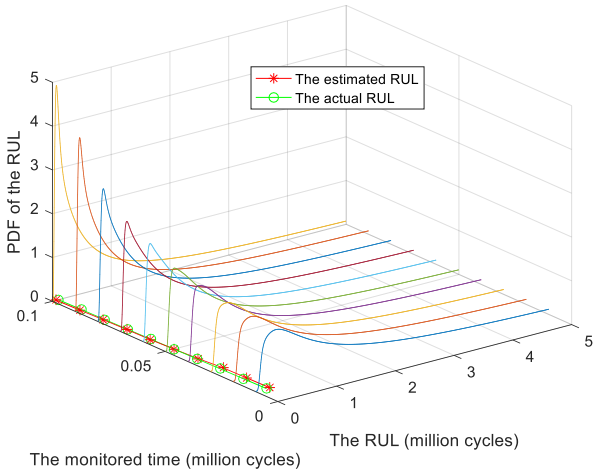

(c) PDF curves of RUL predicted by method VIII

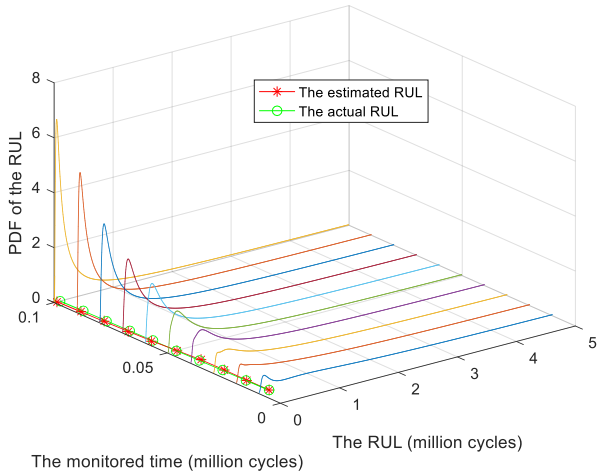

(d) PDF curves of RUL predicted by method IX

Fig.49. PDF curves of RUL predicted by mixed Copula functions.

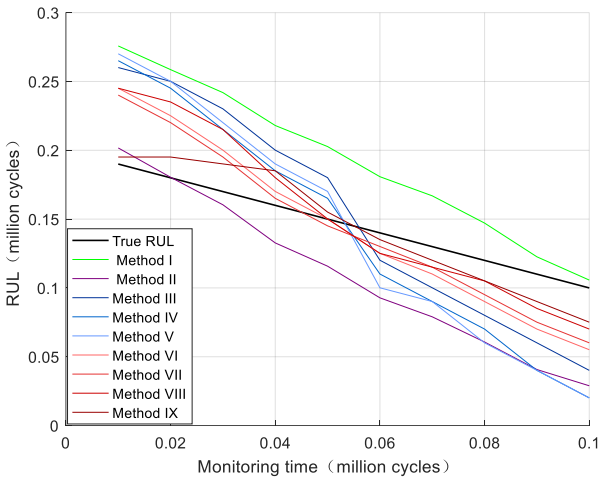

Fig.50. RUL curves predicted by different methods.

From the aforementioned figures, it can be observed that within model M_3, the PDF curves of RUL predicted by the mixed Copula function are higher and sharper than those derived from single Copula functions or single-performance degradation data. This once again demonstrates that predictions using the mixed Copula function exhibit lower uncertainty. Furthermore, comparative analysis with earlier sections reveals that the PDF curves predicted by model M_1 are higher and sharper than those generated by models M_2 and M_3, indicating that model M_1 achieves the smallest prediction uncertainty and is more suitable for degradation modeling and RUL of the metallic equipment. As shown in Fig. 50, the RUL values for metal equipment predicted using the hybrid Copula function-based method are closer to its actual values. The corresponding TMSE, RMSE, and MAE values for each method are presented here in Table 19.

Table 19. Errors of different prediction methods.

Method	TMSE	RMSE	MAE
PC1 (I)	0.0702	0.0029	0.0470
PC2(II)	0.0541	0.0020	0.0381
Frank (III)	0.0464	0.0016	0.0336
Clayton (IV)	0.0478	0.0017	0.0339
Gumbel (V)	0.0525	0.0018	0.0341
k_1Frank+ k_2Clayton (VI)	0.0459	0.0015	0.0331
k_1Frank+ k_3Gumbel (VII)	0.0435	0.0014	0.0325
k_2Clayton+ k_3Gumbel (VIII)	0.0402	0.0012	0.0300
k_1Frank+k_2Clayton+k_3Gumbel (IX)	0.0293	9.8821e-04	0.0280

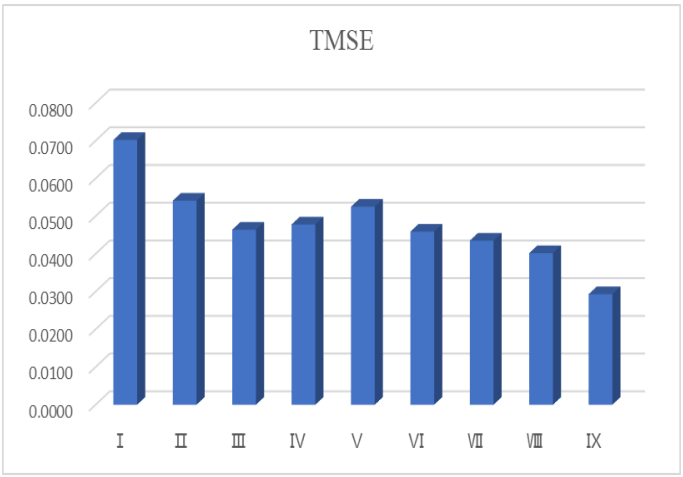

(a) TMSE values for different methods

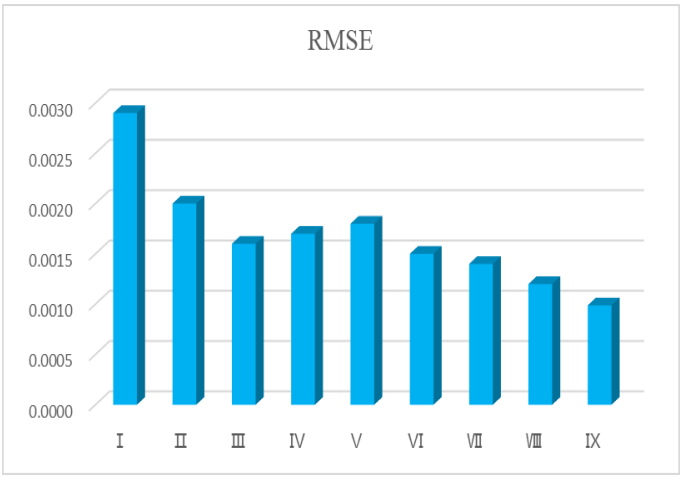

(b) RMSE values for different methods

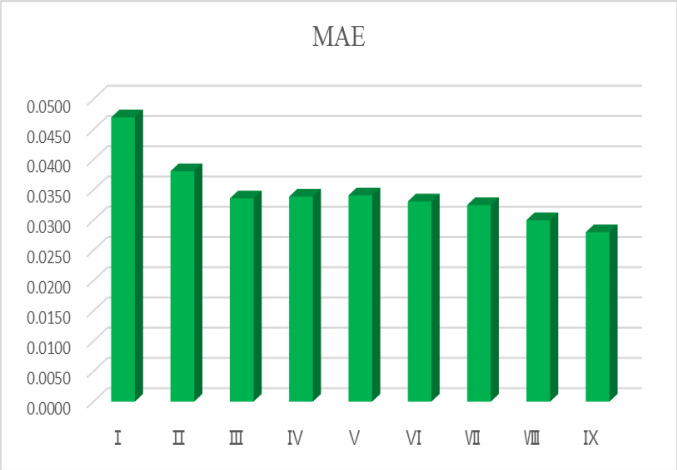

(c) MAE values for different methods

Fig. 51. Comparison of prediction errors across different methods.

From Table 19 and Fig.51, it can be seen that the TMSE, RMSE, and MAE values predicted by the mixed Copula function-based method are smaller than those obtained using single Copula functions or single-performance degradation data. Among these, the mixed Copula function combining Frank Copula, Clayton Copula, and Gumbel Copula yields the smallest TMSE, RMSE, and MAE values, indicating the lowest prediction errors. Furthermore, a comparative analysis with earlier prediction results shows that the TMSE, RMSE, and MAE values predicted by degradation model M_3 are larger than those of model M_1 but smaller than those of model M_2. Therefore, the mixed Copula functions corresponding to degradation model M_1 should be prioritized for predicting the RUL of the metallic equipment. This approach ensures more accurate predictions, thereby reducing long-term maintenance costs.

6. Conclusion

Given that the performance degradation process of equipment exhibits a dual-performance degradation phenomenon with a correlation between the two degradation metrics, using a single performance indicator is insufficient to fully reflect this degradation process. To address this, a binary Wiener process degradation model considering different degradation modes is proposed. By introducing Copula functions, the correlation between the two performance indicators of equipment is analyzed. Since different Copula functions depict correlation differently, this study presents a method based on mixed Copula functions to better integrate data and utilize the distinct characteristics of various Copula functions. Then, based on the properties of the Wiener process and Copula functions, analytical expressions for the joint PDFs of lifetime and RUL under different degradation models based on the FHT principle are derived in detail, and the unknown parameters in the degradation model are estimated using the two-step maximum likelihood estimation method. Finally, the proposed method is validated through simulation data, LED lighting data, and metallic equipment crack propagation data, and the prediction errors of the RUL using single-performance degradation data, single Copula functions, and mixed Copula functions under three different models are compared using TMSE, RMSE, and MAE values. The comparative analysis of the prediction errors indicates that the RUL prediction based on a mixed Copula function for two-performance degradation data yield the smallest errors, resulting in the lowest TMSE, RMSE, and MAE values and more accurate predictions. This research demonstrates that the proposed method has practical applicability, providing effective life information for equipment health status management and holding potential engineering value.

References

1. Lu N, Chen C, Jiang B, Xing Y, Latest progress on maintenance strategy of complex system: from condition-based maintenance to predictive maintenance. Acta Automatica Sinica 2021;47 (01):1-17. https://doi.org/ 10.16383/j.aas.c200227.

2. Wang Z, Chen Y, Cai Z, Xiang H, Wang L. Equipment remaining useful lifetime online prediction based on accelerated degradation modeling with the proportion relationship. Systems Engineering and Electronics 2021;43 (02): 584-592. https://doi.org/10.12305/j.issn.1001-506X.2021.02.34.
3. Hu J, Sun Q., Ye Z, Zhou Q. Joint modeling of degradation and lifetime data for RUL prediction of deteriorating products. IEEE Transactions on Industrial Informatics 2021;17 (07): 4521-4531. https://doi.org/10.1109/TII.2020.3021054.
4. Wang X, Hu C, Ren Z, Xiong W. Performance degradation modeling and remaining useful life prediction for aeroengine based on nonlinear Wiener process. Acta Aeronautica et Astronautica Sinica 2020;41 (02): 195-205. https://doi.org/10.7527/S1000-6893.2019.23291.
5. Yuan Y, Zhang Y, Ding H. Research on key technology of industrial artificial intelligence and its application in predictive maintenance. Acta Automatica Sinica 2020; 46(10):200333. https://doi.org/10.16383/j.aas.c200333.
6. Kan S, Tan C, Mathew J. A review on prognostic techniques for non-stationary and non-linear rotating systems. Mechanical Systems and Signal Processing 2015;62 (63):1-20. https://doi.org/10.1016/j.ymssp.2015.02.016.
7. Lei Y, Li N, Guo L, Li N, Yan T, Lin J. Machinery health prognostics: A systematic review from data acquisition to RUL prediction. Mechanical Systems and Signal Processing 2018;104: 799-834. https://doi.org/10.1016/j.ymssp.2017.11.016.
8. Guo J, Li Z, Li M. A review on prognostics methods for engineering systems. IEEE Transactions on Reliability 2019;69 (03): 1-20. https://doi.org/10.1109/TR.2019.2957965.
9. Meng D, Lv Z, Yang S, Wang H, Xie T, Wang Z.A time-varying mechanical structure reliability analysis method based on performance degradation. Structures 2021:34:3247-3256.https://doi.org/10.1016/J.ISTRUC.2021.09.085.
10. Ma H, Zhu S, Guo Y, Pan L, Yang S, Meng D. Residual useful life prediction of the vehicle isolator based on Bayesian inference. Structures, 2023;58:105518.
11. Wang C, Zhang L, Chen L, Tan T, Zhang C. Remaining useful life prediction of nuclear reactor control rod drive mechanism based on dynamic temporal convolutional network, Reliability Engineering and System Safety 2025; 253:110580.
12. He D, Zhao J, Jin Z, Huang C, Zhang F, Wu J. Prediction of bearing remaining useful life based on a two-stage updated digital twin. Advanced Engineering Informatics 2025; 65:103123.
13. Guan Q, Zuo Z, Teng Y, Zhang H, Jia L. Two-stage remaining useful life prediction based on the Wiener process with multi-feature fusion and stage division. Eksploatacja i Niezawodność – Maintenance and Reliability 2024; 26 (04):189803.
14. Kahle W, Lehmann A. The Wiener process as a degradation model: modeling and parameter estimation, Birkhäuser Boston,2010. https://doi.org/10.1007/978-0-8176-4924-1_9
15. Wang X, Cheng Z, Guo B. Residual life forecasting of metallized film capacitor based on Wiener process. Journal of National University of Defense Technology 2011; 33 (04): 146-151. https://doi.org/10.3969/j.issn.1001-2486.2011.04.028.
16. Li H, Jin G, Zhou J, Zhou Z, Hu C. Momentum wheel Wiener process degradation modeling and life prediction. Journal of Aerospace Power 2011;26 (03):622-627. https://doi.org/10.13224/j.cnki.jasp.2011.03.022.
17. Si X, Chen M, Wang W, Hu C, Zhou D. Specifying measurement errors for required lifetime estimation performance. European Journal of Operational Research 2013;231 (03): 631-644. https://doi.org/10.1016/j.ejor.2013.05.046.
18. Peng C, Tseng S. Statistical lifetime inference with skew-wiener linear degradation models.IEEE Transactions on Reliability 2013;62 (02):338-350. https://doi.org/10.1109/TR.2013.2257055.
19. Zhang J, Hu C, He X, Si X, Liu Y, Zhou D. A novel lifetime estimation method for two-phase degrading systems. IEEE Transactions on Reliability 2019; 68(02): 689-709. https://doi.org/10.1109/TR.2018.2829844
20. Guan Q, Wei X, Bai W, Jia L. Two-stage degradation modeling for remaining useful life prediction based on the Wiener process with measurement errors. Quality and Reliability Engineering International 2022;38 (07): 3485-3512. https://doi.org/10.1002/QRE.3147.
21. Si X, Wang W, Hu C, Zhou D, Pecht M. Remaining useful life estimation based on a nonlinear diffusion degradation process. IEEE Transactions on Reliability 2012;61 (01):50-67. https://doi.org/10.1109/TR.2011.2182221.
22. Tang S, Guo X, Yu C, Zhou Z, Zhou Z, Zhang B. Real time remaining useful life prediction based on nonlinear Wiener based degradation processes with measurement errors. Journal of Central South University 2014;21 (12): 4509-4517. https://doi.org/10.1007/s11771-014-2455-9.
23. Peng C, Qian F, Du X. New nonlinear degradation modeling and residual life prediction. Computer Integrated Manufacturing System

2019;25 (07): 1647-1654. https://doi.org/10.13196/j.cims.2019.07.005.

24. Yu W, Tu W, Kim Y, Mechefske C. A nonlinear-drift-driven Wiener process model for remaining useful life estimation considering three sources of variability. Reliability Engineering and System Safety2021; 212:107631.
25. Long J, Chen C, Liu Z, Guo J, Chen W. Stochastic hybrid system approach to task-orientated remaining useful life prediction under time-varying operating conditions. Reliability Engineering and System Safety 2022; 225: 108568.
26. Lin J, Liao G, Chen M, Yin H. Two-phase degradation modeling and remaining useful life prediction using nonlinear wiener process. Computers & Industrial Engineering 2021; 160:107533.
27. Hu C, Xing Y, Du D, Si X, Zhang J. Remaining useful life estimation for two-phase nonlinear degradation processes. Reliability Engineering and System Safety 2023; 230:108945.
28. Zhou Y, Lü W, Wang S, Sun Y. Statistical analysis method of bivariate degradation data based on dependency modeling via copula function. Journal of Ordnance Equipment Engineering 2018;39 (5):160-165. https://doi.org/10.11809/bqzbgcxb2018.05.035.
29. Song Y, Li H. Typical scene generation of wind and photovoltaic power output based on kernel density estimation and Copula function. Electrical Engineering 2022;23 (01): 56-63.
30. Jin Y, Li J, Sun Y. Bearing remaining useful life prediction based on two-dimensional Wiener process. Chinese Journal of Scientific Instrument 2018;39 (06) :89-95. https://doi.org/10.19650/j.cnki.cjsi.J1803186.
31. Dai Y, Cheng S, Gan Q, Yu T, Wu X, Bi F. Life prediction of Ni-Cd battery based on linear Wiener process. Journal of Central South University 2021;28, (09): 2919-2930. https://doi.org/10.1007/S11771-021-4816-5.
32. Qi J, Li H, Zhang H, Liu X, Yan D. Remaining life prediction of oil-paper insulation of on-board transformers of high-speed trains based on binary correlation degradation. Journal of Safety and Environment 2024;24 (6): 2229-2237. https://doi.org/10.13637/j.issn.1009-6094.2023.1283.
33. Dong Z, Liu K, Peng H. Failure prediction of dry hollow reactor encapsulation material based on binary nonlinear Wiener process. Insulating Materials 2020;53 (05): 101-106. https://doi.org/10.19595/j.cnki.1000-6753.tces.220865.
34. Zhao H, Chang J, Qu Y, Sun C, Guo X. Residual life prediction method of transformer oil-paper insulation based on binary nonlinear Wiener random process. Transactions of China Electrotechnical Society 2023;38 (15): 4040-4049. https://doi.org/10.19595/j.cnki.1000-6753.tces.220865.
35. Li Y, Huang X, Gao T, Zhao C, Li S. A wiener-based remaining useful life prediction method with multiple degradation patterns. Advanced Engineering Informatics 2023; 57:102066.
36. Zhou Y, Guo J, Wan W, Jiang Y, Shao S. A study on reliability benefit assessment of reduced thrust take off based on performance degradation model of Wiener and Copula functions. Journal of Propulsion Technology 2019;40 (03): 667-674. https://doi.org/10.13675/j.cnki.tjjs.180139.
37. Nelsen R. An introduction to Copulas. Technometrics 2000; 42:1271100.
38. Asgari A, Si W, Yuan L, Krishna K, Wei W. Multivariable degradation modeling and life prediction using multivariate fractional Brownian motion. Reliability Engineering and System Safety 2024;248:110146
39. Liu S, Wei J, Li G, He J, Zhang B, Liu B. A two-stage remaining useful life prediction method based on adaptive feature metric and graph spatiotemporal attention rule learning. Reliability Engineering and System Safety 2025;257: 110802.
40. Si X, Zhou D. A generalized result for degradation model-based reliability estimation. IEEE Transactions on Automation Science and Engineering: a publication of the IEEE Robotics and Automation Society 2014;11 (2): 632-637. https://doi.org/10.1109/TASE.2013.2260740.
41. Albahli S, Yar H. Defect prediction using Akaike and Bayesian information criterion. Computer Systems Science and Engineering 2022;41 (03) :1117-1127. https://doi.org/10.32604/CSSE.2022.021750.
42. Chanseok P, Padgett W. Stochastic degradation models with several accelerating variables. IEEE Transactions on Reliability 2006;55 (02): 379-390. https://doi.org/10.1109/TR.2006.874937.
43. Ye Z, Wang Y, Tsui K, Pecht M. Degradation data analysis using Wiener processes with measurement errors. IEEE Transactions on Reliability 2013;62 (04):772-780, https://doi.org/10.1109/TR.2013.2284733.
44. Pecht M, Jaai R. A prognostics and health management roadmap for information and electronics-rich systems. Microelectronics Reliability

2010; 50 (03):317-323. https://doi.org/10.1016/j.microrel.2010.01.006.
45. Meeker W, Escobar L. Statistical methods for reliability data, New York,Wiley,1998.
46. Pan Z, Balakrishnan N, Sun Q. Bivariate constant-stress accelerated degradation model and inference. Communications in Statistics - Simulation and Computation 2011; 40(02):247-257. https://doi.org/10.1080/03610918.2010.534227
47. Sari J K. Multivariate degradation modeling and its application to reliability testing. Singapore: National University of Singapore, 2007.
48. Si X, Hu C, Zhang Z. Data-driven remaining useful life prognosis techniques: stochastic models, methods and applications, New York, Springer, 2017, https://doi.org/10.1007/978-3-662-54030-5

Appendix A. Proof of Eqs. (7), (9), (11)

In order to prove the lifetime probability distribution functions corresponding to the three different degradation models, a stochastic process $\{Z(t), t \geq 0\}$ is defined on the basis of a one-dimensional Wiener process

$$Z(t) = \underset{0 \leq s \leq t}{SUP}\{X(s), s \geq 0\} \tag{A.1}$$

At any given time $t \geq 0$, $Z(t)$ takes the maximum value of $X(t)$ during the time interval $[0, t]$. The probability density function of $Z(t)$ at time t is $g(z, t)$. From the definition of $\{z(t), t \geq 0\}$, it is known that it is a monotonic stochastic process, and the probability of equipment not failing is

$$P(T > t) = P(Z(t) < \omega) = \int_{-\infty}^{\omega} g(z, t)\, dz \tag{A.2}$$

Using the Fokker-Planck equation one can obtain G in the form:

$$g(z, t) = \frac{1}{\delta_B \sqrt{2\pi t}} \left\{ exp\left[-\frac{(z - a\phi(t,b))^2}{2\delta_B^2 t} \right] - exp\left(\frac{2a\omega}{\delta_B^2} \right) exp\left[-\frac{(z - 2\omega - a\phi(t,b))^2}{2\delta_B^2 t} \right] \right\} \tag{A.3}$$

Substituting Eq. (A.3) into Eq. (A.2) yields:

$$P(T > t) = 1 - F(t) = \Phi\left(\frac{\omega - a\phi(t,b)}{\delta_B \sqrt{t}} \right) - exp\left(\frac{2\omega a}{\delta_B^2} \right) \Phi\left(\frac{-\omega - a\phi(t,b)}{\delta_B \sqrt{t}} \right) \tag{A.4}$$

The distribution function of lifetime can be obtained from Eq. (A.4) as follows:

$$F(t) = 1 - \Phi\left(\frac{\omega - a\phi(t,b)}{\delta_B \sqrt{t}} \right) + exp\left(\frac{2\omega a}{\delta_B^2} \right) \Phi\left(\frac{-\omega - a\phi(t,b)}{\delta_B \sqrt{t}} \right) \tag{A.5}$$

The distribution function expressed in the above equation does not take into account the randomness of the drift coefficient a. When the randomness of the drift coefficient a is taken into account and $a \sim N(\mu_a, \delta_a^2)$ is satisfied, the use of the full probability formula for Eq. (A.5) yields

$$F_T(t) = \int_{-\infty}^{+\infty} F(t) p(a)\, da = E_a[F(t)] \tag{A.6}$$

where $p(a)$ is the PDF of the random variable a, and $E_a[.]$ denotes the mathematical expectation of the random parameter a. To solve the expectation of the above equation, Theorem 1 is introduced.

Theorem 1 ([48]) If $Z \sim N(\mu, \delta^2)$,$\omega, v, B, D \in R$,and$C \in R^+$, then

$$E_z[exp\{vZ\}\, \Phi(C + DZ)] = exp\left\{ \frac{v^2}{2} \delta^2 + v\mu \right\} \Phi\left(\frac{C + D\mu + Dv\delta^2}{\sqrt{1 + D^2\delta^2}} \right) \tag{A.7}$$

Based on Eq. (51) and Theorem 1, it can be concluded that:

$$F_T(t) = E_a[F(t)] \quad = 1 - E\left[\Phi\left(\frac{\omega - a\phi(t,b)}{\delta_B \sqrt{t}} \right) \right] + E\left[exp\left(\frac{2\omega a}{\delta_B^2} \right) \Phi\left(\frac{-\omega - a\phi(t,b)}{\delta_B \sqrt{t}} \right) \right] \quad = 1 - E_1(t) + E_2(t) \tag{A.8}$$

If $v = 0$ in Theorem 1, then

$$E_z[\Phi(C + DZ)] = \Phi\left(\frac{C + D\mu}{\sqrt{1 + D^2\delta^2}} \right) \tag{A.9}$$

Let $C = \frac{\omega}{\delta_B \sqrt{t}}, D = -\frac{\phi(t,b)}{\delta_B \sqrt{t}}$. By combining Eq. (A.9), we can obtain

$$E_1(t) = E\left[\Phi\left(\frac{\omega - a\phi(t,b)}{\delta_B\sqrt{t}}\right)\right] = E[\Phi(C + Da)] \qquad = \Phi\left(\frac{C + D\mu_a}{\sqrt{1 + D^2\delta_a^2}}\right) = \Phi\left(\frac{\omega - \mu_a\phi(t,b)}{\sqrt{\delta_a^2\phi^2(t,b) + t\delta_B^2}}\right) \tag{A.10}$$

Similarly, it can be concluded that

$$E_2(t) = E\left[exp\left(\frac{2\omega a}{\delta_B^2}\right)\Phi\left(\frac{-\omega - a\phi(t,b)}{\delta_B\sqrt{t}}\right)\right] = exp\left(\frac{2\omega\mu_a\phi(t,b)}{\delta_B^2 t} + \frac{2\omega^2\delta_a^2\phi^2(t,b)}{\delta_B^4 t^2}\right)\Phi\left(-\frac{(\omega + \mu_a\phi(t,b))\delta_B^2 t + 2\omega\phi^2(t,b)\delta_a^2}{\delta_B^2 t\sqrt{\delta_B^2 t + \delta_a^2\phi^2(t,b)}}\right) \tag{A.11}$$

Based on the above process, it can be concluded that

$$F_T(t) = 1 - \Phi\left(\frac{\omega - \mu_a\phi(t,b)}{\sqrt{\delta_a^2\phi^2(t,b) + t\delta_B^2}}\right) + exp\left(\frac{2\omega\mu_a\phi(t,b)}{\delta_B^2 t} + \frac{2\omega^2\delta_a^2\phi^2(t,b)}{\delta_B^4 t^2}\right)\Phi\left(-\frac{(\omega + \mu_a\phi(t,b))\delta_B^2 t + 2\omega\phi^2(t,b)\delta_a^2}{\delta_B^2 t\sqrt{\delta_B^2 t + \delta_a^2\phi^2(t,b)}}\right) \tag{A.12}$$

When $\phi(t,b) = (t, t^b, e^{bt})$, substituting them into Eq. (A.12) respectively yields the conclusions of Eqs. (7), (9), and (11).

Appendix B Proof of Eqs. (16), (18), (20)

Based on the relationship between lifetime and RUL and the reasoning process in Appendix A, the probability distribution function of RUL corresponding to the degradation model is known as

$$F(l_{t_i}) = 1 - \Phi\left(\frac{\omega - X(t_i) - \mu_a\phi(l_{t_i}, b)}{\sqrt{\delta_a^2\phi^2(l_{t_i}, b) + l_{t_i}\delta_B^2}}\right) + exp\left(\frac{2(\omega - X(t_i))\mu_a\phi(l_{t_i}, b)}{\delta_B^2 l_{t_i}} + \frac{2(\omega - X(t_i))^2\delta_a^2\phi^2(l_{t_i}, b)}{\delta_B^4 l_{t_i}^2}\right)$$

$$\times\Phi\left(-\frac{\left(\omega - X(t_i) + \mu_a\phi(l_{t_i}, b)\right)\delta_B^2 l_{t_i} + 2(\omega - X(t_i))\phi^2(l_{t_i}, b)\delta_a^2}{\delta_B^2 l_{t_i}\sqrt{\delta_B^2 l_{t_i} + \delta_a^2\phi^2(l_{t_i}, b)}}\right) \tag{B.1}$$

When $\phi(l_{t_i}, b) = (l_{t_i}, l_{t_i}^b, exp(bl_{t_i}))$, substituting them into Eq. (B.1) respectively yields the conclusions of Eqs. (16), (18), and (20).